

Dissertation
submitted to the
Combined Faculties for the Natural Sciences and for Mathematics
of the Ruperto-Carola University of Heidelberg, Germany

for the degree of

Doctor of Natural Sciences

presented by

MSc. Ivelina Kadiyska

Born in Dupnitsa, Bulgaria
Oral examination: 13.07.2016

**Implications of a genetically
determined nitric oxide deficit for
endothelial cell-leukocyte
interaction and cardiovascular
disease**

Referees:

Prof. Dr. Markus Hecker

Prof. Dr. Gudrun Rappold

Contents

Contents	iii
List of Figures	vii
List of Tables	ix
Abbreviations & Symbols	xi
1 Introduction	1
1.1 Nitric oxide and vascular homeostasis	1
1.1.1 The NO synthases	2
1.1.2 Regulation of NOS-3 activity	2
1.1.3 Shear stress-dependent transcriptional regulation of NOS-3 ex- pression	3
1.2 Hallmark of endothelial dysfunction is the impaired bioavailability of NO	4
1.3 Atherosclerosis	5
1.3.1 Role of monocytes/macrophages in atherosclerosis	5
1.3.2 Role of neutrophils in atherosclerosis	7
1.3.3 Role of T cells in atherosclerosis	7
1.4 Endothelial dysfunction in chronic inflammatory diseases	9
1.5 Genetic susceptibility to atherosclerosis	11
1.5.1 The T-786C SNP of the <i>NOS3</i> gene as a genetic determinant of endothelial dysfunction	13
1.6 Prostanoids	14
1.7 Aims of the thesis	16
2 Materials	19
2.1 Chemicals and reagents	19
2.2 Kits	21
2.3 Consumables	21
2.4 Equipment	22
2.5 Oligonucleotides	23

2.6	Antibodies	26
2.7	Stimulants and inhibitors	27
2.8	Growth media, buffers and solutions	28
3	Methods	31
3.1	Cell biology methods	31
3.1.1	Cell isolation and culture	31
3.1.1.1	Isolation and culture of human umbilical vein endothelial cells (HUVECs)	31
3.1.1.2	Isolation of human naïve CD4 ⁺ T cells	31
3.1.1.3	<i>In vitro</i> clonal expansion and differentiation of CD4 ⁺ T cells	32
3.1.1.4	THP-1 cell suspension culture	32
3.1.1.5	HEK293 and HeLa adherent cell culture	32
3.1.2	Intracellular cytokine staining to monitor Th1 cell differentiation	33
3.1.3	Monitoring CD4 ⁺ T cell proliferation with CFSE	33
3.1.4	Flow Cytometry	34
3.1.5	Application of unidirectional shear stress	34
3.1.6	Orbital shear stress <i>in vitro</i> transmigration system	35
3.1.7	<i>In vitro</i> Transmigration assay	36
3.1.8	Transfection	38
3.1.8.1	Viromer GREEN	38
3.1.8.2	Magnet-assisted transfection (MATra) of siRNAs	38
3.1.8.3	Lipofectamine 3000-mediated transfection of DNA plasmids	39
3.1.9	Decoy oligodeoxynucleotides (dODNs)	39
3.1.10	Treatments	39
3.2	Molecular biology methods	40
3.2.1	Isolation of human genomic DNA from blood	40
3.2.2	Isolation of RNA from cultured cells	40
3.2.3	Reverse transcription (RT)	41
3.2.4	Real-time quantitative reverse transcription polymerase chain reaction (Real-time qRT-PCR)	41
3.2.5	Conventional PCR	42
3.2.6	Agarose gel electrophoresis	44
3.2.7	Genotyping	44
3.2.8	DNA plasmid amplification	45
3.2.9	Introduction of deletion mutations in the <i>IL-1B</i> gene promoter using site-directed mutagenesis	45
3.2.10	Luciferase reporter gene assay	46
3.3	Biochemical methods	47
3.3.1	Total protein extraction	47
3.3.2	Nuclear extraction	47
3.3.3	Immunoblotting (Western blotting)	48
3.3.4	Electrophoretic mobility shift analysis (EMSA)	48
3.3.5	Chromatin Immunoprecipitation (ChIP)	49
3.3.6	15d-PGJ ₂ enzyme immunoassay	50

3.4	Sample collection and diagnosis of CHD	50
3.5	Quantification of 15d-PGJ ₂ concentration in CHD patients plasma	51
3.5.1	Chemicals	51
3.5.2	Preparation of internal standard stock and working solutions	51
3.5.3	Lipid extraction from blood plasma	51
3.5.4	Chromatography	52
3.5.5	Tandem mass spectrometry	52
3.6	Statistical analysis	53
4	Results	55
4.1	Characterization of a 15d-PGJ ₂ -mediated mechanism compensating for the relative lack of NO formation in endothelial cells (ECs) of individuals homozygous for the T-786C SNP of the <i>NOS3</i> gene	55
4.1.1	CC-genotype ECs impede monocyte activation and transendothelial migration independent of NO	55
4.1.2	COX-2 and L-PGDS are up-regulated in CC-genotype ECs upon FSS	56
4.1.3	CC-genotype HUVECs produce increased levels of 15d-PGJ ₂ , which has potent anti-migratory and anti-inflammatory activities <i>in vitro</i>	58
4.1.4	L-PGDS up-regulation in CC-genotype HUVECs is driven by the relative lack of NO	59
4.2	Investigation of molecular mechanisms underlying the anti-inflammatory activity of 15d-PGJ ₂ in human monocytes	60
4.2.1	15d-PGJ ₂ and Bardoxolone induce Nrf2 signaling in human THP-1 monocytes	63
4.2.2	15d-PGJ ₂ and Bardoxolone cause the nuclear accumulation of <i>de novo</i> synthesized Nrf2	66
4.2.3	Constitutive Nrf2 activation attenuates expression of IL-1 β	66
4.2.4	HO-1 is not a direct mediator of the anti-inflammatory activity of 15d-PGJ ₂ in THP-1 monocytes	67
4.2.5	15d-PGJ ₂ inhibits <i>IL-1B</i> gene expression at the transcriptional level	72
4.2.6	Silencing of Nrf2 does not abrogate the transcriptional repressor activity of 15d-PGJ ₂	74
4.2.7	Deletion of ARE-like motifs 2 and 3 in the <i>IL-1B</i> promoter may attenuate the transcriptional repressor activity of 15d-PGJ ₂	75
4.2.8	Bach1 knockdown does not affect the suppressive activity of 15d-PGJ ₂ on the <i>IL-1B</i> gene	78
4.2.9	Inhibition of histone deacetylase and p300/CBP histone acetyltransferase activities does not reverse the repressor effect of 15d-PGJ ₂ on the <i>IL-1B</i> promoter transcriptional activity	81
4.3	Increased 15d-PGJ ₂ plasma levels in patients suffering from coronary heart disease	83
4.4	Implications of the T-786C <i>NOS3</i> SNP for T helper cell-endothelial cell interactions	84
4.4.1	Isolation and expansion of human T helper cells	84
4.4.2	15d-PGJ ₂ inhibits the transmigration of Th1 lymphocytes	85
5	Discussion	89

5.1	Characterization of the 15d-PGJ ₂ -mediated compensatory mechanism in CC-genotype carriers	90
5.2	Investigation of molecular mechanisms underlying the anti-inflammatory activity of 15d-PGJ ₂	94
5.2.1	The Nrf2-Keap-1 pathway as a mediator of the anti-inflammatory activities of 15d-PGJ ₂	95
5.2.2	Verifying a role for the Nrf2-Keap-1 pathway in THP-1 monocytes	96
5.2.3	Investigating the mechanism of action of Nrf2 in THP-1 cells . . .	98
5.3	Clinical relevance of 15d-PGJ ₂ in patients with chronic inflammatory diseases such as CHD	102
5.4	Implications of the T-786C <i>NOS3</i> SNP for T helper cell-endothelial cell interactions	105
	Summary	109
	Zusammenfassung	111
	Bibliography	113
	Acknowledgements	130

List of Figures

1.1	Development of an atherosclerotic plaque.	6
1.2	The atherosclerotic plaque (a) shares many common features with rheumatoid arthritic synovium (b).	10
1.3	Biosynthesis of 15d-PGJ ₂	15
3.1	Snapshots of the direction and distribution of shear stress within single well of a 6-well Transwell [®] plate on an orbital shaker at different speed settings.	36
3.2	Schematic representation of <i>in vitro</i> transmigration assay.	37
3.3	RFLP pattern	44
4.1	Characterization of the 15d-PGJ ₂ mediated compensatory mechanism in CC-genotype HUVECs.	56
4.2	15d-PGJ ₂ inhibits the transmigration and pro-inflammatory activation of THP-1 monocytic cells.	59
4.3	Relative lack of NO facilitates genotype-dependent differential L-PGDS expression.	60
4.4	Inhibition of 15d-PGJ ₂ effector signaling pathways in THP-1 monocytes.	61
4.5	15d-PGJ ₂ induces Nrf2 DNA-binding activity in THP-1 monocytes.	64
4.6	15d-PGJ ₂ and Nrf2 activator, Bardoxolone, induce nuclear accumulation and activation of Nrf2 in THP-1 cells.	65
4.7	15d-PGJ ₂ and Bardoxolone induce accumulation of <i>de novo</i> synthesized Nrf2 in the nucleus.	67
4.8	Knockdown of the negative Nrf2 regulator Keap-1 attenuates IL-1 β expression.	68
4.9	A model for compensatory anti-inflammatory mechanism in endothelial cells (ECs) with insufficient NO synthesis.	69
4.10	HO-1 inhibition does not abrogate the suppressor effect of 15d-PGJ ₂ on <i>IL-1B</i> gene transcription.	71
4.11	15d-PGJ ₂ inhibits the expression of the <i>IL-1B</i> gene at the transcriptional level.	73
4.12	Deletion of ARE-like Nrf2-binding sites in the <i>IL-1B</i> promoter does not alter the transcriptional repressor activity of 15d-PGJ ₂	74

4.13	Knockdown of Nrf2 does not abrogate the transcriptional repressor activity of 15d-PGJ ₂ on the <i>IL-1B</i> promoter-reporter gene construct.	76
4.14	Length of the <i>IL-1B</i> promoter insert does not influence the basal and TNF- α -induced expression of the luciferase reporter construct.	77
4.15	Disruption of DNA sequence motifs ARE2 and ARE3 attenuates the inhibitory effect of 15d-PGJ ₂ in an improved <i>IL-1B</i> promoter-reporter gene assay.	78
4.16	Bach1 knockdown does not affect the repressor activity of 15d-PGJ ₂ on the <i>IL-1B</i> gene.	80
4.17	Inhibition of HDACs and p300/CBP HATs does not reverse the repressor activity of 15d-PGJ ₂ on the <i>IL-1B</i> gene.	82
4.18	Prevalence of the -786C-allele is greater in patients suffering from CHD.	83
4.19	Increased 15d-PGJ ₂ plasma levels in patients suffering from CHD.	84
4.20	Isolation and expansion of human T helper cells.	86
4.21	15d-PGJ ₂ impedes the transendothelial migration of <i>in vitro</i> differentiated Th1 cells.	87
5.1	15d-PGJ ₂ is an activator of the Nrf2-Keap-1 pathway.	97
5.2	Repression of Nrf2-mediated gene transactivation by the p65 subunit of NF- κ B.	101
5.3	15d-PGJ ₂ balances for the anti-inflammatory properties of NO in ECs with genetically determined NO deficit.	108

List of Tables

2.1	Chemicals and reagents	19
2.2	Kits	21
2.3	Consumables	21
2.4	Equipment	22
2.5	RT-PCR primers	23
2.6	qRT-PCR primers	23
2.7	Genotyping primers	23
2.8	ChIP primers	24
2.9	Mutagenesis primers	24
2.10	Decoy oligodeoxynucleotides	24
2.11	EMSA oligodeoxynucleotides	24
2.12	Small interfering RNAs	25
2.13	Primary antibodies	26
2.14	Secondary antibodies	26
2.15	Stimulants and inhibitors	27
2.16	List of growth media used for mammalian/bacterial cell growth and transfection	28
2.17	List of buffers and solutions	29
3.1	PCR Master mix HO-1	42
3.2	PCR Master mix <i>IL-1B</i> ARE-2 (ChIP assay)	43
3.3	PCR Master mix T-786C SNP <i>NOS3</i> genotyping	43
3.4	PCR program HO-1	43
3.5	PCR program <i>IL-1B</i> ARE-2 (ChIP assay)	43
3.6	PCR program T-786C <i>NOS3</i> SNP genotyping	43
4.1	Differences in arachidonic acid-metabolizing enzymes transcript levels in TT and CC-genotype ECs following exposure to FSS for 24 hours.	58

Abbreviations & Symbols

$^{\circ}\text{C}$	Degree Celsius
μ	Micro
AA	Arachidonic acid
ARE	Antioxidant response element
BARD	Bardoxolone-methyl
bp	Base pairs
Ca^{2+}	Calcium
CAM	Cell adhesion molecule
cAMP	Cyclic adenosine monophosphate
cGMP	Cyclic guanosine monophosphate
CHD	Coronary heart disease
CHX	Cycloheximide
CO	Carbon monoxide
COX	Cyclooxygenase
CyPGs	Cyclopentenone prostaglandin
DMSO	Dimethyl sulfoxide
dODN	Decoy oligodeoxynucleotide
EC	Endothelial cell
ECM	Extracellular matrix
EpRE	Electrophile response elements
FAD	Flavin adenin dinucleotide
FMN	Flavin mononucleotide
FSS	Fluid shear stress
GLuc	<i>Gaussia</i> Luciferase
GWAS	Genome-wide association study
HO-1	Heme-oxygenase-1
HUVEC	Human umbilical vein endothelial cell

ICAM	Intercellular adhesion molecule 1
IFNγ	Interferon- γ
IL-1β	Interleukin-1 β
Keap-1	Kelch-like ECH-associated protein-1
KLF-2	Krüppel-like factor 2
LD	linkage disequilibrium
LDL	Low-density lipoprotein
LOX	Lipoxygenase
MCP-1	Monocyte chemoattractant protein-1
MMPs	Matrixmetalloproteinases
NADPH	Nicotinamide adenine dinucleotide phosphate (reduced)
NETs	Neutrophil extracellular traps
NF-κB	Nuclear factor kappa-light-chain enhancer of activated B cells
NO	Nitric oxide
NOS	Nitric oxide synthase
Nrf2	Nuclear factor (erythroid-derived 2)-like 2
NQO-1	NADPH:quinone oxidoreductase 1
O$_2^-$	Superoxide anion
PBMCs	Peripheral blood mononuclear cells
PBS	Phosphate buffered saline
PG	Prostaglandin
L-PGDS	Lipocalin-type prostaglandin-D synthase
15d-PGJ$_2$	15-deoxy- $\Delta^{12,14}$ -prostaglandin J $_2$
PrxI	Peroxiredoxin 1
RA	Rheumatoid arthritis
ROS	Reactive oxygen species
rpm	Revolutions per minute
SLE	Systemic lupus erythematosus
SMCs	Smooth muscle cells
SNP	Single nucleotide polymorphism
SOD	Superoxide dismutase
TBS	Tris buffered saline
TF	Transcription factor
TGF-β	Transforming growth factor-beta
Th	T helper
THP-1	Human monocytic cell line
TNF-α	Tumor necrosis factor- α
Tregs	Regulatory T cells
TXA$_2$	Thromboxane A $_2$
VCAM1	Vascular cell adhesion molecule 1
ZnPP	Zinc protoporphyrin IX

1.1 Nitric oxide and vascular homeostasis

A functional endothelium is required for a healthy cardiovascular system. The endothelium plays a key role in vascular homeostasis both as a sensor of mechanical and biochemical stimuli as well as a source of pleiotropic vasoactive autacoids. In non-inflamed tissue, the endothelium maintains blood fluidity, regulates vascular tone by coordinating the balance between vasoconstriction and vasodilation, controls vascular permeability and preserves the anti-inflammatory environment within the vessel wall. Among the variety of messengers released by the endothelium, nitric oxide (NO) has been recognized as the principal mediator of these regulatory properties, thereby maintaining vessel wall homeostasis.

NO is the primary physiological vasodilator, released by endothelial cells (ECs) in response to mechanostimulation and biochemical stimuli to regulate blood flow, blood pressure and tissue oxygen supply (for review, see Pober and Sessa (2007); Förstermann and Sessa (2012)). From ECs NO diffuses to the underlying smooth muscle cells (SMCs) where it acts in various ways to promote smooth muscle relaxation. In SMCs, NO binds to soluble guanylyl cyclase causing a rapid rise in cyclic guanosine monophosphate (cGMP) levels. This activates protein kinase G, which in turn causes sequestration of intracellular calcium (Ca^{2+}) as well as activation of potassium channels leading to membrane hyperpolarization, hence closure of voltage-dependent Ca^{2+} channels, and thus relaxation.

Endothelial NO is not only a potent vasodilator but also an effective anti-thrombotic and anti-inflammatory agent (for review, see Förstermann and Sessa (2012)). Through cGMP-dependent inhibition of Ca^{2+} influx and release from intracellular stores, endogenous NO can also inhibit platelet adhesion and aggregation, thus maintaining an

anti-coagulant surface of blood vessels (reviewed by Pober and Sessa (2007)). In addition, NO controls the expression of genes involved in the development of atherosclerosis and by that contributes to quiescence of the resting endothelium. NO inhibits the expression of chemoattractant protein MCP-1 and various surface adhesion molecules, thereby preventing leukocyte adhesion to the endothelium and transmigration into the arterial vessel wall. This preserves the anti-inflammatory state of the blood vessel and confers protection against early phases of atherogenesis. Endothelium-derived NO prevents oxidative modification of low-density lipoprotein cholesterol in the arterial vessel wall, further contributing to its atheroprotective properties. Finally, endogenous NO has also been documented to exert anti-proliferative and anti-migratory effects on vascular SMCs, thereby protecting the vessel wall against vascular lesion formation and neointimal hyperplasia (Jeremy et al. (1999)).

1.1.1 The NO synthases

NO is generated in a vast number of cell types by the three mammalian isoforms of the enzyme NO synthase (NOS), i.e., constitutive neuronal NOS (nNOS/NOS-1), inducible NOS (iNOS/NOS-2) and endothelial NOS (eNOS/NOS-3). Under physiologic conditions, however, NOS-3 is the primary source of EC-derived NO. All three isozymes utilize the amino acid L-arginine as a substrate, and molecular oxygen and reduced nicotinamid adenine dinucleotide phosphate (NADPH) as co-substrates. NOS-3 is a homodimeric protein with each monomer consisting of an N-terminal oxygenase domain, which contains binding sites for heme, L-arginine and the co-factor, tetrahydrobiopterin (BH₄), and a reductase domain with binding sites for NADPH, flavin mononucleotide (FMN), flavin adenine-dinucleotide (FAD) and calmodulin (for review, see Fleming (2010); Förstermann and Sessa (2012)).

NO is enzymatically synthesised through the sequential oxidation of L-arginine to yield equimolar amounts of NO and L-citrulline. During NO synthesis, NADPH-derived electrons are transferred via the flavins (FAD and FMN) in the reductase domain to the heme located in the oxygenase domain. At the heme center, the electrons are used to reduce and activate molecular oxygen, which subsequently oxidizes L-arginine to L-citrulline and NO. Binding of calmodulin is generally accepted to activate the stepwise synthesis of NO by facilitating electron transfer directed from the reductase to the oxygenase domain (reviewed by Fleming (2010); Förstermann and Sessa (2012)).

1.1.2 Regulation of NOS-3 activity

The dynamic adaptation of both NOS-3 activity and expression to the demand is pivotal for the maintenance of vascular tone and the anti-inflammatory state of the endothelium. Although NOS-3 is constitutively expressed, basal synthesis of NO is greatly enhanced

by receptor-dependent agonists such as bradykinin or histamine, as well as in response to hypoxia, an acute increase in shear stress, and other receptor-independent stimuli.

An increase in the intracellular concentration of Ca^{2+} is the common denominator for endothelial NO production as NOS-3 activity is strongly dependent on Ca^{2+} -activated calmodulin. Elevated intracellular Ca^{2+} and its subsequent activation of calmodulin bound to the NOS-3 enzyme (Hemmens and Mayer (1998)) in response to receptor-dependent agonist stimulation disrupts an auto-inhibitory loop (Rafikov et al. (2011)) and facilitates the electron transfer from NADPH in the reductase domain to the heme in the oxygenase domain, hence driving the synthesis of NO.

However, NOS-3 can also be activated by stimuli that do not produce a sustained increase in intracellular Ca^{2+} , the best characterized of which is fluid shear stress (FSS) that is generated by the viscous drag of blood flowing over the EC surface. The FSS-driven phosphorylation of multiple serine residues augments the catalytic efficiency and the sensitivity of NOS-3 to Ca^{2+} leading to sustained activity of the enzyme and NO formation at resting Ca^{2+} levels (reviewed by Fleming (2010); Förstermann and Sessa (2012)).

1.1.3 Shear stress-dependent transcriptional regulation of NOS-3 expression

Besides regulating the activity of NOS-3, blood flow-generated FSS and in particular unidirectional FSS acts as the principal physiologic determinant of *NOS3* gene expression in ECs. In this context, it is noteworthy to emphasize that unidirectional shear stress maintains rather than up-regulates *NOS3* expression while NOS-3 activity is rapidly altered in response to, e.g. an acute increase in unidirectional shear stress.

The signaling pathways involved in the regulation of NOS-3 expression are relatively complex, but important roles have been ascribed to the transcription factors (TFs) nuclear factor-kappa B (NF- κ B) and Krüppel-like factor-2 (KLF-2) in mediating the shear stress-driven increase in *NOS3* transcription (for review, see Balligand et al. (2009)). Nonetheless, the precise temporal and spatial transcriptional mechanism(s) by which unidirectional shear stress regulates *NOS3* expression is still largely unknown. In fact, NF- κ B has been demonstrated to up-regulate *NOS3* gene transcription only upon acute short-term exposure to FSS (i.e., an experimental setting in which ECs cultured under static conditions are suddenly exposed to FSS for seconds to min, generally for <24 hours), which mimics the *in vivo* response of injured or activated endothelium to FSS rather than the effects of physiological shear stress on the endothelium. In addition, *in vitro* experiments done with short-term shear stress stimulation have led to the historical misinterpretation of the "shear-stress-responsive element" found in the promoters of genes induced during the acute response to shear stress (e.g., mostly genes encoding pro-inflammatory proteins such as MCP-1 and ICAM-1), which turned out to be the

NF- κ B binding site (Boon and Horrevoets (2009)). Moreover, although KLF-2 has been postulated as the shear-stress-responsive TF eliciting *NOS3* gene expression under conditions of prolonged laminar flow, to date, there has been no direct demonstration of such a KLF-2-mediated transcriptional mechanism. On the other hand, there is some evidence for a long-term epigenetic regulation of the *NOS3* gene (reviewed by Dunn et al. (2015); Jiang et al. (2015)). It still remains elusive, however, how such a mechanism could contribute to the adaptation of NOS-3 expression to transient alterations in shear stress.

1.2 Hallmark of endothelial dysfunction is the impaired bioavailability of NO

Disturbances in the expression and/or activity of NOS-3 may lead to inadequate NO formation and endothelial dysfunction, a key event in the pathogenesis of vascular diseases such as atherosclerosis. In this regard, atherosclerosis preferentially develops at sites of disturbed blood flow such as bifurcations or curvatures of large conduit arteries. At these atherosclerosis-predilection sites hemodynamics is altered in such a way that unidirectional shear stress largely declines becoming oscillatory because of the disturbed flow pattern at these sites (for review, see Cattaruzza et al. (2012); chapter 3). Consequently, endothelial NO production is strongly diminished as both the expression and activity of NOS-3 are chiefly dependent on the presence of a sufficiently large unidirectional shear stress.

In addition, rhythmic distensions of the vessel wall due to augmented reflections of the arterial pulse wave, e.g., from the protrusion of the bifurcation into the opposite vessel wall, result in elevated cyclic stretching of the cells within the arterial vessel wall. This in turn up-regulates the expression and activity of NADPH oxidases leading to an increased formation of superoxide anions (O_2^-) both in endothelial and smooth muscle cells. Enhanced levels of O_2^- accelerate neutralization of endothelium-derived NO to peroxynitrite ($ONOO^-$) and thus further reduce the bioavailability of NO in atherosclerosis-prone regions. As a consequence, failure of the endothelium to fulfill its homeostatic functions at areas of diminished NO bioavailability can cause permanent pro-inflammatory alterations in the EC phenotype, collectively referred to as endothelial dysfunction, characterized by increased expression of pro-inflammatory gene products and an elevated permeability for leukocytes (Förstermann (2010)).

This inadequate endothelial activation promotes the accumulation of chemokines (e.g., monocyte chemoattractant protein-1 (MCP-1), also known as CCL-2, and CCL-5), cell adhesion molecules (e.g., vascular cell adhesion molecule-1 (VCAM-1) and intercellular cell adhesion molecule-1 (ICAM-1), selectins (e.g., E- and P-selectin) (for review, see

Galkina and Ley (2007)) and pro-inflammatory cytokines (e.g., tumor necrosis factor- α (TNF- α) and interleukin-1 β (IL-1 β)) in ECs, facilitating the recruitment and activation of pro-inflammatory leukocytes. Because of the marked deceleration of blood flow velocity near arterial branch points, circulating leukocytes, mainly granulocytes, monocytes and T cells, are able to adhere and roll over the EC surface and eventually to transmigrate into the sub-endothelial space where they initiate or exacerbate atherosclerotic lesion formation (for review, see Cattaruzza et al. (2012), chapter 3).

1.3 Atherosclerosis

Inflammation is a hallmark of atherosclerosis and a key driving force at each stage of disease development. Both innate and adaptive cellular components of immunity participate in the onset and progression of atherosclerosis.

1.3.1 Role of monocytes/macrophages in atherosclerosis

Atherosclerosis results from a maladaptive inflammatory response driven by the accumulation of lipid-laden macrophages in the arterial wall (for reviews, see Moore and Tabas (2011); Moore et al. (2013); Libby et al. (2013)). Endothelial dysfunction in atherosclerosis-prone regions confers an increased permeability to cholesterol-rich lipoproteins, particularly low-density lipoprotein (LDL), and accumulation of extracellular matrix (ECM) proteins that facilitate the retention of these atherogenic particles in the vessel intima (Figure 1.1). Once infiltrated into the arterial wall, cholesterol-containing lipoproteins undergo various modifications, including oxidation, enzymatic/non-enzymatic cleavage and aggregation, which renders them pro-inflammatory and which triggers local vascular and immune cell responses. The sequestration of lipids in the arterial wall enhances endothelial activation and further promotes the recruitment of circulating monocytes to the vessel wall where they differentiate into macrophages (reviewed by Moore et al. (2013)). The accumulated mononuclear phagocytes ingest oxidized LDL and transform into cholesterol-laden foam cells that play a central role in the formation of early plaques (i.e., fatty streaks).

Lesion macrophages have a diminished capacity to migrate and therefore fail to exit from the inflamed plaque and resolve the ongoing inflammation in the vessel wall. Monocytes continue to enter plaques and differentiate into macrophages, thereby promoting progression of the disease from early lesions to more advanced plaques wherein other immune cell subsets and vascular SMCs become involved in the inflammatory process. In these advanced plaques, activated macrophages perpetuate and amplify the ongoing inflammatory response through secretion of pro-inflammatory mediators (including chemokines, cytokines and reactive oxygen/nitrogen species) and ECM-degrading matrix metalloproteinases (MMPs) in the arterial intima. Many of these foam cells eventually die causing

the accumulation of apoptotic bodies and necrotic debris in the lesion. The impaired phagocytic clearance (i.e., efferocytosis) of apoptotic macrophage debris triggers the formation of a “necrotic” core in evolving plaques. The lipid content and tissue factor released from dying macrophages are pro-thrombotic and may thus contribute to the rupture of the plaque. The rupture site of advanced plaques is usually found in close vicinity to the necrotic core and it is associated with thinning of the protective scar (i.e., fibrous cap) covering the inflamed lesion. Macrophages inhibit collagen synthesis and proliferation of lesion SMCs, which together with macrophage-derived MMPs promote thinning of the fibrous cap and thus the formation of a “vulnerable” (i.e., rupture-prone) plaque.

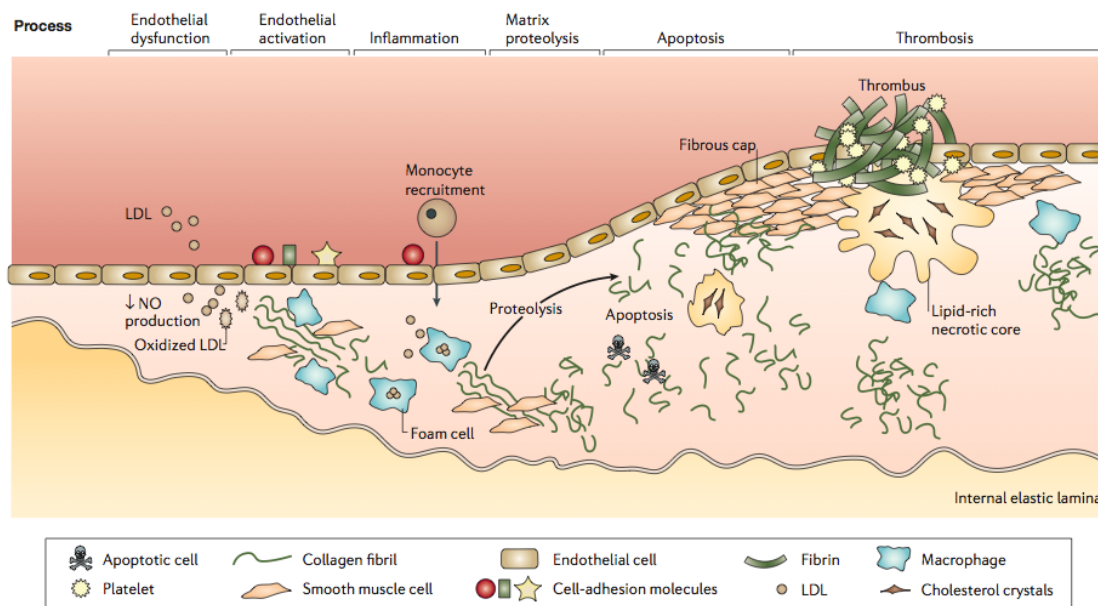


Figure 1.1: Development of an atherosclerotic plaque. A simplified illustration of the processes of atherogenesis: from pre-lesional endothelial dysfunction (left) through monocyte recruitment to thrombotic complication of the advanced plaque (right). Endothelial dysfunction is characterized by reduced production of NO, which promotes the up-regulation of endothelial cell adhesion molecules. Plasma lipoproteins such as LDL and oxLDL accumulate in the subendothelial space. Several types of immune and inflammatory cells are recruited to the atherosclerotic plaque, including monocytes differentiating into macrophages, which take up oxLDL particles resulting in intracellular cholesterol accumulation and subsequent formation of foam cells. An atherosclerotic lesion has a cholesterol crystal-rich necrotic core consisting of living and apoptotic cells covered with a fibrous cap made of smooth muscle cells and collagen. Inflammatory cell infiltration, smooth muscle cell apoptosis and matrix degradation through proteolysis generate vulnerable plaque. Plaque disruption leads to thrombosis, which may cause vessel occlusion (Watkins and Farrall (2006)).

Fissure of the atherosclerotic plaque exposes components of the underlying ECM, namely collagen, to the flowing blood, thus favoring platelet adhesion and activation. Local platelet activation stimulates the further recruitment of platelets to eventually form a

thrombus, which may lead to myocardial infarction (acute coronary syndrome), peripheral occlusion in peripheral arterial occlusive disease, and in some cases to ischemic stroke (for review, see Badimon et al. (2012); Bentzon et al. (2014)).

1.3.2 Role of neutrophils in atherosclerosis

Macrophages, however, are not alone in contributing to atherosclerotic lesion formation. Other crucial players in the initiation and progression of atherosclerosis are the neutrophilic polymorphonuclear leukocytes (i.e., neutrophils) (for review, see Noels and Weber (2011)). A disturbed lipid balance increases the number of circulating neutrophils and facilitates their recruitment to early atherosclerotic lesions (Drechsler et al. (2010)). Upon extravasation, neutrophils release granule proteins (e.g., azurocidin, cathepsin G and LL-37) that trigger monocyte recruitment and extravasation directly or indirectly through up-regulation of endothelial cell adhesion molecules. In addition, apoptotic neutrophils maintain monocyte recruitment by various “find-me” and “eat-me” signals (i.e., signals released (“find-me”) or exposed (“eat-me”) by apoptotic cells that attract phagocytes, such as scavenging macrophages). Activated neutrophils can release nuclear content (i.e., chromatin) that forms a web-like structure containing anti-microbial proteases (e.g., elastase, proteinase-3) referring to as neutrophil extracellular traps (NETs). NETs can be harmful in the context of atherosclerosis. NET formation and proteolysis of the tissue factor pathway inhibitor by neutrophil-derived proteases (Massberg et al. (2010)) could promote atheroprogession and thrombus formation. Furthermore, extracellular cholesterol crystals interact with neutrophils to trigger the release of NETs, which prime macrophages for inflammasome activation and IL-1 β production (the inflammasome is a multi-protein cytoplasmic complex which mediates the maturation and release of pro-inflammatory cytokines such as IL-1 β and IL-18), hence propagating inflammation in murine atherosclerosis (Warnatsch et al. (2015)).

1.3.3 Role of T cells in atherosclerosis

As the fatty streaks evolve into mature atherosclerotic plaques, additional inflammatory and immune cell types such as eosinophils, B cells or mast cells get recruited and contribute to the atherogenic process. In addition, CD4⁺ T cells traffic to the atherosclerotic lesions and there they become the dominant force in enhancing the ongoing inflammatory process. Although most of the cells in the fatty streak are macrophage-derived foam cells, T cells are also present in early lesions and maintain a prominent role at all stages of the disease. Once in the arterial intima, CD4⁺ T cells undergo activation (upon local autoantigens such as oxLDL and HSP60) and differentiate into effector T subsets of the T helper1 (Th1), T helper2 (Th2), T helper17 (Th17) and other lineages, in response to the local milieu of cytokines. Major mediators of the lymphocytic influence on atherogenesis are T cells from the Th1-cell subtype, which differentiate due to IL-12

and IL-18 released by macrophages and SMCs in the plaque. Th1 cells produce high levels of pro-inflammatory cytokines, such as interferon- γ (IFN- γ) and TNF- α , which fuel the inflammatory process by recruiting more monocytes/macrophages and further drive lesion macrophage foam cells to produce more pro-inflammatory mediators and MMPs. Moreover, IFN- γ inhibits vascular SMC proliferation and collagen production, reducing the cell and collagen content of the fibrous cap and thus stability of the plaque. The interaction between activated T cells and macrophages through the co-stimulatory CD40-CD40 ligand dyad, in addition, results in expression of pro-coagulant tissue factor and MMPs contributing to the thinning of the plaque fibrous cap and subsequent plaque rupture (for review, see Galkina and Ley (2009); Noels and Weber (2011); Tse et al. (2013); Ketelhuth and Hansson (2016)).

Similar to Th1 cells, an unusual subset of T cells that lack CD28 and elaborate high levels of IFN- γ and TNF- α has been suggested to modulate atherosclerosis in humans. Nonetheless, their involvement in the cause of the disease remains speculative (for review, see Libby et al. (2013); Tse et al. (2013); Ketelhuth and Hansson (2016)). Additionally, the contribution of Th17 cells and their cytokines to atherosclerosis has been extensively studied. Th17 cells have been proposed to modulate lesion formation and composition. However, various attempts to deplete the expression of IL-17A, the signature Th17 cytokine, and its receptor IL-17RA, yielded conflicting results, obscuring their role in disease development (reviewed by Tse et al. (2013); Ketelhuth and Hansson (2016)).

The heterogeneous role of adaptive T cell immunity in atherogenesis is further demonstrated by the participation of Th2 cells, which seem to have atheroprotective effects (reviewed by Libby et al. (2013); Tse et al. (2013); Ketelhuth and Hansson (2016)). Through secretion of IL-4, IL-5, IL-13 and particularly IL-10, Th2 cells can antagonize the pro-atherogenic immune responses of Th1 cells and thereby confer atheroprotection. Besides opposing Th1 effects and lineage commitment, Th2 cytokines (e.g., IL-4 and IL-5) also influence other cell types implicated in atherogenesis such as mast cells and eosinophils, making their role in atherosclerosis challenging to elucidate. Targeted deletion of Th2 cytokines, IL-5 and IL-13, in mice, accelerates disease progression, suggesting that Th2 cells are atheroprotective (Ketelhuth and Hansson (2016)). On the other hand, studies have shown that IL-4 production exacerbates atherosclerosis through up-regulation of MMPs, cell adhesion molecules and chemokines by vascular cells (Tse et al. (2013)). IL-4 deficiency in hypercholesterolemic mice, conversely, alleviated disease severity (Tse et al. (2013); Ketelhuth and Hansson (2016)), implying a controversial role of Th2 cells in atherosclerosis.

The balance between Th1 and Th2 cells is controlled by other T-lymphocyte subtypes - regulatory T cells (Tregs) (Ait-Oufella et al. (2006)). Tregs are generally defined as T cells that suppress the activation or effector function of other T cells, thus limiting excessive immune responses to maintain immune homeostasis and prevent immunopathology. Tregs carry out their immunosuppressive functions via several mechanisms, including

cell-contact inhibition and/or secretion of anti-inflammatory cytokines such as IL-10 and transforming growth factor (TGF)- β (reviewed in Gotsman et al. (2008)). Studies have reported that IL-10 and TGF- β have atheroprotective properties (Mallat et al. (1999); Caligiuri et al. (2003); Robertson et al. (2003)).

1.4 Endothelial dysfunction in chronic inflammatory diseases

Chronic inflammatory diseases correlate with increased risk of premature cardiovascular mortality due to accelerated atherosclerosis. Increased cardiovascular mortality in patients with rheumatoid arthritis (RA), for example, has been attributed to the greater risk of coronary heart disease (CHD) and myocardial infarction secondary to coronary atherosclerosis in these populations (reviewed by Full et al. (2009); Steyers and Miller (2014); Mason and Libby (2015)). As chronic inflammation plays a central role in the pathogenesis of atherosclerosis, chronic inflammatory diseases and atherosclerosis may share a common pathophysiologic basis that is relevant for their development. In this respect, characterization of shared pathologic features between atherogenesis and systemic inflammatory diseases such as RA, systemic lupus erythematosus (SLE), psoriasis, chronic inflammatory bowel disease, and others, has fuelled intense basic and clinical research. Similar to an atherosclerotic plaque, the pannus tissue in the synovium of an RA joint is characterized by the enhanced expression of cell adhesion molecules and chemokines by locally activated endothelium, which promotes the extravasation of blood-borne pro-inflammatory leukocytes. The up-regulation of cytokines and ECM-degrading proteases, underlying the erosion of cartilage and bone in the RA joint, is also fundamental to the pathogenesis of atherosclerosis. Furthermore, in both diseases, recruited immune cells alter the phenotype of resident cell types, which then become involved into the inflammatory process and tissue destruction (Figure 1.2) (Full et al. (2009)).

Endothelial dysfunction largely contributes to the pathogenesis of both atherosclerosis and rheumatic diseases. Besides, patients with chronic inflammatory diseases (e.g., RA and SLE) manifest endothelial dysfunction rather early in the course of the disease, suggesting that endothelial dysfunction may be the common denominator. Therefore, the mechanisms underlying the development of the two types of diseases may be integrated at the level of the endothelium.

Multiple factors, produced during local vascular and systemic inflammation, including circulating pro-inflammatory cytokines, such as TNF- α and IL-1 β , reactive oxygen species (ROS), oxLDL, autoantibodies, as well as the traditional cardiovascular risk factors – hypertension, diabetes mellitus, dyslipidaemia, and smoking – are strongly linked to endothelial activation and subsequent endothelial dysfunction. Nonetheless,

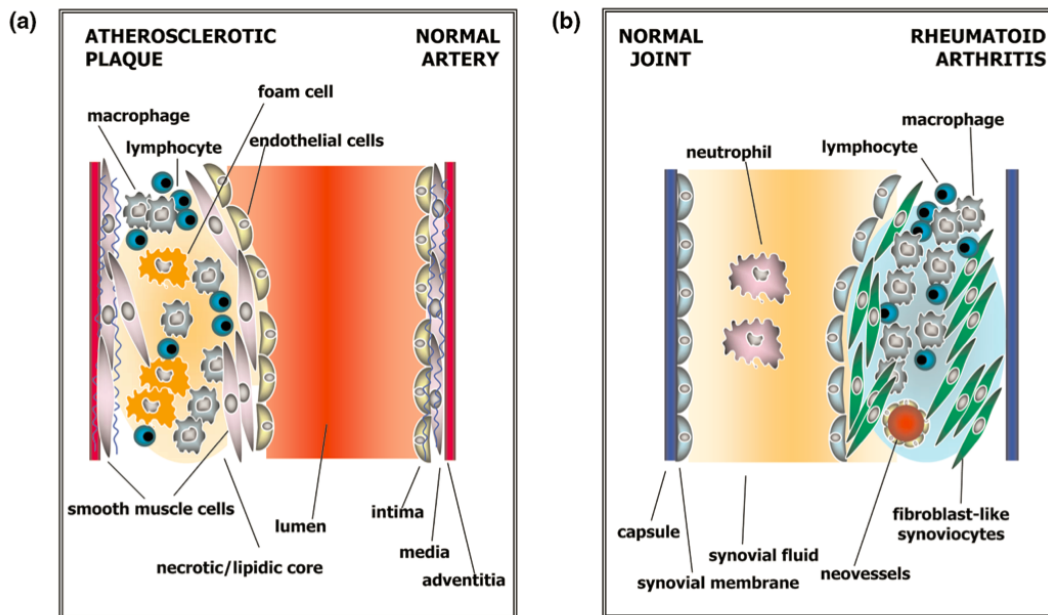


Figure 1.2: The atherosclerotic plaque (a) shares many common features with rheumatoid arthritic synovium (b). Endothelial dysfunction is a hallmark of both atherosclerosis and RA. Persistent endothelial activation associated with chronic systemic inflammation is characterized by reduced production of NO and enhanced expression of cell adhesion molecules and chemokines, resulting in the recruitment of blood-borne mononuclear cells such as monocytes and T lymphocytes. Elevated levels of inflammatory cytokines and MMPs contribute to inflammation and tissue destruction in both atherosclerotic and RA synovitis lesions. Deregulated immune responses against endogenous vascular and synovial cell types underlie both diseases (Full et al. (2009)).

the traditional risk factors alone have proved insufficient to explain the occurrence of cardiovascular morbidity and mortality in patients with rheumatic diseases. It appears that presence of systemic chronic inflammation is the major cause of accelerated endothelial dysfunction in affected individuals.

Cytokine up-regulation is a general characteristic of inflammatory diseases and could be a potential mechanism that links the increased incidence of endothelial dysfunction in patients with chronic inflammatory diseases, including SLE and RA. Several pro-inflammatory cytokines could contribute to the pathogenesis of atherosclerosis (reviewed by Steyers and Miller (2014)). Prolonged exposure of vascular endothelium to circulating TNF- α , a cytokine that plays a primary role in the pathogenesis of RA, for example, leads to impaired endothelium-dependent vasodilation, both in mice and humans. In addition, multiple studies have demonstrated that TNF- α attenuates the expression of NOS-3 and thus reduces the bioavailability of NO in ECs, a critical step linking TNF- α and endothelial dysfunction. Moreover, TNF- α contributes via multiple mechanisms to the increased cell adhesion molecule expression and thus endothelial adhesiveness for pro-inflammatory leukocytes.

Chronic inflammatory diseases are associated with increased oxidative stress. Pro-inflammatory cytokines, in particular TNF- α , are largely responsible for the increased production of ROS in these diseases. As mentioned above, the levels of ROS largely modulate the bioavailability of NO. ROS contribute to the “uncoupling” of NOS-3 activity resulting in an enhanced generation of O₂⁻ and reduced production of NO, thus causing a shift in cellular redox state towards a pro-oxidant, pro-atherogenic environment. Chronic inflammation has also been shown to structurally alter lipoproteins and modify the levels of plasma LDL and high-density lipoprotein (HDL) cholesterol. Elevated ROS production, in addition, promotes the oxidative modification of LDL, which in turn suppresses further the activity of NOS-3, augments the expression of endothelial cell adhesion molecules and intensifies the ongoing inflammation owing to an increased release of TNF- α . In addition, failure of regulatory feedback mechanisms, such as the production of the anti-inflammatory cytokines IL-10 and TGF- β by Tregs, may contribute to the increased cardiovascular burden in patients with rheumatic diseases. Nadkarni et al. demonstrated that in RA patients, CD4⁺CD25⁺ Tregs display defective suppressive functions, which were overcome during an anti-TNF- α therapy. Treatment with anti-TNF- α antibody gave rise to a CD4⁺CD25⁺FoxP3⁺ Treg cell population, which restored the suppression of pro-inflammatory cytokine production via TGF- β and IL-10 (Nadkarni et al. (2007)).

1.5 Genetic susceptibility to atherosclerosis

Atherosclerosis and its main life-threatening manifestations, myocardial infarction, ischemic stroke and heart failure, have become the most frequent cause of death worldwide (Murray et al. (2012); Libby et al. (2013)). Globally, a total number of 17.3 million people die from cardiovascular disease every year, representing 30% of all deaths. Until the manifestation of a full-blown disease, atherosclerosis is clinically silent, hampering its early detection. Scientists must, therefore, identify targets for prevention and early treatment in apparently healthy individuals harboring the disease.

The risk of developing atherosclerosis is shaped by the complex interplay between environmental factors and factors with a genetic component. Although epidemiological studies over the last 60 years have revealed a number of risk factors for atherosclerosis, the primary (and most significant) of which comprise arterial hypertension, cigarette smoking, type 2 diabetes, dyslipidaemia, and systemic chronic inflammation, a causal role has been proven only for some of them (i.e., dyslipidaemia and hypertension). In addition, even though environmental factors such as diet, smoking and sedentary lifestyle play an important role in atherosclerosis development, genetic factors significantly influence susceptibility to the disease. Studies with identical twins and families have documented the importance of genetics in determining the risk of atherosclerosis, revealing that the heritability of atherosclerosis (i.e., the fraction of disease explained by genetics)

exceeds 50%. Technical advances have permitted the unbiased identification of genetic polymorphisms (i.e., single nucleotide polymorphisms or SNPs), candidate genes and susceptibility loci associated with atherosclerosis/cardiovascular disease most recently by using genome-wide association studies (GWAS) (for review, see Lusi (2012)). To date, GWAS has reported a total of 48 loci associated with atherosclerosis and CHD at genome-wide significance, and their number is rapidly increasing (The CARDIoGRAM-plusC4D Consortium, Deloukas et al. (2012) - 45 loci identified; The CARDIoGRAM-plusC4D Consortium, Nikpay et al. (2015) - 48 loci identified). However, genetic variants at these loci explain only a small fraction (i.e., $\sim 10\%$) of the heritability of atherosclerosis/cardiovascular disease. Likely reason for this may be the polygenic nature of genetic determinants, i.e., multiple major genes contributing to manifestation of the disease, and the relatively small observed effect sizes of the identified susceptibility loci. It is therefore possible that many genuinely disease-associated loci do not reach genome-wide significance and are thus not detected because of their very small effect size. Indeed, there has been increasing evidence that multiple causative small-effect loci underlie the large effect of complex traits (i.e., traits derived from the interaction of multiple genes) (Yang et al. (2011)). An additional level of complexity is added by the linkage disequilibrium (LD) existing between disease-associated polymorphisms, i.e., linked inheritance and association between alleles at separate loci. A genetic variant may therefore be linked to a disease, not because it has any effect, but because it is genetically linked with a polymorphism that does. The LD between variants with opposing or additive effects, as well as the different degree of LD between SNPs in different ethnic populations, may further obscure the identification of true effects of disease-associated polymorphisms by GWASs.

The genetic risk of atherosclerosis is partially conferred through the traditional risk factors, including elevated blood pressure, dyslipidaemia, diabetes and obesity, systemic inflammation, etc. (i.e., risk factors with a strong genetic component), however, these factors alone do not account for the entire contribution to the risk of developing atherosclerosis and CHD. Interactions between risk factors could play a decisive role in determining individual's global cardiovascular risk as well (Kovacic and Bakran (2012); Lusi (2012)). For example, the effects of hypertension on CHD progression are markedly augmented if the levels of pro-atherogenic lipoproteins are elevated. Epigenetic changes such as aberrant DNA methylation and histone modification patterns have also proven to be contributing factors in the pathogenesis of atherosclerosis (for review, see Baccarelli et al. (2010); Wierda et al. (2010); Xiong et al. (2015)). As a matter of fact, epigenetics has provided an explanation of how diet, lifestyle and environment may contribute to the development of atherosclerosis and cardiovascular disease.

1.5.1 The T-786C SNP of the *NOS3* gene as a genetic determinant of endothelial dysfunction

Apart from environmental factors influencing endothelial function, intrinsic impairment of the expression or activity of NOS-3 may predispose to or accelerate atherosclerosis and thus CHD, as well as other chronic inflammatory disorders. Accordingly, characterization of genetic alterations and common genetic polymorphisms in the *NOS3* gene may help define genetic risk factors for these diseases. Several polymorphic sites have been described in the human *NOS3* gene, including SNPs, variable number of tandem repeats, microsatellites and insertions/deletions (reviewed by Oliveira-Paula et al. (2016)). Amongst these, the frequent (up to 13% of the Caucasian population) SNP at position -786 (-786 T/C variance; rs2070744) in the *NOS3* gene promoter, which does not occur in other mammals, plays a decisive role (Cattaruzza et al. (2004); Melchers et al. (2006)). This thymine-to-cytosine transition leads to a remarkable decrease in *NOS3* promoter activity, resulting in a reduced NOS-3 expression and endothelial capacity to generate NO (Cattaruzza et al. (2004), Asif et al. (2009a)). Homozygosity for the C-type promoter variant renders the gene largely insensitive to diverse stimuli such as shear stress or IL-10, an anti-Th1 cytokine known to maintain NOS-3 expression in ECs under pro-inflammatory conditions (Cattaruzza et al. (2003); Cattaruzza et al. (2004)). Consequently, individuals homozygous for the C-variant develop endothelial dysfunction and have an increased risk of contracting cardiovascular (Nakayama et al. (1999); Nakayama et al. (2000); Miyamoto et al. (2000); Colombo et al. (2003); Rossi et al. (2003), Cattaruzza et al. (2004)) and rheumatic diseases (Melchers et al. (2006); An et al. (2012); Löffers et al. (2015)). In particular, the promoter polymorphism is an independent predictor for chronic vascular inflammation such as e.g., CHD or hypertension-induced arterial remodeling as well as chronic inflammation of the joints with secondary involvement of vasculature like e.g., RA, polymyalgia rheumatica, systemic sclerosis; or systemic diseases with primary manifestation in the skin such as, e.g., psoriasis. Association with these diseases, however, holds true for Caucasians only, presumably because of the interethnic differences in the prevalence of the SNP. Thus, the T-786C SNP is much more prevalent in the Caucasian population as compared to Asians and Africans (Tanus-Santos et al. (2001)).

Increased NOS-3 expression is one mechanism through which IL-10 (i.e., a cytokine which is generally elevated in patients with RA) exerts its anti-inflammatory effects in chronic inflammatory diseases (Cattaruzza et al. (2003)). Exposure to IL-10 up-regulates endothelial NOS-3 expression through binding of the TF signal transducer and activator of transcription-3 (STAT-3) to a STAT consensus motif at position -856 to -830 in the *NOS3* promoter, which is less than 50 nucleotides upstream of the T-786C SNP. In the C-type promoter this STAT-3 binding site, although not directly altered, has proven to be insensitive to IL-10 (Melchers et al. (2006)). As a functional consequence, CC-genotype ECs do not provide sufficient NO-mediated protection against pro-inflammatory stimuli

in response to IL-10. Accordingly, the inability of CC-genotype endothelium to maintain sufficient NO production under pro-inflammatory conditions promotes endothelial dysfunction, thereby increasing the risk of contracting RA (Melchers et al. (2006)) and other rheumatic diseases (Löffers et al. (2015)) by individuals homozygous for the -786C allele.

Interestingly, even though homozygosity for the -786C allele associates with chronic inflammatory disorders, manifestation of these diseases does not seem to occur prematurely nor is the course of the diseases more severe as compared to patients without this genetic defect (Cattaruzza et al. (2004); Colombo et al. (2003); Rossi et al. (2003); Melchers et al. (2006)). Moreover, GWASs have failed to associate the T-786C SNP with any of the aforementioned diseases, pointing to the existence of a mechanism(s) in CC-genotype carriers to compensate for the inadequate endothelial NO synthesis.

In fact, exclusively in ECs from CC-genotype individuals our group discovered that FSS up-regulates expression of manganese-containing superoxide dismutase (SOD-2), a mitochondrial enzyme, which scavenges superoxide anions (Asif et al. (2009a); Asif et al. (2009b)). This genotype-dependent increase in SOD-2 levels was brought about by the increased activity of the NO-sensitive TF Egr1, the expression of which was up-regulated only in CC-genotype ECs challenged with FSS. Such an increase in cellular SOD-2 content may account for the greater resistance of CC-genotype ECs to oxidative stress, substantiated by the significantly higher superoxide anion-quenching capacity of these cells upon exposure to FSS than that of cells derived from TT-genotype individuals (Asif et al. (2009a)). Up-regulation of NO-protective anti-oxidant enzymes can therefore constitute a common compensatory mechanism in dysfunctional CC-genotype ECs by which the smaller amounts of NO synthesized by these cells are better protected against neutralization by superoxide anions, and as a result maintain a critical level of bioavailable NO.

Furthermore, in endothelial cells homozygous for the -786C allele of the *NOS3* gene, our group recently uncovered an enhanced FSS-dependent formation and release of the anti-inflammatory prostanoid, 15-deoxy- $\Delta^{12,14}$ -prostaglandin J₂ (15d-PGJ₂), which potentially underlies a second mechanism compensating for the reduced bioavailability of NO and its atheroprotective properties in these cells.

1.6 Prostanoids

Prostaglandins (PGs) and thromboxane A₂ (TXA₂), collectively referred to as prostanoids, comprise a large group of structurally related lipid autacoids produced by cells in response to various extrinsic stimuli to sustain homeostatic functions as well as to modulate pathologic processes (for review, see Ricciotti and FitzGerald (2011); Surh et al. (2011)). Prostanoids derive from the 20-carbon poly-unsaturated fatty acid, arachidonic

acid (AA), released from membrane phospholipids by phospholipase A₂ (PLA₂). The rate-limiting step in prostaglandin biosynthesis is the conversion of AA to the unstable endoperoxide intermediate, prostaglandin H₂ (PGH₂), by cyclooxygenases 1 and 2 (COXs). COXs are bifunctional enzymes that comprise both a cyclooxygenase and a peroxidase activity and exist in two isoforms, constitutive COX-1 and inducible COX-2. Although COX-1 has initially been postulated to fulfil mainly housekeeping functions, and COX-2 to be the primary source of prostanoid formation during inflammation, today both enzymes are known to contribute to the generation of homeostatic prostanoids but also to prostanoid release upon inflammatory signals. PGH₂ is subsequently metabolised to a series of bioactive prostanoids, including prostaglandin D₂ (PGD₂), PGE₂, PGF₂ α , prostacyclin (PGI₂), and thromboxane A₂, through the action of specific isomerases referred to as PG synthases (Figure 1.3).

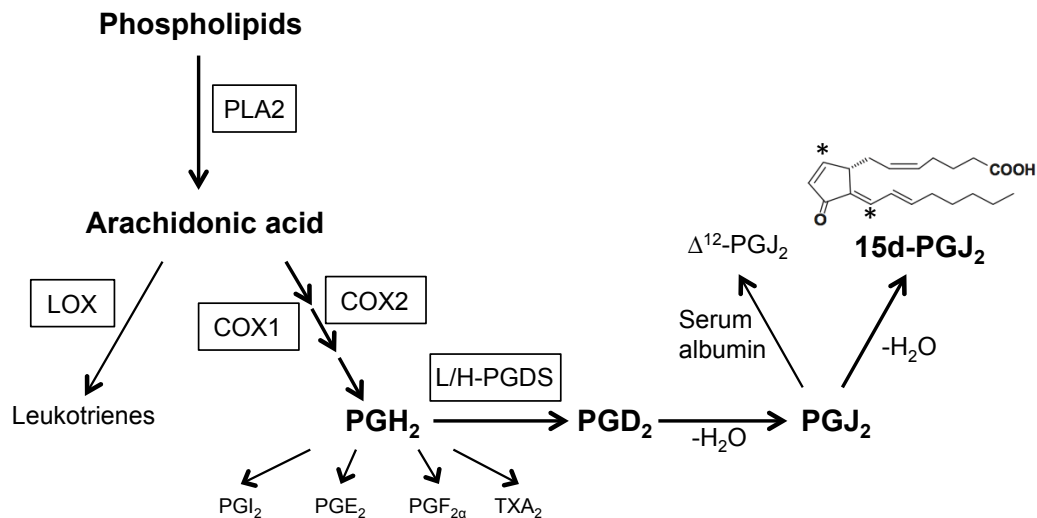


Figure 1.3: Biosynthesis of 15d-PGJ₂. Phospholipase A₂ catalyzes the hydrolysis of membrane phospholipids to produce arachidonic acid (AA). Cyclooxygenases (COX-1 and COX-2) or lipoxygenases (LOX) convert AA to prostanoids or leukotrienes, respectively. PGD₂ is non-enzymatically converted into prostaglandins of the J₂ series in a serum albumin-dependent or independent manner. PGJ₂ undergoes spontaneous dehydration to yield 15d-PGJ₂. Asterisks indicate positions of the reactive carbon centers in the 15d-PGJ₂ molecule.

Prostanoids are ubiquitously produced and act as autocrine or paracrine lipid mediators to maintain local homeostasis in the body. Each cell type generates usually one or two dominant prostanoid products exerting effects on various biological processes, including regulation of vascular and non-vascular SMC tone, platelet aggregation, mediating inflammation and allergic reactions, modulation of nerve cell functions, etc. Furthermore, both the levels and the spectrum of prostanoids change profoundly during inflammation. PG production is generally kept very low in uninflamed tissues but rises dramatically upon acute inflammation prior to the recruitment of immune cells. The

profile of prostanoid production is determined by the differential expression of PG synthases within cells present at the site of inflammation or, in general, within cell types of a particular tissue. Alterations in the profile of prostanoid synthesis occur also during cellular activation. For example, upon exposure to bacterial lipopolysaccharide, PGE₂ becomes the predominant prostanoid over TXA₂ in activated macrophages, whereas the production of TXA₂ prevails in resting cells (Tilley et al. (2001)).

PGs exert their effects by activating the prostanoid G protein-coupled heptahelical membrane receptors (GPCRs) consisting of eight members, i.e., the EP1, EP2, EP3 and EP4 subtypes of the PGE₂ receptor (E prostanoid receptor), the PGD₂ receptor DP1, the PGF₂α receptor (FP), the PGI₂ receptor (IP), and the TXA₂ receptor (TP) (reviewed by Alfranca et al. (2006); Ricciotti and FitzGerald (2011)). In addition, a ninth receptor, the DP2 receptor, also known as chemoattractant receptor-homologous molecule expressed on T helper 2 cells (CRTH2) receptor, also responds to PGD₂ but belongs to the large family of chemokine receptors. Prostanoid receptors elicit a broad range of intracellular signalling pathways depending on what type of G protein they are coupled to. For example, EP2 receptor signalling can be coupled to adenylyl cyclase activation through G_s, thereby elevating intracellular cyclic adenosine monophosphate (cAMP). EP1 receptor ligation can trigger activation of phospholipase C through G_q and activation of protein kinase C and mobilization of intracellular Ca²⁺ as a result of phosphatidylinositol-4,5-bisphosphate metabolism. Several prostanoids could also stimulate activation of small Rho GTPase signalling, for example by binding to the TP, EP3 or FP receptors. Generally, the same prostanoid receptor can induce different signalling pathways based on the G protein they act through. On the other hand, different isoforms of the same receptor can exert opposing effects by activating or inhibiting the same signalling pathway. Finally, some prostanoids are capable of binding to different receptors with distinct affinity (e.g., PGD₂, as well as its dehydration derivative, 15d-PGJ₂, bind to both DP1 and DP2). Hence, depending on which of its cognate receptors are locally expressed, one prostanoid can activate multiple signalling pathways and thus exert different biological effects.

1.7 Aims of the thesis

The shear stress-dependent expression of endothelial NO synthase (NOS-3) is central to vascular homeostasis. Disturbances in the expression and/or activity of this enzyme may therefore lead to insufficient NO formation and endothelial dysfunction, a key event in the pathogenesis of vascular diseases such as atherosclerosis. Endothelial dysfunction has been recognized as the common denominator of cardiovascular and rheumatic diseases that is relevant to the pathogenesis of both types of inflammatory disorders. In this context, a common genetic variant of the *NOS3* gene, i.e. a T to C transition at position -786 of the promoter of the gene, predisposes to endothelial dysfunction and

has proven to be an independent and strong predictor for both coronary heart disease and rheumatoid arthritis in conventional association studies. However, compensatory mechanisms minimizing the effects of this single nucleotide polymorphism (SNP) have limited the early onset of these diseases and could therefore constitute a general strategy to prevent endothelial dysfunction. One such mechanism involves the increased expression of the superoxide anion-scavenging enzyme, SOD-2, in homozygous carriers of the T-786C SNP, thereby better protecting the low amounts of NO produced by endothelial cells of these individuals. Furthermore, a striking increase in the release of the anti-inflammatory prostanoid 15d-PGJ₂ by ECs derived from individuals homozygous for the -786C-allele in response to fluid shear stress was noted, which provided the starting point for this thesis. Its main aims can be summarized as follows:

1. To characterize the function of the anti-inflammatory 15d-PGJ₂ in clonally expanded endothelial cells from individuals homozygous for the T-786C SNP of the *NOS3* gene.
2. To establish an *in vitro* transmigration assay to study the interactions between atherosclerosis-related leukocytes (monocytes and T cells) and TT or CC-genotype ECs.
3. To investigate the molecular mechanisms underlying the anti-inflammatory activity of endothelial cell-derived 15d-PGJ₂ in monocytes.
4. To evaluate the clinical relevance of 15d-PGJ₂ in patients with coronary heart disease.

2.1 Chemicals and reagents

TABLE 2.1: Chemicals and reagents

Chemical/reagent	Supplier
Agar	Roth
Agarose	Sigma-Aldrich
Ampicillin	Sigma-Aldrich
Ammoniumpersulfate	Roth
Bacto-tryptone	BD
Boric acid	Sigma-Aldrich
Bovine Serum Albumin	Sigma
Chemiluminescence substrate Luminata™ Forte	Merck Millipore
Deoxyribonuclease I	Worthington
DNA from herring sperm	Sigma-Aldrich
DNA ladders	Thermo Scientific
D-PBS	Gibco, Life Technologies
Disodium hydrogen phosphate	Roth
Dispase	Gibco, Life Technologies
Dithiothreitol (DTT)	Roth
EDTA	AppliChem
EGTA	Roth
Ethidium bromide	Roth
Fixable Viability Dye eFluor® 780	eBioscience
Fungizone	Gibco, Life Technologies
Gelatin	Merck
Glucose	Merck

Glycine	Sigma Aldrich
Heat-inactivated fetal bovine serum (FCS)	Gibco, Life Technologies
HEPES	Sigma
KCl	AppliChem
Leupeptin A	Sigma
L-glutamine	Life technologies
Magnesium chloride	AppliChem
Magnesium sulfate	AppliChem
Methanol	Sigma-Aldrich
M-MLV reverse transcriptase	Promega
Nonidet-P-40	Fluka
N-Z-Amine [®] A	Sigma
Oligo dT	Promega
Paraformaldehyde	Sigma
Penicillin	Gibco, Life Technologies
Pefabloc	Fluka
Pepstatin A	Sigma
Polyacrylamide	Roth
Potassium dihydrogen phosphate	Riedel-de Haën
Precision Plus Protein Dual Color Standard [™]	BioRad
Paraffin Paraplast [®] Plus [™]	Leica
Sodium dodecyl sulfate (SDS)	Serva
Sodium chloride	Sigma Aldrich
Sodium hydrogen carbonate	J.T.Baker
Streptomycin	Gibco, Life Technologies
Sodium hydroxide	Sigma Aldrich
Sodium orthovanadate	Sigma
TEMED	Roth
Trypsin	Gibco, Life Technologies
Tween 20	Roth
Tris	Roth
Triton-X 100	Sigma
Taq polymerase	Bioron
Yeast extract	Roth

2.2 Kits

TABLE 2.2: Kits

Kit	Cat. No.	Supplier
NucleoSpin [®] Plasmid extraction kit	740588	Macherey-Nagel
NucleoBond Xtra Maxi EF kit	740424	Macherey-Nagel
NucleoSpin [®] RNA extraction kit	740955	Macherey-Nagel
QuikChange II XL Site-directed mutagenesis kit	200521	Stratagene, Agilent Technologies
QuantiTect SYBR Green [®] PCR kit	204143	Qiagen
Naïve CD4 ⁺ T Cell Isolation kit II	130-094-131	Miltenyi Biotec
Dead Cell Removal kit	130-090-101	Miltenyi Biotec
Pierce [™] Gaussia Luciferase Glow Assay kit	16160	Thermo Fisher Scientific
Viromer [®] GREEN, transfection kit	VG-01LB-00	Lipocalyx GmbH
Lipofectamine [®] 3000, transfection reagent	L3000008	Thermo Fisher Scientific
MATra-si, transfection reagent	7-2021-020	IBA-Life Sciences
15d-PGJ ₂ ELISA kit	ADI-900-023	Enzo Life Sciences

2.3 Consumables

TABLE 2.3: Consumables

Material	Supplier
Bacterial culture round-bottom tubes	Sarstedt
Cell culture dishes	TPP
Cell culture flasks (T-25, T-75)	Sarstedt
Cell culture plates	Sarstedt, Greiner
Filter papers	Munktell
PCR tubes	Sarstedt
Pipette tips	Sarstedt
Serologic pipettes	Sarstedt
PVDF transfer membranes Immobilon [®] -P	Merck Millipore
SafeSeal Micro tubes	Sarstedt
Sterile filters	GE Healthcare

2.4 Equipment

TABLE 2.4: Equipment

Equipment	Model	Supplier
Universal power supply	PowerPack P25	Biometra
Bacterial incubator	Innova 4230	New Brunswick Scientific
CO ₂ incubator	Innova CO-170	New Brunswick Scientific
CO ₂ incubator	BB-16	Heraeus Instruments
Laminar flow hood	HS18 Hera safe	Heraeus Instruments
Real-Time PCR system	LightCycler 1.5	Roche
Digital Imaging System	ImageQuant LAS 4000 mini	GE Healthcare
NanoDrop Spectrophotometer	ND-1000	Thermo Fisher Scientific
PCR cyclor	Thermocycler	Biometra
Microplate spectrophotometer	PowerWave XS	BIO-TEK
Power supply for electrophoresis and blotting	PowerPac TM HC	BioRad
SDS-PAGE system	Mini-Protean [®] Tetra Cell	BioRad
Sonicator	UP50H	Dr. Hielscher GmbH
Mini Trans-blot [®] Cell	Mini-Protean	BioRad
Agarose gel imager	Gel Doc TM XR System	BioRad
Luminescence plate reader	MicroLumat LB 96P	Berthold Technologies
Orbital shaker	PSU-10i	Biosan, SIA
Plate-and-cone viscometer		Martin-Luther University Halle-Wittenberg
Refrigerated centrifuge	Z323K	HERMLE
Centrifuge	Universal 32	Hettich Zentrifugen
Mini centrifuge	SPROUT TM	Biozym
Table top centrifuge	Pico 21	Heraeus
Table top refrigerated centrifuge	Mikro22R	Hettich Zentrifugen
Light microscope	Axiovert 25 (inverted)	Carl Zeiss
Light microscope	CKX41 (inverted)	Olympus

2.5 Oligonucleotides

TABLE 2.5: RT-PCR primers

Gene product	Primer sequence	T _{Annealing}
Human HO-1	For 5'-CAGTCAGGCAGAGGGTGATA-3' Rev 5'-GCTCTGGTCCTTGGTGTCAT-3'	58°C

TABLE 2.6: qRT-PCR primers

Gene product	Primer sequence	T _{Annealing}
Human IL-1 β	For 5'-TGGAGCAACAAGTGGTGT-3' Rev 5'-TGGGATCTACTCTCCAGC-3'	60°C
Human RPL32	For 5'-AGGCATTGACAACAGGGTTC-3' Rev 5'-GTTGCACATCAGCAGCACTT-3'	56°C
Human HPRT-1	For 5'-CAAGCTTGCTGGTGAAAAGGAC-3' Rev 5'-GTCAAGGGCATATCCTACAACAAA-3'	60°C
Human Bach-1	For 5'-TGCGATGTCACCATCTTTGT-3' Rev 5'-CCTGGCCTACGATTCTTGAG-3'	60°C
Human IL-8	For 5'-TGTAAGCTTTCTGATGGA-3' Rev 5'-CTCTTCAAAACTTCTCC-3'	58°C
Human IL-6	Proprietary (Hs_IL6_1.LSG-QiantiTect Primer assay #QT00083720) (Qiagen)	55°C
Human Keap-1	For 5'-GGAGTGTTACGACCCAGATA-3' Rev 5'-AGAAACAAAAGTGCCTCAAC-3'	60°C
Human L-PGDS	For 5'-GCTTCACAGAGGATAACCATT-3' Rev 5'-GAAGGAACAGAGCAGAGACA-3'	60°C
Human GAPDH	For 5'-CCACTCCTCCACCTTTGAC-3' Rev 5'-ACCCTGTTGCTGTAGCCA-3'	60°C
Human Nrf-2	For 5'-AAACCAGTGGATCTGCCAAC-3' Rev 5'-GACCGGGAATATCAGGAACA-3'	56°C
Human CD40	For 5'-GCATGCAGAGAAAAACAGTACCT-3' Rev 5'-GTGCAGTCACTCACCAGTTTCT-3'	60°C

TABLE 2.7: Genotyping primers

Gene	Primer sequence	T _{Annealing}
T-786C NOS3 SNP	For 5'-GAGTCTGGCCAACACAAATCC-3' Rev 5'-GACCTCTAGGGTCATGCAGGT-3'	60°C

TABLE 2.8: ChIP primers

Gene	Primer sequence	T _{Annealing}
Human <i>IL-1B</i> ChIP	For 5'-GAGTCTGGCCAACACAAATCC-3' Rev 5'-GACCTCTAGGGTCATGCAGGT-3'	55°C

TABLE 2.9: Mutagenesis primers

Gene	Primer sequence	T _{Annealing}
Δ ARE1 (7831–7834)	Sense 5'-GGAAAACAATGCATATTTGCATGT ACATTTGCAAAATGTGTCATAG -3' Anti-sense 5'-CTATGACACATTTTGCAAATGTA CATGCAAATATGCATTGTTTTCC -3'	60°C
Δ ARE2 (7896–7899)	Sense 5'-CCATGAACCAGAGAATTATGTTTA TTAGTCCCCCTCCCC -3' Anti-sense 5'-GGGGAGGGGACTAATAAACATA ATTCTCTGGTTCATGG-3'	60°C
Δ ARE3 (7995–7998)	Sense 5'-GAAATCAGGTATTCAACAGAGAAA TTTGCCCTCCTACTTCTG-3' Anti-sense 5'-CAGAAGTAGGAGGCAAATTTCT CTGTTGAATACCTGATTTC-3'	60°C

TABLE 2.10: Decoy oligodeoxynucleotides - *indicate phosphorothioate groups

Gene	Primer sequence
Egr1 dODN	5'- A*C*ATGTGGGGGCGTGAT*G*T-3' 5'- A*C*ATCACGCCCCCACAT*G*T-3'
Egr1 mutODN	5'- A*C*ATGTGTAGTAGTGAT*G*T-3' 5'- A*C*ATCACTACTACACAT*G*T-3'

TABLE 2.11: EMSA oligodeoxynucleotides

Gene	Primer sequence	Supplier
NF-E1 consensus	5'- TGGGGAACCTGTGCTGAGTCACTGGAG-3' 3'-ACCCCTTGGACACGACTCAGTGACCTC-5'	Santa Cruz (sc-2527)
NF-E2 mutant	5'- TGGGGAACCTGTGCTAGGTCAGTGGAG-3' 3'-ACCCCTTGGACACGATCCAGTGACCTC-5'	Santa Cruz (sc-2528)

2.5. Oligonucleotides

TABLE 2.12: Small interfering RNAs

Gene	Target sequence	Supplier
Bach-1 siRNA (human)	5'-CCCGACAACATTTGTTATGCA-3'	Qiagen Hs_BACH1_2 SI00309876
Nrf-2 siGenome TM SMART Pool (human)	5'-GAGAAAGAAUUGCCUGUAA-3' 5'-CCAAAGAGCAGUUCAAUGA-3' 5'-UAAAGUGGCUGCUCAGAAU-3' 5'-UGACAGAAGUUGACAAUUA-3'	Dharmacon TM M-003755-02
siGenome TM Control Non-targeting Pool #2	5'-UAAGGCUAUGAAGAGAUAC-3' 5'-AUGUAUUGGCCUGUAUUAG-3' 5'-AUGAACGUGAAUUGCUCAA-3' 5'-UGGUUUACAUGUCGACUAA-3'	Dharmacon TM D-001206-14-05
Keap-1 Stealth RNAi TM duplex siRNA (human)	Sense strand 5'-UGGCUGUCCUCAAUCGUC UCCUUUA-3' Anti-sense strand 5'-UAAAGGAGACGAUUGA GGACAGCCA-3'	Invitrogen KEAP1 HSS190639
L-PGDS siRNA (human)	Sense strand 5'-CACAAUAAACUCCGGAAGC AAUU-3' Anti-sense strand 5'-UUGCUCUCCGGAGUUUA UUGUGUU-3'	Thermo Scientific AKDA-000009
scambled L-PGDS siRNA	Sense strand 5'-GACACUGACAACAACCAUA GAUU-3' Anti-sense strand 5'-UUCUAUGGUUGUUGUC AGUGUCUU-3'	Thermo Scientific AKDA-000011
AllStar Negative Control siRNA	Proprietary	Qiagen SI03650318

2.6 Antibodies

TABLE 2.13: Primary antibodies

Antibody	Supplier	Reference	Dilution
Rabbit monoclonal α -Nrf-2 [EP1808Y]	Abcam	ab62352	1:2000 WB ¹
Rabbit polyclonal α -Nrf-2	Santa Cruz	sc-722X	1:500 ChIP ²
Mouse monoclonal α -HO-1	BD	#610712	1:1000 WB
Rabbit polyclonal α -Keap-1	ProteinTech	#10503-2-AP	1:2000 WB
Rabbit polyclonal α - α -tubulin	Cell signaling	# 2144	1:3000 WB
Rabbit polyclonal α -histone H3	Abcam	ab1791	1:3000 WB
PE-conjugated mouse α -CD3 Human	BD Pharmingen	#561803 Clone: HIT3a	10 μ l/test FC ³
FITC-conjugated mouse α -CD4	BD Pharmingen	#561005 Clone: RPA-T4	10 μ l/test FC
APC-conjugated mouse α -CD45RA	BD Pharmingen	#561884 Clone: HI100	10 μ l/test FC
APC/Cy7-conjugated mouse α -CD62L	BioLegend	#304813 Clone: DREG-56	5 μ l/test FC
APC-conjugated mouse α -IL-4	BD Pharmingen	#561223 Clone:	5 μ l/test FC
APC-conjugated mouse IgG1 κ isotype control	BD Pharmingen	#550854 Clone: MOPC-21	20 μ l/test FC
PE/Cy7-conjugated mouse α -IFN gamma	eBioscience	#25-7319 Clone: 4S.B3	5 μ l/test FC
PE/Cy7-conjugated mouse IgG1 κ isotype control	eBioscience	#25-4714 Clone: P3.6.2.8.1	5 μ l/test FC
Purified NA/LE rat α -IL-4	BD Pharmingen	#554481 Clone: MP4-25D2	5 μ g/ml Neutralization

TABLE 2.14: Secondary antibodies

Antibody	Supplier	Reference	Dilution
Goat α -rabbit peroxidase	Sigma	A6154	1:5000–1:10.000 WB
Goat α -mouse peroxidase	Sigma	A4416	1:5000 WB

¹WB: Western blot²ChIP: Chromatin Immunoprecipitation³FC: Flow cytometry

2.7 Stimulants and inhibitors

TABLE 2.15: Stimulants and inhibitors

Product	Concentration	Reference	Supplier
BWA868C, DP-1 antagonist	0.2 μ M	12060	Cayman Chemicals
CAY10471, DP-2 antagonist	1 μ M	10006735	Cayman Chemicals
GW9662, PPAR- γ antagonist	10 μ M	M6191	Sigma-Aldrich
SC-514, IKK β inhibitor	50 μ M	SML-0557	Sigma-Aldrich
C646, p300/CBP inhibitor	10 μ M	SML-0002	Sigma-Aldrich
Trichostatin A, HDAC inhibitor	1 μ M	T8552	Sigma-Aldrich
Bardoxolone-methyl (CDDO methyl ester)	50 nM	11883	Cayman Chemicals
15d-PGJ ₂	10 μ M	BML-PG050-0001	Enzo Life Biosciences
D,L-Sulforaphane	0.5-1 μ M	S4441	Sigma-Aldrich
Interleukin-2	50 U/ml	202-IL-010	R&D Systems
Interleukin-12	2.5 ng/ml	219-IL-005	R&D Systems
TNF- α	1000 U/ml	50435	Biomol GmbH
Anti-CD3/CD28 T cell activator Dynabeads [®]	1:1 cell-to-bead ratio	11161D	Gibco, Life Technologies
CCL5/RANTES	100 ng/ml	278-RN-010	R&D Systems
CCL-2/MCP-1	30 ng/ml	279-MC-010	R&D Systems
Protein transport inhibitor cocktail (500X)	BrefeldinA 10.6 μ M Monensin 2 μ M	00-4980	eBioscience

2.8 Growth media, buffers and solutions

TABLE 2.16: List of growth media used for mammalian/bacterial cell growth and transfection

Media	Purpose	Composition
Growth medium	Propagation of HUVECs	Endothelial cell basal medium (PromoCell) + 5% FCS + Penicillin/Streptomycin/Fungizone + supplement (without hydrocortisone)
Growth medium	Propagation of THP-1 cells and primary T cells	RPMI 1640 (1x) + GlutaMAX TM + Penicillin/Streptomycin/Fungizone + HEPES + 10% FCS
LB agar	Propagation of bacteria	1.5% (w/v) Agar in LB medium + 100 μ g/ml ampicillin
LB medium	Propagation of bacteria	1.0% Bacto TM Trypton + 0.5% (w/v) Yeast extract + 1.0% (w/v) NaCl
NZY⁺ broth	Propagation of XL10-Gold ultracompetent bacteria	10 g NY amine (casein hydrolysate) + 5 g Yeast extract + 5 g NaCl H ₂ O to 1 l Supplement freshly with: 12.5 ml MgCl ₂ ·6H ₂ O 12.5 ml MgSO ₄ ·7H ₂ O 20 ml of 20% (w/v) glucose
Opti-MEM[®] Reduced Serum Media	Cationic lipid transfection	Gibco, Life Technologies

TABLE 2.17: List of buffers and solutions

Buffer	Composition
Agarose gel electrophoresis loading buffer	10 mM Tris HCl, pH=7.5 10 mM EDTA, pH=8.0 30% Glycerol 0.01% Bromophenol blue 0.01% Xylene green
Blocking buffer for WB	4-5% milk powder or Blotto [®] in TBST
DNase I solution	0.5% (w/v) solution in PBS
dODN hybridization buffer	10 mM Tris-HCl, pH=7.0 1 mM EDTA 150 mM NaCl
FACS buffer	PBS supplemented with: 5% FCS 0.5% BSA 0.05% Na ₃ N
IC Fixation buffer	eBioscience, # 00-8222
MACS buffer	PBS supplemented with: 0.5% (w/v) BSA 2 mM EDTA
Lysis buffer (whole cell lysates)	10 mM HEPES, pH=7.9 10 mM KCl 0.1 mM EDTA 0.1 mM EGTA 1 mM DTT 1 mg/ml Pefabloc 12 μ l/ml Protease inhibitor mix 20 mM Na ₃ VO ₄ 15 mM NaF
Lysis buffer I for nuclear extraction	10 mM HEPES, pH=7.9 10 mM KCl 0.1 mM EDTA 0.1 mM EGTA 0.15% Nonidet-P-40 Supplement freshly with: 20 mM Na ₃ VO ₄ 15 mM NaF 1 mM DTT 1 mg/ml Pefabloc 12 μ g/ml Protease inhibitor mix

Lysis buffer II for nuclear extraction	20 mM HEPES, pH=7.9 400 mM NaCl 1 mM EDTA 1 mM EGTA 0.5% Nonidet-P-40 Supplement freshly with: 20 mM Na ₃ VO ₄ 15 mM NaF 1 mM DTT 1 mg/ml Pefabloc 12 μg/ml Protease inhibitor mix
Pefabloc	15 mM HEPES Puffer, pH=7.4 4% Pefabloc-SC
Permeabilization buffer (10×)	eBioscience, # 00-8333
Phosphate-buffered saline (PBS)	8.0 g NaCl 0.2 g KCl 1.44 g Na ₂ HPO ₄ 0.2 g KH ₂ PO ₄
Protease inhibitor mix (PIM)	1% Pepstatin A in 20% DMSO und 80% 15 mM HEPES, pH=7.4 1% Leupeptin in 20% DMSO und 80% 15 mM HEPES, pH=7.4
SDS-PAGE running buffer	25 mM Tris HCl, pH=8.3 192 mM Glycine 0.1% SDS 5× TBE buffer 450 mM Tris 450 mM Boric acid 20 mM EDTA, pH=8.0
TBST	0.05% Tween 20 in TBS
Tris-buffered saline (TBS)	6.1 g Tris (0.5 M) 8.75 g NaCl (1.5 M) to 1 liter H ₂ O
Wet Blotting buffer (Towbin buffer)	25 mM Tris 192 mM Glycine, pH 8.3 20% Methanol

3.1 Cell biology methods

3.1.1 Cell isolation and culture

3.1.1.1 Isolation and culture of human umbilical vein endothelial cells (HU-VECs)

The isolation and culture of ECs from fresh human umbilical cords were approved by the local ethics committee. In brief, the two ends of the umbilical vein were cannulated and blood was flushed out with 20 ml of D-PBS buffer. The endothelial cells were dislodged using Dispase solution (3.1 g/l) by filling the cords through the cannula and tying up the two ends. The cords filled with the Dispase solution were incubated at 37°C for 30 min. Finally, the contents were emptied into a 50 ml Falcon tube. The vein was flushed with D-PBS buffer to collect the remaining cells. The tube was centrifuged for 5 min at 1000 rpm (160×g). The cell pellet was re-suspended in endothelial cell growth medium. The cells were routinely grown on 2% (w/v) gelatin-coated 60-mm polystyrene dishes or Collagen I-coated Transwell[®] inserts at 37°C in a 5% CO₂ atmosphere. Cells passaged once (P1) were used in all experiments.

3.1.1.2 Isolation of human naïve CD4⁺ T cells

Buffy coat preparations from whole blood supplemented with anti-coagulants (citrate-phosphate dextrose, citrate and/or ACD-A) were obtained from the DRK-Blutspendedienst Baden-Württemberg-Hessen in Mannheim, Germany. Peripheral blood mononuclear cells (PBMCs) were isolated by gradient-density centrifugation using the T cell separation medium Pancoll human (density 1.077 g/ml, PAN-Biotech) at 500×g for

30 min at 20°C in a swinging-bucket rotor without brake. For platelets depletion, PBMCs were washed four times in 50 ml D-PBS supplemented with 2 mM EDTA at low-speed centrifugation (200×g for 10 min at 20°C with brake). Naïve T cells were isolated by depletion of magnetically labeled non-T helper cells and memory CD4⁺ T cells from the purified PBMC fraction using the Naïve CD4⁺ T Cell Isolation Kit II (Miltenyi Biotec) according to the manufacturer's instructions. The purity of isolated cell populations was assessed by flow cytometry using FITC-conjugated anti-CD4 (BD Pharmingen™), PE-conjugated anti-CD3 (BD Pharmingen™), APC-conjugated anti-CD45RA (BD Pharmingen™) and APC-Cy7-conjugated anti-CD62L antibodies (BioLegend) (for antibody concentrations, see Table 2.13). Samples were analyzed on a BD FACSCanto™ II Cell Analyzer system (BD Biosciences) (flow cytometric data acquisition and analysis were performed by Philipp Rößner, DKFZ, Heidelberg).

3.1.1.3 *In vitro* clonal expansion and differentiation of CD4⁺ T cells

Purified naïve T cells (seeding density of 1×10⁶ cells/ml) were cultured in RPMI 1640 GlutaMAX™ medium (Gibco, Life Technologies) supplemented with 10% heat-inactivated fetal bovine serum and 1% of penicillin/streptomycin (Life Technologies) at 37°C in a 5% CO₂ atmosphere. Cells were activated and clonally expanded in the presence of rIL-2 (50 U/ml; R&D Systems) and anti-CD3/CD28 T cell activator Dynabeads® (bead-to-cell ratio of 1:1; Gibco, Life Technologies). To direct Th1 differentiation, rIL-12 (2.5 ng/ml; R&D Systems) and anti-IL-4 neutralizing antibody (5 µg/ml; BD Pharmingen™) were added to the expansion medium (Cousins et al. (2002)). After 3 days cells were sub-cultured at a density of 1×10⁶ cells/ml and expanded under the same conditions in the absence of activator Dynabeads for additional 4 days. The magnetic activator beads were removed prior to downstream experiments.

3.1.1.4 THP-1 cell suspension culture

THP-1 human monocytic cell line was cultured in RPMI 1640 GlutaMAX® medium supplemented with 10% heat-inactivated fetal bovine serum and 1% of penicillin/streptomycin at 37°C in a 5% CO₂ atmosphere. Cultures were maintained either by the addition of fresh medium or replacement of medium with subsequent re-suspension at 2–4×10⁵ viable cells/ml. Cells were sub-cultured upon reaching a concentration of 8×10⁵ cells/ml, usually every 2 to 3 days. Cell concentration was not allowed to exceed 1×10⁶ cells/ml.

3.1.1.5 HEK293 and HeLa adherent cell culture

Cell lines HEK293 (human embryonic kidney) and HeLa (human cervical carcinoma) were maintained in DMEM-Low glucose GlutaMAX® medium, supplemented with

10% heat-inactivated fetal bovine serum and 1% penicillin/streptomycin at 37°C in a 5% CO₂ atmosphere. Cell monolayers were routinely sub-cultured at 80% confluence. Briefly, cells were rinsed with D-PBS and dislodged with Trypsin-EDTA (0.05%) solution, followed by reaction quenching with complete medium. Cell suspensions were seeded into new cell culture-treated plastic flasks (T-25; T-75) (Sarstedt, Germany) at 1:5–1:10 split ratios (seeding density 50,000–100,000 cells/cm²). Culture medium was renewed every 2 to 3 days.

3.1.2 Intracellular cytokine staining to monitor Th1 cell differentiation

Resting T cells were stimulated with human anti-CD3/CD28 activator Dynabeads[®] in the presence of 1× protein transport inhibitor cocktail (eBioscience) for 5 hours. Cells were harvested and stained with fixable viability dye eFluor[®] 780 (eBioscience) (diluted 1:1000 in D-PBS) for 30 min at 4°C in the dark. 5×10⁵ cells were stained per condition. The cells were thereafter washed twice with ice-cold FACS buffer (centrifugation at 1500 rpm (270×g) for 5 min at 4°C) and fixed for 30 min at room temperature using the IC Fixation buffer (eBioscience). Next, the cells were permeabilized for 5 min with 1× Permeabilization buffer (eBioscience) followed by a 30 min incubation with PE-Cy7-conjugated anti-IFN-γ (eBioscience) and APC-conjugated anti-IL-4 antibodies (BD Pharmingen[™]), diluted in permeabilization buffer at room temperature in the dark (for antibody concentrations, see Table 2.13). Finally, stained permeabilized cells were washed and re-suspended in FACS buffer (staining protocol was established with the help of Philipp Rößner, DKFZ, Heidelberg). Viable cells were analyzed for cytokine expression on a BD FACSCanto[™] II Cell Analyzer system (BD Biosciences). Dead cells were excluded by gating off the eFluor[®] 780 fluorescence-positive cells. At least 20,000 viable cells were assessed for cytokine expression per sample. Background staining was subtracted using fluorophore- and concentration-matched isotype control antibodies from the respective host species. Resting, non-activated cells served as a reference for the basal expression of cytokines in differentiated (i.e., Th1)/non-differentiated (i.e., Th0) activated T cells.

3.1.3 Monitoring CD4⁺ T cell proliferation with CFSE

Activation-induced CD4⁺ T cell proliferation (see section clonal expansion and differentiation of CD4⁺ T cells) was monitored with the intracellular fluorescent dye carboxyfluorescein diacetate succinimidyl ester (CFSE). CFSE labeling was performed according to the protocol published by Quah et al. (2007) (Nature Protocols; also available as a video article). Briefly, T cells were re-suspended in 1ml PBS containing 5% (v/v) FCS at a concentration of 2×10⁶ cells/ml. The tube was laid horizontally to prevent pre-mixing of the cell suspension with the CFSE labeling solution. 110 μl of PBS were added to the non-wetted portion of the tube (i.e., at the top of the tube), and in this droplet, 1.1 μl

of 5 mM CFSE were re-suspended (final concentration of CFSE in the cell suspension: 5 μ M). After an immediate mixing (i.e., by inverting the tube and pulse-vortex), cells were incubated with the dye for 5 min at room temperature followed by three washing steps with PBS/5% FCS (i.e., the labeled cell suspension was first washed with 10 volumes of PBS/5% FCS, followed by two washings of the cell pellet with 10ml of PBS/5% FCS). Thereafter, labeled T cells were stimulated or not with anti-CD3/CD28 T cell activator Dynabeads[®] and rIL-2 (50 U/ml) and cultured for 3 days at 37°C in a 5% CO₂ atmosphere. Division-dependent reduction in CFSE fluorescence intensity was detected by flow cytometry. Unlabeled, non-activated and labeled, non-activated cell controls were included as references for minimum and maximum CFSE fluorescence, respectively.

3.1.4 Flow Cytometry

Freshly isolated naïve CD4⁺ T cells were washed once with ice-cold FACS buffer and stained with the respective fluorochrome-conjugated antibodies (see section 3.1.1.2) in a 100 μ l staining volume for 30 min at 4°C in the dark. Cells were thereafter fixed with 1% paraformaldehyde for 15 min at room temperature in the dark and washed three times with 200 μ l FACS buffer (centrifugation at 1500 rpm (270 \times g) for 5 min). For each donor, 1×10^5 cells were used to determine the percentage of naïve CD45RA⁺ CD62L⁺ cells within the isolated CD4⁺ T-cell population (gated on CD3⁺CD4⁺), referred to as purity of isolation. All samples were analyzed on a BD FACSCanto[™] II Cell Analyzer system (BD Biosciences), and fluorescence data were processed using the BD FACSDiva[™] v8.0.1 software (flow cytometric data acquisition was performed by Philipp Rößner, DKFZ, Heidelberg).

3.1.5 Application of unidirectional shear stress

Cells were subjected to unidirectional shear stress upon reaching confluence in a cone-and-plate viscometer (Martin-Luther University, Halle-Wittenberg) (Sdougos and Busolari (1984)). Briefly, this viscometer consists of a cone with an angle of 0.5 degrees rotating on top of a 60 mm cell culture dish. Unidirectional shear stress of ~ 30 dyn/cm² (arterial levels of shear stress) was applied by a constant angular velocity in a humidified environment with 5% CO₂ at 37°C. Three percent of polymer poly(vinyl pyrrolidone) (PVP) (average molecular weight 360,000 g/mol) was added to the HUVEC growth medium to increase its viscosity. In all experiments each cell culture dish was accompanied by a control from the same HUVEC preparation incubated with cell culture medium supplemented with 3% PVP for 24 hours in the absence of shear stress.

3.1.6 Orbital shear stress *in vitro* transmigration system

In order to mimic the process of leukocyte extravasation *in vivo*, we have established a model in which leukocytes transmigrate through endothelial cell monolayers in the presence of fluid shear stress. Unlike the traditional cell migration assays where leukocytes transmigrate under static conditions, our model system provides an *in vitro* hydrodynamic shear stress environment, combining both chemical and mechanical stimuli, that makes it a more relevant representation of the physiological process of leukocyte diapedesis.

For this purpose, a modified Boyden multi-well transmigration system is used. The chamber consists of upper and lower compartments, separated by a micro-porous filter membrane constituting a physical barrier that prevents the passive movement of cells through the pores. The pore size of the filter membrane is selected according to the size of the cells to be investigated (for transmigration of monocytes and Th1 cells, a 8 μm pore-size filters were used). To obtain tight endothelial cell monolayers, HUVECs are plated on collagen-I-coated 6-well Transwell[®] filter inserts and subsequently cultured for 48 hours before application of different experimental conditions. Among others tested, fibrillar collagen coating proved to be the only one able to withstand the application of shear stress, and at the same time, to ensure the stability of the HUVEC monolayers under hydrodynamic shear conditions. After forming a confluent monolayer, HUVECs are primed by exposure to shear stress for 24 hours. To generate shear stress in this system, the entire 6-well transmigration setup (i.e., Transwell[®] inserts in a companion 6-well plate) was placed on an orbital shaker (PSU-10i, Biosan, SIA., Riga, Latvia). The magnitude of shear stress exerted onto the cells within the Transwell inserts is regulated by adjusting the agitation speed of the shaker platform (usually 100 rpm). Next, leukocytes isolated from freshly drawn human blood/buffy coats, such as monocytes or T lymphocytes, are allowed to transmigrate through the already pre-conditioned HUVEC monolayers, in the presence of shear flow and various stimuli. Finally, the transmigrated cells are quantitated and characterized for phenotypic changes.

Within blood vessels, the flow pattern and magnitude of shear stress varies with the architecture of the vessel. Regions of endothelium exposed to low and irregular blood flow, such as at vessel bifurcations, are predisposed to atherosclerosis (see section 1.2). The orbital shaker technique creates a waveform of shear, which represents a good approximation of the disturbed, non-unidirectional flow at atherosclerotic-prone areas of the vasculature. A wave of culture medium swirls around the Transwell[®] as a result of the rotation of the shaker platform, which creates different patterns of shear stress at different locations within the wells. Figure 3.1 depicts the pattern of shear stress at different shaking speeds.

Hence, the orbital shear stress model of transmigration could provide an invaluable tool to study EC-leukocytes interactions in the context of atherosclerosis and beyond.

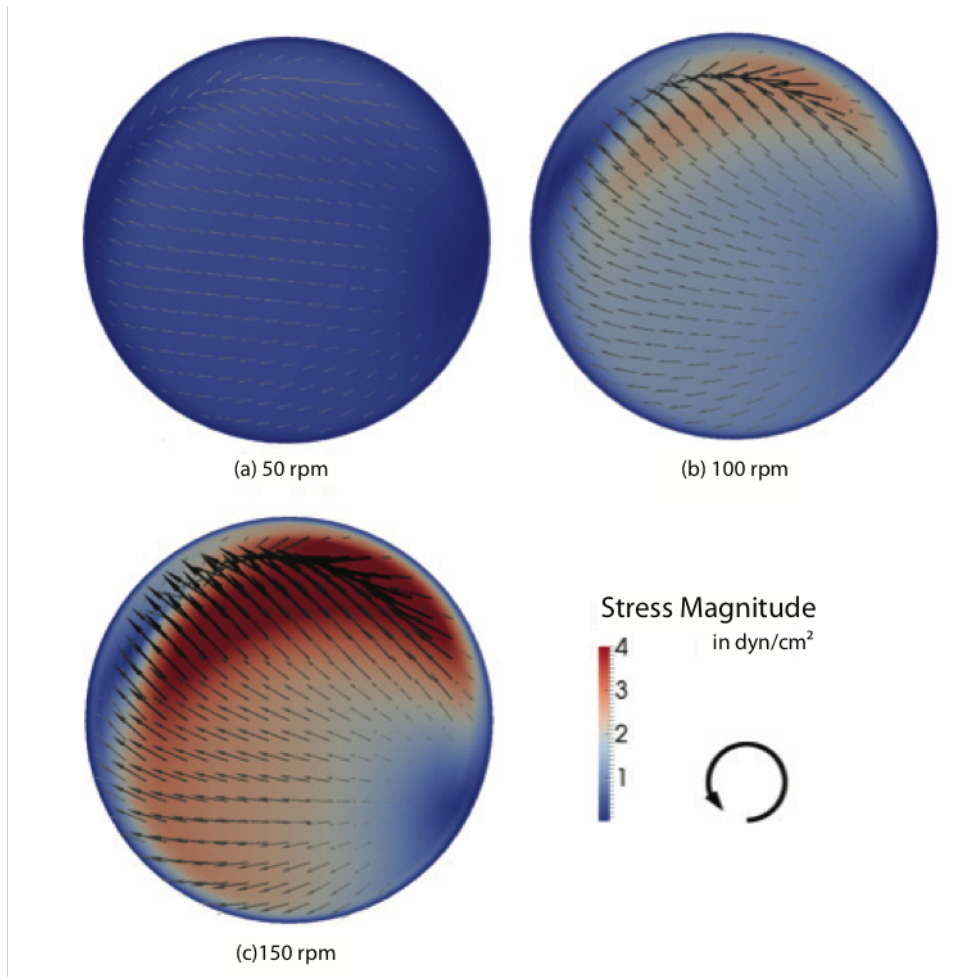


Figure 3.1: Snapshots of the direction and distribution of shear stress within single well of a 6-well Transwell[®] plate on an orbital shaker at different speed settings. The color code corresponds to the magnitude of shear stress throughout the Transwells[®]. Images, as well as calculations of the orbital shear stress, were generated in collaboration with Prof. Dr. Thomas Richter from the Numerical Methods Group at the Heidelberg University, now University of Erlangen-Nürnberg.

3.1.7 *In vitro* Transmigration assay

This assay has been used to study interactions between endothelial cells and THP-1 monocytes or T helper1 cells (Figure 3.2). In brief, Transwell[®] inserts (8 μm pore size; PET; 6-well format; Corning, NY, USA) were coated with rat-tail collagen-I (10 $\mu\text{g}/\text{cm}^2$, i.e., 100 $\mu\text{g}/\text{ml}$; 500 μl per Transwell) for 1 hour at 37°C in a 5% CO_2 atmosphere and placed in a 6-well companion plate (Corning, NY, USA). Coated Transwells were thereafter washed three times with D-PBS and equilibrated in an endothelial cell growth medium (see Media, Table 2.16) for 30 min. Trypsinized HUVECs were seeded at a density of $\sim 150,000/\text{cm}^2$, i.e., 700,000 cells per insert and allowed to form tight monolayers for 72 hours (medium volume in the upper chamber: 2 ml; lower chamber: 3 ml). Within the last 24 hours of culture, the HUVEC monolayers were exposed to orbital shear

3.1. Cell biology methods

stress (shaking speed 100 rpm (i.e., 3–4 dyn/cm²); medium volume in upper chamber: 1 ml; lower chamber: 1.5 ml) to mimic the endothelial cell phenotype at atherosclerosis predilection sites of disturbed blood flow. After shear stress pre-conditioning of the monolayers, leukocytes were pretreated with 10 μM 15d-PGJ₂ or DMSO for 1 hour in endothelial cell growth medium in a separate culture vessel. Cells were then washed once with pre-warmed D-PBS (i.e., pulsed treatment) and loaded onto the HUVEC monolayers for a transmigration assay. Lower chamber was supplemented with MCP-1, 30 ng/ml (for THP-1 cells) or CCL-5, 100 ng/ml (for Th1 cells) to generate a chemotactic gradient directing the migration of the cells. Subsequently, cells were allowed to transmigrate across the HUVEC monolayers for 6 hours at 37°C in a 5% CO₂ atmosphere. The number of transmigrated cells was determined by using a hemocytometer or a handheld automated cell counter (Scepter™ 2.0, Millipore). Activation-induced dead/dying Th1 cells were removed prior to the transmigration assay using the Dead Cell Removal kit of Miltenyi Biotec.

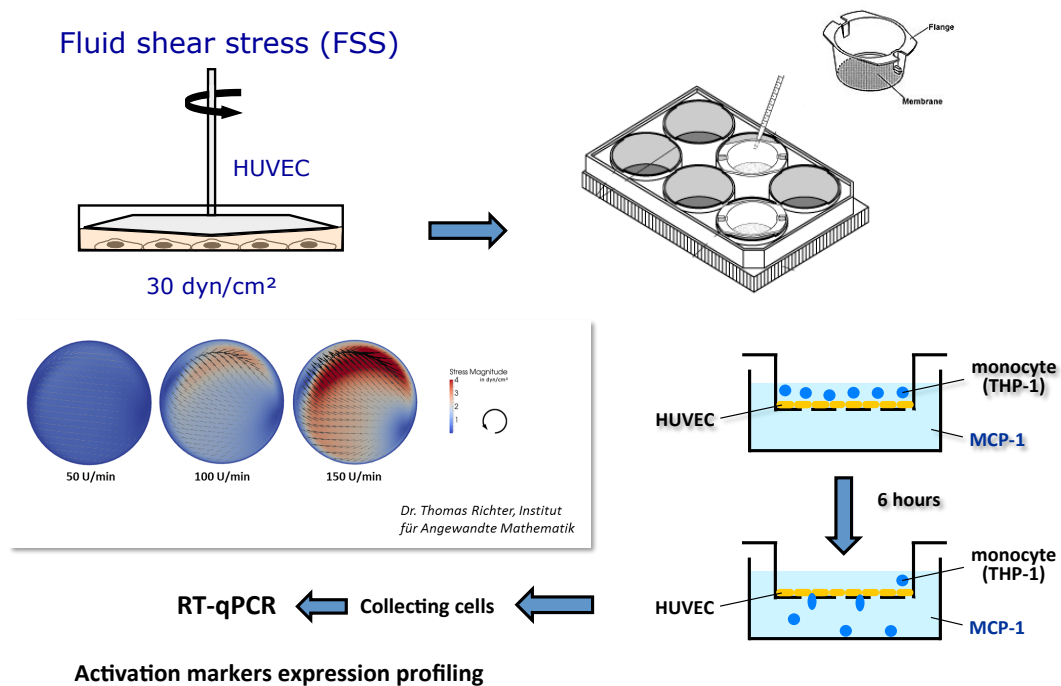


Figure 3.2: Schematic representation of *in vitro* transmigration assay. HUVEC monolayers seeded onto porous membrane filters are primed with unidirectional or orbital shear stresses of various magnitudes. Monocytic (THP-1) cells or primary Th1 cells (not shown on the scheme) are allowed to transmigrate along a chemotactic gradient composed of MCP-1 (or CCL-5 in the case of Th1 cells) added to the lower chamber. The number of transmigrated cells is quantitated 6 hours post-transmigration. The degree of activation of transmigrated cells is determined by analyzing the expression of prototypic marker genes using qRT-PCR.

3.1.8 Transfection

Three separate methods were used for the transient transfection of nucleic acids in monocytic THP-1, HEK293 and HeLa cells.

3.1.8.1 Viromer GREEN

As electroporation and standard lipofection of THP-1 cells yielded a poor transfection efficiency and high cytotoxicity, the Viromer[®] technology was chosen as a tool for the transient transfection of Keap-1-targeting siRNAs (Stealth RNAi[™] siRNA, Invitrogen) in these cells. Viromer[®] are polymeric transfection reagents which mimic viral membrane fusion mechanism. The cationic polyamine backbone of Viromer binds to nucleic acids resulting in a neutral polymer-nucleic acid particle. When endocytosed, Viromer[®] becomes exposed to an acidic environment rendering the fatty acid moieties of the polymer uncharged and hydrophobic. This facilitates the so-called "active endosome escape" of the transfected nucleic acids. We used the specifically optimized manufacturer's protocol for the forward transfection of THP-1 cells. Cells were seeded 24 hours before transfection at a density of 125,000 cells/ml in a 6-well culture plate. At first, Keap1-targeting as well as scrambled control siRNAs were diluted down to 11 μ M in Buffer F. In the second step, the Viromer[®] GREEN transfection reagent was diluted in the Buffer F by adding 90 \times the volume of transfection reagent. Both working solutions were combined and incubated for 15 min at room temperature. To reach a final siRNA concentration of 100 nM and 50 μ M Viromer GREEN, 200 μ l of complexes were transferred per well. Culture medium was exchanged 6 hours post-transfection. Cell viability was routinely monitored by Live/dead viability/cytotoxicity kit for mammalian cells (Molecular Probes[™], Invitrogen).

3.1.8.2 Magnet-assisted transfection (MATra) of siRNAs

The MATra technology (IBA) was employed to knock down endogenous human Nrf-2 in HEK293 cells. For each well of a 6-well plate, 3 μ g of human Nrf-2 siGenome[™] SMART-pool siRNAs (GE Dharmacon) or siGenome[™] Control Non-targeting siRNA pool #2 (GE Dharmacon) were diluted in a serum-reduced Opti-MEM medium to yield a final volume of 200 μ l (100 nM). Thereafter, 4 μ l of MATra-si reagent, containing magnetic beads, was added to the diluted siRNAs and allowed to complexate the nucleic acids at room temperature for 20 min. The siRNA-magnetic beads mixture was added dropwise to the cells and the plate was immediately placed on a powerful magnet (Universal Magnet Plate, IBA) for 30 min to allow the delivery of siRNAs into the cells. As the MATra transfection technology is compatible with serum-containing culture media and transfection efficiency proved to be unaltered by the presence of serum and antibiotics, the cells were left untouched before the addition of the bead-siRNA complexes. Culture

medium was replaced 6 hours post-transfection. The efficiency of gene knockdown was assessed at the mRNA and protein levels using real-time qPCR and/or Immunoblotting, 24 to 72 hours post-transfection (depending on the half-life of the protein of interest).

3.1.8.3 Lipofectamine 3000-mediated transfection of DNA plasmids

Given that suspension THP-1 monocytic cells are hard to transfect, the transfection of large overexpression or reporter DNA constructs was performed in the cell lines HEK293 and/or HeLa. Delivery of DNA plasmids was carried out using the Lipofectamine 3000 transfection reagent according to the manufacturer's protocol. Lipofectamine 3000 is an improved cationic-lipid transfection reagent which forms liposomes in an aqueous environment and complexes negatively charged nucleic acid molecules to assist their cellular internalization. 24 hours prior transfection, each cell line was seeded at a density of $\sim 1 \times 10^5$ cells/cm² for HEK293 and $0.3\text{--}0.5 \times 10^5$ cells/cm² for HeLa cells ($\sim 70\%$ confluence at the time of transfection). For transfection in a 6-well format, 2.5 μg of Nrf-2 overexpression or luciferase reporter constructs were mixed with the transfection reagent and allowed to complexate for 5 min at room temperature. Thereafter, the lipid-DNA complexes were added dropwise to the respective cell line and transfectants were cultured for 24-48 hours prior to analysis. Culture medium was replaced 6 hours post-transfection. Transfection efficiency and non-specific effects were monitored using a GFP-expressing control construct.

3.1.9 Decoy oligodeoxynucleotides (dODNs)

The activity of the transcription factor Egr-1 was blocked by using double-stranded dODNs (see Table 2.10 for sequence) mimicking the Egr-1-binding DNA sequence motifs in the human *PTGDS* gene promoter. In the cell, dODNs modify target gene expression by mimicking TF binding sites in the promoter of these genes. Decoy ODNs can readily enter cells without the aid of transfection reagents (Morishita et al. (1998)), therefore, no auxiliary means were used to introduce these DNA oligos. To prevent binding of Egr-1 to the *PTGDS* gene promoter, HUVECs of both TT and CC genotypes were pre-incubated with dODNs for 4 hours (at a $C_{\text{final}}=10 \mu\text{M}$) prior to their exposure to unidirectional shear stress ($\sim 30 \text{ dyn/cm}^2$) for another 12 hours. In addition, a scrambled ODN with similar base content was used as a specificity control. The expression of the *PTGDS* gene was subsequently analyzed by real-time qRT-PCR.

3.1.10 Treatments

THP-1 cells were pre-treated with 10 μM 15d-PGJ₂ or 50 nM Bardoxolone-methyl for 1 hour, followed by stimulation with 1000 U/ml TNF- α for 6 hours, unless stated otherwise. Treatment with HDACs (TSA, 0.5–1 μM) and p300/CBP HAT (C646, 10–15 μM)

inhibitors was performed prior to the addition of 15d-PGJ₂. Inhibition of signaling pathways modulated by 15d-PGJ₂ was carried out 1 hour before the addition of 15d-PGJ₂ and subsequent stimulation with TNF- α . For Nrf-2 nuclear translocation studies, THP-1 cells were treated with 10 μ M 15d-PGJ₂ or 50 nM Bardoxolone-methyl or 0.5-1 μ M sulforaphane for 4 hour prior to nuclear extraction. Small interfering RNA-mediated knockdown of the respective proteins was carried out 48 hours before the exposure to inhibitors and/or stimulants.

For transmigration assays with *in vitro* differentiated Th1 cells, cells were pulse-treated with 10–20 μ M 15d-PGJ₂ for 1 hours, followed by a washing step and exposure to the chemoattractant, 100 ng/ml CCL-5/RANTES.

HUVEC monolayers were pre-conditioned with unidirectional (\sim 30 dyn/cm²) or orbital fluid shear stress (100 rpm shaking speed) for 24 hours before their use in the leukocyte transmigration assay.

Reporter gene construct-transfected HEK293 cells were pre-treated with 10 μ M 15d-PGJ₂ or 50 nM Bardoxolone-methyl for 1 hour, followed by stimulation with 1000 U/ml TNF- α for 18 hours to allow the secretion of the reporter *Gaussia* luciferase. Treatment with HDACs (TSA, 0.5-1 μ M) and p300/CBP HATs (C646, 10-15 μ M) inhibitors was performed prior to the addition of 15d-PGJ₂. Small interference RNA-mediated knockdown of the respective proteins was carried out 24-48 hours before the exposure to inhibitors and/or stimulants.

HeLa cells were stimulated with 1000 U/ml TNF- α for 6 hours after transfection with Nrf-2 or control GFP overexpression vectors.

3.2 Molecular biology methods

3.2.1 Isolation of human genomic DNA from blood

Genomic DNA was isolated from fresh or frozen EDTA-treated whole human blood using the QIAamp[®] DNA Blood Mini Kit (Qiagen) according to the manufacturer's protocol. DNA binds specifically to the QIAamp silica-gel membrane inside the spin columns while contaminants and PCR inhibitors such as divalent cations and proteins pass through. Pure genomic DNA was eluted in 50–100 μ l elution buffer provided with the kit and used as a template for RFLP-PCR analysis of the T-786C *NOS3* SNP genotype.

3.2.2 Isolation of RNA from cultured cells

Adherent cells were rinsed with ice-cold D-PBS and lysed with 350 μ l RA1 (Macherey-Nagel) lysis buffer containing 1% β -mercaptoethanol. Suspension cells were pelleted

and washed once with ice-cold D-PBS prior to lysis with 350 μl of the same buffer. Total RNA was isolated using the NucleoSpin[®] spin column-based RNA extraction kit (Macherey-Nagel) according to the manufacturer's instructions. In brief, homogenized lysates were mixed with 70% ethanol to create binding conditions favoring the adsorption of RNA to the column silica membrane. DNA was removed by on-column digestion with recombinant DNase. A series of washing steps remove salts, metabolites and macromolecular cellular components. Total pure RNA was eluted in 30–60 μl of RNase-free water under low ionic strength conditions. Elution volumes were selected depending on the amount of starting material. Concentration and purity of the extracted total RNA was determined using a spectrophotometer (NanoDrop ND-1000).

3.2.3 Reverse transcription (RT)

1 μg of the total RNA template (volume of 13 μl) was mixed with 1 μl of oligo dT primer (0.5 $\mu\text{g}/\mu\text{l}$) and heated to 70°C for 10 min to melt secondary structure within the template. The mixture was immediately cooled on ice to prevent reformation of secondary structures and briefly centrifuged. An RT master mix containing 4 μl of 5 \times first strand reaction buffer (250 mM Tris-HCl pH=8.3, 375 mM KCl, 15 mM MgCl₂, 50 mM DTT), 1 μl of 10 mM dNTPs (0.5 mM) and 1 μl of 200 U/ μl Moloney Murine Leukemia Virus Reverse Transcriptase (M-MLV RT) was prepared. The resultant mixture was incubated at 42°C for 1 hour for a first-strand cDNA synthesis. The RT reaction was terminated by incubation at 70°C for 10 min and the reaction batch was cooled on ice. The synthesized cDNA (20 μl) was diluted 1:10 with DNA/DNase-free water and used as a template in conventional semi-quantitative and/or real-time quantitative PCR.

3.2.4 Real-time quantitative reverse transcription polymerase chain reaction (Real-time qRT-PCR)

Real-time qRT-PCR was performed using the LightCycler 1.5 instrument (Roche Diagnostics, Germany) and the QuantiTect SYBR Green[®] kit (Qiagen, Hilden, Germany). Briefly, 5 μl cDNA (\sim 25 ng), 1 μl each of forward and reverse primer (10 μM), 3 μl of RNase-free water, and 10 μl of SYBR Green Master mix were added to obtain a final PCR reaction volume of 20 μl . The annealing temperatures used for the respective primer pairs are tabulated in Table 2.6. Changes in gene expression were analyzed by using either absolute (i.e., based on number of copies of the gene product) or relative quantification (i.e., based on the comparative $\Delta\Delta C_t$ method; C_t or threshold cycle value is the cycle number at which the fluorescence generated within the PCR reaction crosses the fluorescence threshold). The real-time qRT-PCR data were standardized using at least one stably expressed reference gene and by corrections for PCR efficiency and inter-run variations (e.g., by using a calibrator sample) (Pfaffl (2001); Vandesompele et al.

(2002); Willems et al. (2008)). The standard deviation of quantification C_t values between technical replicates was typically less than 0.3 cycles (Hellemans et al. (2007)). All replicates with a standard deviation over 0.3 cycles were excluded. GAPDH, the 60S ribosomal protein L32 (RPL32) and HPRT-1 were used as reference genes to correct for variations in the qRT-PCR workflow, e.g., to normalize for differences in RT efficiency, differences in the amount of PCR template used, etc. For absolute quantification, a standard curve was generated based on serial dilutions of plasmid DNA (of known concentration) encoding the amplified gene sequence. DNA plasmid standards were constructed by amplification of the desired sequence using conventional RT-PCR and cloning it into a vector for bacterial expression. For relative quantification, fold-change in gene expression was calculated as follows:

$$\Delta C_t = C_{t\text{target}} - C_{t\text{reference}} \quad (3.1)$$

$$\Delta\Delta C_t = \Delta C_{t\text{treated}} - \Delta C_{t\text{untreated}} \quad (3.2)$$

(untreated, i.e., calibrator sample; treated, i.e., test sample)

$$\text{Fold change} = 2^{-\Delta\Delta C_t} \quad (3.3)$$

PCR amplification efficiency (E) was calculated as follows:

$$E(\%) = (10^{-1/\text{slope}-1}) \times 100 \quad (3.4)$$

3.2.5 Conventional PCR

In this study, conventional, semi-quantitative RT-PCR was used to analyze the expression of the HO-1 gene in THP-1 and HEK293 cells upon different treatments or siRNA-mediated gene silencing. Conventional PCR was used to amplify the immunoprecipitated DNA in ChIP assays and for genotyping of the T-786C SNP of the *NOS3* gene. The PCR reaction mixtures (see Tables 3.1–3.3) were loaded on an automated PCR thermocycler (Biometra, Göttingen, Germany) programmed with the following cycling parameters (see Tables 3.4–3.6).

TABLE 3.1: PCR Master mix HO-1

Complete PCR buffer (10×)	5 μ l
dNTPs (10 mM)	1 μ l
Fwd primer (10 μ M)	2 μ l
Rev primer (10 μ M)	2 μ l
cDNA	3 μ l (~15 ng)
Taq polymerase (Boiron)	0.2 μ l
ddH ₂ O	to 50 μ l

TABLE 3.2: PCR Master mix *IL-1B* ARE-2 (ChIP assay)

Complete PCR buffer (10×)	5 μ l
dNTPs (10 mM)	1 μ l
Fwd primer (10 μ M)	1 μ l
Rev primer (10 μ M)	1 μ l
immunoprecipitated DNA	5 μ l
Taq polymerase (Boiron)	0.2 μ l
ddH ₂ O	to 50 μ l

TABLE 3.3: PCR Master mix T-786C SNP *NOS3* genotyping

Complete PCR buffer (10×)	2.5 μ l
dNTPs (10 mM)	0.5 μ l
Fwd primer (10 μ M)	1 μ l
Rev primer (10 μ M)	1 μ l
genomic DNA	1 μ l (~25–50 ng)
Taq polymerase (Boiron)	0.2 μ l
ddH ₂ O	to 25 μ l

TABLE 3.4: PCR program HO-1

94°C 5 min	
94°C 30 s	} 31×
58°C 30 s	
72°C 1 min	
72°C 5 min	

TABLE 3.5: PCR program *IL-1B* ARE-2 (ChIP assay)

94°C 5 min	
94°C 45 s	} 35×
55°C 45 s	
72°C 45 s	
72°C 5 min	

TABLE 3.6: PCR program T-786C *NOS3* SNP genotyping

94°C 5 min	
94°C 30 s	} 40×
60°C 30 s	
72°C 1 min	
72°C 5 min	

3.2.6 Agarose gel electrophoresis

Agarose gel electrophoresis was used for the separation of DNA fragments according to their size in an agarose gel matrix. This method was employed to confirm the specificity of amplified PCR products as well as for restriction analysis of expression and reporter DNA constructs. Agarose gels of different density (1-2% agarose) were used depending on the size of the DNA fragment to be resolved. Briefly, agarose was melted in 100 ml of TBE buffer followed by addition of 5 μ l ($C_{\text{final}}=0.5 \mu\text{g/ml}$) of ethidium bromide to stain the DNA fragments. The resultant solution was poured in an electrophoresis chamber. Samples (PCR products or restriction digests) were mixed with 6 \times loading buffer and loaded into the gel pockets. Electrophoresis was carried out at 100 V for approximately 1 hour. The GeneRulerTM DNA ladders of varying range (Thermo Scientific) were used to verify the size of the separated DNA fragments. DNA samples were visualized using the GelDoc XRTM imaging system and data were acquired and analyzed using the Quantity One[®] 1-D Analysis software package, version 4.6.9 (BioRad Laboratories, Germany).

3.2.7 Genotyping

Genotyping was performed by PCR-based restriction fragment length polymorphism (RFLP) analysis. Genomic DNA isolated from umbilical artery specimens or human patient blood was used for genotyping of the T-786C *NOS3* SNP. A 657 bp fragment of the promoter region (GenBank accession No. D26607; -1113 to -456) comprising the SNP was amplified by PCR (for Master mix composition and PCR program see Tables 3.3 & 3.6). The resulting PCR product was digested using restriction endonuclease *HpaII* yielding a specific RFLP pattern (Figure 3.3) depending on the presence or absence of the C allele.

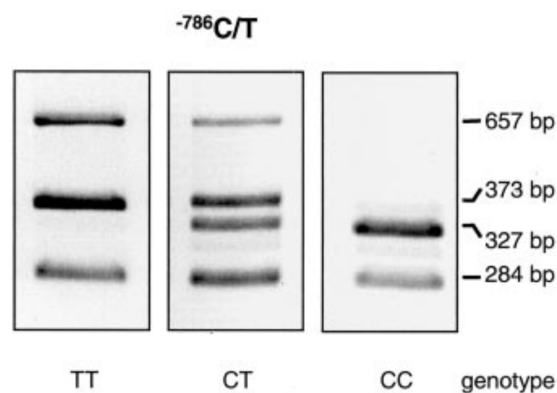


Figure 3.3: Restriction fragment length polymorphism (RFLP) analysis of the T-786C SNP of the *NOS3* gene.

3.2.8 DNA plasmid amplification

The Nrf-2 mammalian expression plasmid (Gene accession No.: NM_006461.2; vector pJ603:137670-AmpR), as well as the corresponding GFP-encoding control construct (vector pJ603:149883-AmpR), were purchased from DNA 2.0, Inc. (Menlo Park, CA, USA) The human *IL-1B* promoter-reporter construct was purchased from GeneCopoeia, Inc. (Rockville, MD, USA) (Catalog No.: HPRM14646-PG04; Gene accession No.: NM_000576; vector pEZX-PG04-Gaussia luciferase (GLuc)-KanR; GLuc-ON promoter reporter clone series). The promoter clone comprises a \sim 1.6 kb-fragment of the human *IL-1B* promoter (-1367bp to +212bp relative to the transcription start site). The full-length *IL-1B* promoter clone (\sim 4.0 kb-fragment of the human *IL-1B* promoter; -3880bp to +212bp relative to the transcription start site) was synthesized and inserted into the pEZX-PG04-GLuc-reporter vector by GenScript USA, Inc. (Piscataway, NJ, USA).

All DNA plasmids were amplified in a competent *E. coli* bacterial strain, DH5- α . 20–50 ng of purchased plasmid was transformed into 100 μ l of competent cells, followed by incubation for 30 min on ice. The cells were thereafter exposed to heat shock at 42°C for 2 min and immediately placed on ice for another 30 sec. Thereafter, 900 μ l of LB broth (with no antibiotics) was added to the cells and the resulting suspension was incubated at 37°C for 1 hour with continuous shaking at 250 rpm. Sterile LB-agar plates containing ampicillin (100 μ g/ml) or kanamycin (50 μ g/ml) were pre-equilibrated to 37°C. Fifty microliters, 100 μ l and 200 μ l of transformed bacterial cell suspension were streaked out onto three separate LB-agar plates using a sterile Drigalski spatula. Bacterial colonies were allowed to grow overnight at 37°C in an incubator. Transformed single colonies were randomly picked with a sterile pipette tip and a starter culture was set up as follows: 3–5 ml of LB broth with appropriate antibiotics were inoculated with a single bacterial colony and cultured at 37°C for 8 hours with continuous shaking at 250 rpm. Large-scale overnight culture was inoculated by diluting the starter culture 1:1000 into 100 ml of LB broth containing the appropriate selective antibiotic. Culture was grown at 37°C with continuous agitation at 125 rpm for \sim 16 hours. For long-term storage, a glycerol stock of each DNA plasmid was prepared and kept at -80°C. Plasmid DNA was purified using a maxi prep endotoxin-free kit (NucleoBond Xtra Maxi prep EF kit, Macherey-Nagel) and all vector inserts (i.e., Nrf-2 and GFP coding sequences, as well as all *IL-1B* promoter clones) were sequenced prior to downstream applications.

3.2.9 Introduction of deletion mutations in the *IL-1B* gene promoter using site-directed mutagenesis

The core sequences of the identified three Nrf-2-like binding sites were deleted in the experimental *IL-1B* promoter-reporter gene construct using the PCR-based QuikChange II XL Site-directed mutagenesis kit (Stratagene, Agilent Technologies) according to the manufacturer’s protocol. In brief, complementary mutagenic primers were designed

using the QuikChange[®] Primer Design Program (for sequences, see Table 2.9). The mutagenic reaction is divided into three steps: 1) mutant strand synthesis reaction; 2) *Dpn I* digestion of the amplification products; 3) transformation of mutated plasmid molecules into competent bacterial cells (XL10-Gold ultracompetent cells). Transformed bacteria were streaked onto LB/kanamycin (50 $\mu\text{g}/\text{ml}$) agar plates and grown overnight at 37°C. Ten transformed bacterial colonies were randomly selected and plasmid DNA was extracted. The *IL-1B* promoter insert was sequenced to verify that the selected clones contain the desired deletion mutation. Large-scale cultures (grown in 100 ml LB broth containing 50 $\mu\text{g}/\text{ml}$ of kanamycin at 37°C overnight) were set up from the deletion mutation-positive clones, and mutant plasmid DNA was purified using a maxi prep endotoxin-free kit (NucleoBond Xtra Maxi prep EF kit, Macherey-Nagel).

3.2.10 Luciferase reporter gene assay

HEK293 cells were transiently transfected in a 6-well plate at 70% confluence (1×10^6 cells seeded 24 hours prior to the transfection) with 2.5 μg or 0.25 μg of wild type or ARE-mutated *IL-1B* promoter-*Gaussia* luciferase reporter gene constructs using Lipofectamine 3000 according to manufacturer's protocol. After 6 hours, the transfected cells were trypsinized and equal numbers were transferred in 24-well plate ($\sim 125,000$ cells/well, i.e., 1 well of a 6-well plate was split into 8 wells of a 24-well plate). Because the transfectants were split into equal portions, normalization for transfection efficiency was not necessary. Twenty-four hours post-transfection, cell culture medium was replaced to eliminate any background secreted *Gaussia* luciferase prior to cell treatment. The passaged cells were thereafter subjected to a 1-hour pre-treatment with 10–20 μM 15d-PGJ₂ or 50 nM Bardoxolone-methyl, followed by a stimulation with TNF- α (1000 U/ml) for 18 hours to induce activity of the experimental *IL-1B* promoter. Promoter activation leads to the expression of secreted luciferase protein into the medium. Stimulation was performed for 18 hours to allow secretion of the reporter *Gaussia* luciferase protein. Culture supernatants were harvested at the end-point of the experiment and were assayed for extracellular luciferase activity. In brief, 10 μl of supernatant and substrate reaction buffer were added to a white opaque microtiter 96-well plate, and after a 10 min incubation (to allow signal stabilization) the luminescence light output was recorded from an average of 15 counts at 1 sec exposure time, using the MicroLumat LB 96P luminometer (Berthold Technologies, Bad Wildbad, Germany). Raw bioluminescence values (expressed in relative light units, RLU) were background-subtracted using supernatants of mock-transfected cells.

To analyze the effect of Nrf-2 or Bach-1 protein knockdowns, siRNAs were introduced into the cells before or after the transfection of the *IL-1B* promoter-reporter construct (depending on the half-life of the depleted protein), i.e., Nrf-2 siRNAs were introduced 24 hours after the reporter construct transfection, whereas the siRNAs against Bach1 were transfected 24 hours before the delivery of the reporter construct into the cells.

Pretreatment with HDACs and p300/CBP HATs inhibitors was performed before the addition of 15d-PGJ₂ and TNF- α .

3.3 Biochemical methods

3.3.1 Total protein extraction

For isolation of total cellular protein, adherent cells were washed with ice-cold D-PBS and scraped off in 50–100 μ l of hypotonic swelling buffer supplemented with protease and phosphatase inhibitors, and transferred into 1.5 ml Eppendorf tubes. Alternatively, suspension cells were first pelleted and washed once with ice-cold D-PBS, followed by re-suspension in 50–100 μ l of hypotonic swelling buffer supplemented with protease and phosphatase inhibitors. After incubation on ice for 30 min, Triton X-100 to a $C_{\text{final}}=0.5\%$ was added to the cell homogenates, which were incubated on ice for another 10 min. A complete cell lysis as well as DNA shearing to reduce the lysates viscosity was assured by an ultrasonication step (3 \times 5 sec at 50% sonication amplitude with cooling on ice in between; UP50H sonicator). The resulting cell lysates were cleared from cellular debris/unlysed cells by a high-speed centrifugation (13,000 rpm (20,000 \times g) for 15 min at 4°C . The lysate was either snap frozen and stored at -80°C or used for downstream analyses. Total protein concentration and yield was determined by a colorimetric Bradford protein assay. Light absorbance at 595 nm wavelength, which is proportional to the protein concentration, was recorded on a Microplate spectrophotometer (PowerWave XS, BIO-TEK).

3.3.2 Nuclear extraction

Cell lysates were fractionated into cytosolic and nuclear (including membranes) portions to monitor subcellular localization of proteins. Suspension THP-1 cells were harvested by centrifugation and washed once with ice-cold D-PBS. Cells were re-suspended vigorously in 100 μ l of Lysis buffer I supplemented with protease and phosphatase inhibitors (see Materials) and incubated for 10 min on ice (samples were vortexed 5 \times 10 sec to break open the cells). Alternatively, adherent cells were washed once with ice-cold D-PBS and harvested by scraping in 100 μ l of Lysis buffer I. Lysates were homogenized by passing them through a 26-gauge needle three times and transferred into 1.5 ml Eppendorf tubes. Nuclei (including the membrane fraction) were pelleted at 12,000 \times g at 4°C for 15 min and the supernatants (cytosolic fraction) were transferred to new tubes. Cytosolic extracts were either snap frozen and stored at -80°C or used for downstream analyses. The nuclear pellets were washed once very carefully with ice-cold D-PBS and re-suspended in 50 μ l Lysis buffer II (supplemented with protease and phosphatase inhibitors). Nuclear lysates were incubated for 15 min on ice and sonicated 3 \times 5 seconds

at 50% sonication amplitude with cooling on ice in between to shear chromatin (UP50H sonicator). After centrifugation (12,000×g at 4°C for 15 min), supernatants containing the nuclear fraction were transferred to new tubes and were either snap frozen and stored at -80°C or used for downstream analyses. The protein concentration was determined in both cellular fractions (see section 3.3.1), and fractions were subsequently used for Western blot analyses.

3.3.3 Immunoblotting (Western blotting)

Protein samples were separated by 10% denaturing sodium dodecylsulfate polyacrylamide gel electrophoresis (SDS-PAGE). Samples were boiled in 1× reducing sample-loading buffer for 5 min at 95°C, and equal amounts of total protein (40 µg/lane) were resolved by 10% denaturing sodium dodecylsulfate polyacrylamide gel electrophoresis (SDS-PAGE). Gels (thickness = 1.5 mm) were run for 20 min at 80 V to allow protein stacking followed by an increase in voltage to 120 V to finish the run in about 1.5 hours. Dual color protein marker from BioRad was used to estimate the approximate molecular mass of the separated proteins. Proteins were blotted onto methanol-activated Immobilon PVDF membranes (Millipore Corp., Belford, MA, USA; pore size: 0.45 µm) using a wet transfer system (Biorad, Germany). Gels and membranes were equilibrated in 1× Towbin transfer buffer (20% methanol), and proteins were transferred at a constant current of 350 mA for 1.5 hours. After blocking with 4% (w/v) nonfat dried Blotto[®] milk dissolved in TBS-Tween 20 0.05% (v/v) (TBST) for 30 min -1 hour (blocking time depends on the amount of loaded protein), membranes were incubated with the respective primary antibodies overnight at 4°C. Thereafter, blotted proteins were washed 4 times with TBST for 5 min each and incubated with species-specific horseradish peroxidase-conjugated secondary antibodies for 1 hour at room temperature. Finally, the membrane was washed 4 times with TBST and once with TBS and visualized using enhanced chemiluminescence (LuminataTM Forte substrate, Millipore). Images were acquired using the ImageQuant LAS 4000 mini imaging system, and quantification of the protein bands intensity was performed using the ImageJ software.

3.3.4 Electrophoretic mobility shift analysis (EMSA)

EMSAs were performed by PD Dr. Andreas Wagner, Institute of Physiology and Pathophysiology, Heidelberg University. Nuclear extracts from 15d-PGJ₂/DMSO or TNF- α -treated THP-1 monocytic cells were prepared as described by Schreiber et al. (1989). The double-stranded gel shift oligodeoxynucleotides (Biomers.net, Ulm, Germany) for the anti-oxidant response element (ARE) were end-labelled with [γ -³²P]ATP by using the 5'-end labelling kit from GE Healthcare, formerly Amersham Biosciences (Wagner et al. (2002)). The specificity of the binding reaction was monitored by performing the assay in parallel with the same samples in the presence of a 100-fold excess of

the non-labelled oligonucleotide. Aliquots of nuclear protein (10 μg) were incubated with 10–20,000 counts per minute of the radiolabeled oligonucleotides in binding buffer containing 1.33 mmol/l DTT and 1 μg poly(d(I-C)) in a total volume of 15 μl at ambient temperature for 30 min. The resulting protein-DNA complexes were analyzed by non-denaturing polyacrylamide gel (4%) electrophoresis and autoradiography by exposing the dried gels to Kodak X-OMAT AR X-ray film (Sigma-Aldrich). Specificity of the ARE-protein interaction was ascertained by incubation with scrambled radiolabeled ARE oligonucleotides.

3.3.5 Chromatin Immunoprecipitation (ChIP)

To detect binding of Nrf-2 to the human proximal *IL-1B* promoter, a ChIP assay was performed. THP-1 cells were treated with DMSO or 15d-PGJ₂ for 4 hours at a concentration of 3.5×10^5 cells/ml. DNA-protein crosslinking in living cells was carried out at room temperature using 1% formaldehyde for 15 min. After cell lysis, chromatin was sheared by sonication (UP50H sonicator; 4 pulses of 15 seconds at 50% of maximum output with cooling on ice in between) resulting in DNA fragments in the range of 500 to 800 bp. Ten per cent of the total sonicated chromatin was kept as the input material. Sheared chromatin was immunoprecipitated with 4 μg of anti-Nrf-2 antibody (C20: SC-722X, Santa Cruz Biotechnology, Inc., TX, CA) at 4°C overnight and protein-DNA complexes were pulled down with herring sperm DNA-blocked Dynabeads[®] Protein G (Life Technologies). As a negative control a no-antibody immunoprecipitation was performed in parallel (NAC, no-antibody control). Immunoprecipitated chromatin was reverse cross-linked with 0.2 M NaCl and deproteinated with 40 $\mu\text{l/ml}$ Proteinase K at 65°C for 4 hours. DNA was extracted with phenol/chloroform/isoamyl alcohol (25:24:1) and amplified by conventional PCR. The optimal number of PCR cycles was adjusted to avoid amplification saturation. Nrf-2 binding was detected with specific primers (see Table 2.8) spanning the identified ARE-2 region of the *IL-1B* promoter (PCR product size: 136 bp). The ARE-2 region was amplified from 5 μl of purified soluble chromatin before immunoprecipitation to show input DNA. The PCR cycling parameters used to amplify immunoprecipitated DNA were as follows: 35 cycles of a denaturing step at 94°C for 45 sec, an annealing step at 55°C for 45 sec, and an extension step at 72°C for 45 sec. PCR products were separated on a 2% agarose gel containing ethidium bromide and imaged using the GelDoc XR[™] imaging system (BioRad Laboratories, Germany). Data were acquired and analyzed using the Quantity One[®] 1-D Analysis software package, version 4.6.9 (BioRad Laboratories, Germany). Data were normalized to input control.

3.3.6 15d-PGJ₂ enzyme immunoassay

Quantitative determination of 15d-PGJ₂ in culture supernatants was performed using the 15d-PGJ₂ ELISA kit according to the manufacturer's instructions (Enzo Life Sciences, Lausen, Switzerland). The 15d-PGJ₂ ELISA kit is a colorimetric competitive enzyme immunoassay designed to measure 15d-PGJ₂ in biological fluids. In brief, alkaline phosphatase (AP)-labeled 15d-PGJ₂ competes with the unlabeled 15d-PGJ₂ from the analyzed sample for binding sites on polyclonal anti-15d-PGJ₂ antibodies. After incubation with an AP chromogenic substrate, the enzymatic reaction is stopped and light absorbance is read at 405 nm wavelength using a microplate reader. The level of color development is inversely proportional to the concentration of 15d-PGJ₂ in the analyzed samples. The absolute 15d-PGJ₂ concentrations were calculated by interpolation from a standard curve based on dilution series of a 15d-PGJ₂ standard supplied by the manufacturer.

3.4 Sample collection and diagnosis of CHD

Blood samples were collected in a blinded fashion from randomly selected patients undergoing elective coronary catheterization (samples were collected by Dr. Florian Leuschner, University Hospital Heidelberg, Antragsnummer: S-390/2011). Inclusion criteria for patients were: 1) patients were considered CHD-positive when the luminal diameter in at least one coronary artery was reduced by 50% as confirmed by coronary angiography; 2) lack of acute myocardial infarction or unstable angina; 3) lack of chronic inflammatory diseases known to influence the plasma prostanoid spectrum, e.g., rheumatic diseases, inflammatory bowel disease, etc. Average age of the CHD study group was 71.3±12.7 years; range 44 to 91 years; n=32; 28% female/72% male subjects. CHD-free age-matched patients were included as a control group (samples were kindly provided by Prof. Peter Bugert, Medical Faculty Mannheim, Heidelberg University and Dr. Maik Brune, University Hospital Heidelberg). Average age of the CHD-free control study group was 64±3 years; range 60 to 69 years; n=108; 50% female/50% male subjects. Primary risk factors were defined as follows: hypertension, current treatment with antihypertensive agents; hypercholesterolemia, total plasma cholesterol >4.8 mmol/l; diabetes, fasting glucose >5.5 mmol/l or current treatment with insulin or oral hypoglycemic agents, and smoking.

Blood was drawn from the brachial or femoral arteries in EDTA-blood collection tubes prior to heparin injection. Plasma was separated from the whole blood specimens within 4 hours after blood drawing by centrifugation at 2500×g for 10 min. Plasma was aliquoted (500 μl aliquots), snap frozen in liquid nitrogen and stored at -80°C until mass spectrometric (MS) quantification analysis. The stability of 15d-PGJ₂ under these conditions was confirmed using liquid chromatography-MS/MS (for MS quantification

of 15d-PGJ₂, see section quantification of 15d-PGJ₂ concentration in CHD patients plasma).

All specimens were collected after obtaining informed consent from the patients. All procedures were approved by the local ethics committee.

3.5 Quantification of 15d-PGJ₂ concentration in CHD patients plasma

All plasma 15d-PGJ₂ quantification analyses were performed by Jacob Morgenstern, University Hospital Heidelberg.

3.5.1 Chemicals

High-purity acetonitrile, ammonium acetate, ethyl acetate, methanol and water purchased from Sigma-Aldrich (Steinheim, Germany). Formic acid was purchased from Biosolve (Valkenswaard, Netherlands). Unlabeled 15-Deoxy- $\Delta^{12,14}$ -prostaglandin J₂ (15d-PGJ₂) (2-4 mg), and 15-Deoxy- $\Delta^{12,14}$ -prostaglandin J₂-d4 (15d-PGJ₂-d4, i.e., deuterated 15d-PGJ₂) (50 μ g), were used as internal standards for the quantification of 15d-PGJ₂ by liquid chromatography tandem mass spectrometry (LS-MS/MS) (purity > 98%; standards were purchased from Cayman chemicals - QuantPAK; local distributor: Biomol; Hamburg, Germany).

3.5.2 Preparation of internal standard stock and working solutions

Internal standard solvents were evaporated under a stream of nitrogen, reconstituted in methanol and stored at -80°C at a concentration of 1.5 mg/ml (unlabeled 15d-PGJ₂) and 250 μ g/ml (deuterated 15d-PGJ₂). Working solutions were prepared in methanol and kept at -80°C at all times. For better precision, the deuterated 15d-PGJ₂-d4 standard was quantified against the more precisely weighed unlabeled 15d-PGJ₂ standard by generating a standard curve of MS peak intensity ratios (deuterated vs. unlabeled). The calibration range of 15d-PGJ₂ was as follows: unlabeled 15d-PGJ₂ standard at 100, 250, 500, 1000, 2500, 5000 pg/ml plus 1 ng of 15d-PGJ₂-d4 for each calibrator.

3.5.3 Lipid extraction from blood plasma

Lipids were extracted from plasma by liquid-liquid-extraction (LLE). In brief, 50 μ l of internal standard (1 ng 15d-PGJ₂-d4) was added to 300 μ l of plasma followed by an acidification of the mixture with formic acid to pH=2. Lipids were extracted thrice with

2 volumes of ethylacetate, and the total organic phase was evaporated in a speed vacuum pump for 15 min at room temperature. The lipid extracts were thereafter reconstituted in a mixture of acetonitrile:water (25:75) with 0.1% ammonium acetate (mobile phase) and were separated by ultra performance liquid chromatography (UPLC).

3.5.4 Chromatography

All chromatographic analyses were performed on a Waters[®] ACQUITY UPLC-I Class system (Waters, Eschborn, Germany) equipped with a binary-based solvent delivery system and an online degasser. Prostaglandins were separated on a reversed-phase Waters[®] ACQUITY UPLC BEH C18 column (1.7 μm , 2.1 mm \times 50 mm) at a flow rate of 0.3 ml/min and a column temperature of 40°C. All samples were stored during analyses in the UPLC autosampler at 4°C and the sample injection volumes were varied between 1 to 5 μl . Solvent A consisted of 0.1% ammonium acetate in water and solvent B was 0.1% ammonium acetate in a mixture of acetonitrile:water (95:5). For each run a gradient elution was performed and no pre-equilibration was needed: 0 \rightarrow 2 min, 75 \rightarrow 70% solvent A; 2 \rightarrow 2.5 min, 70 \rightarrow 5% solvent A; 2.5 \rightarrow 8 min, 5 \rightarrow 70% solvent A; 8 \rightarrow 10 min, 70 \rightarrow 75%. The column eluent was directed into a mass spectrometer for analysis. Data were processed using the Waters[®] MassLynx[™]XS software.

3.5.5 Tandem mass spectrometry

The detection of 15d-PGJ₂ was carried out on a XEVO TQ-S tandem quadrupole mass spectrometer (Waters[®]) equipped with an electrospray ionization source (ESI) operated in negative ion mode. Analyte detection was performed using multiple reaction monitoring (MRM). Source parameters were set as follows: capillary voltage - 3.8 kV; desolvation temperature - 300°C; desolvation gas flow - 850 l/h; source temperature - 150°C; cone gas flow - 250 l/h; collision gas flow - 0.15 ml/min; nebuliser gas flow - 5 bar. Cone and collision voltage were optimized for each compound separately and are summarized in table 3. Data was acquired using the Waters[®] MassLynx 4.1 software and quantitative analyses were performed using the TargetLynx[™] 2.7 Application Manager. Rt - retention time; CV - cone voltage; CE - collision energy.

analyte	R _t [min]	MRM – quantifier (m/z)	MRM – qualifier (m/z)	CV [V]	CE [V]
15d-PGJ ₂	3.91	315.1 > 271.1	315.1 > 203.1	35	15
15d-PGJ ₂ -d4	3.90	319.1 > 275.2	319.1 > 203.1	33	14

3.6 Statistical analysis

All data represent mean \pm standard error of the mean (SEM) of "n" independent observations, unless stated otherwise. Tests for statistical significance were computed using the GraphPad Prism 6 software. When comparing two groups, the unpaired Student's t-test was performed; in case of multiple comparisons, a one-way ANOVA followed by Tukey's multiple comparisons test was performed to determine statistically significant differences between the means. A probability value of $p < 0.05$ was considered significant.

4.1 Characterization of a 15d-PGJ₂-mediated mechanism compensating for the relative lack of NO formation in endothelial cells (ECs) of individuals homozygous for the T-786C SNP of the *NOS3* gene

Given that NO is an essential endogenous modulator of leukocyte adhesion and transendothelial migration, we investigated the impact of the T-786C *NOS3* SNP on interactions between dysfunctional CC-genotype ECs and human leukocytes. At first, to analyze the transmigration of leukocytes through endothelial cells of different genotype, we developed an *in vitro* leukocyte extravasation model using monolayers of CC or TT-genotype human umbilical vein endothelial cells (HUVECs) and the human monocyte-like cell line, THP-1. Exposure to unidirectional shear stress for 24 hours at 30 dyn/cm² was used to restore physiological levels of NOS-3 expression in the HUVEC monolayers, thereby mimicking the atheroprotective phenotype of healthy ECs *in vivo*.

4.1.1 CC-genotype ECs impede monocyte activation and transendothelial migration independent of NO

Surprisingly, prior exposure of HUVECs to physiological levels of FSS effectively reduced THP-1 cell migration, not only through TT, but also through NO-deficient CC-genotype ECs (Figure 4.1A). Moreover, the relative number of THP-1 cells transmigrating through the CC-genotype HUVEC monolayer was even lower as compared to the TT-genotype monolayer. This effect was more pronounced when THP-1 cells were allowed to transmigrate along a gradient of monocyte chemotactic protein-1 (MCP-1), indicating a decreased chemokine responsiveness of these cells upon interaction with dysfunctional CC-genotype HUVECs. Even more surprisingly, expression of interleukin-8 (IL-8), a marker

for their pro-inflammatory activation, was greatly suppressed in the THP-1 cells that had transmigrated through FSS-exposed CC-genotype HUVECs (Figure 4.1B).

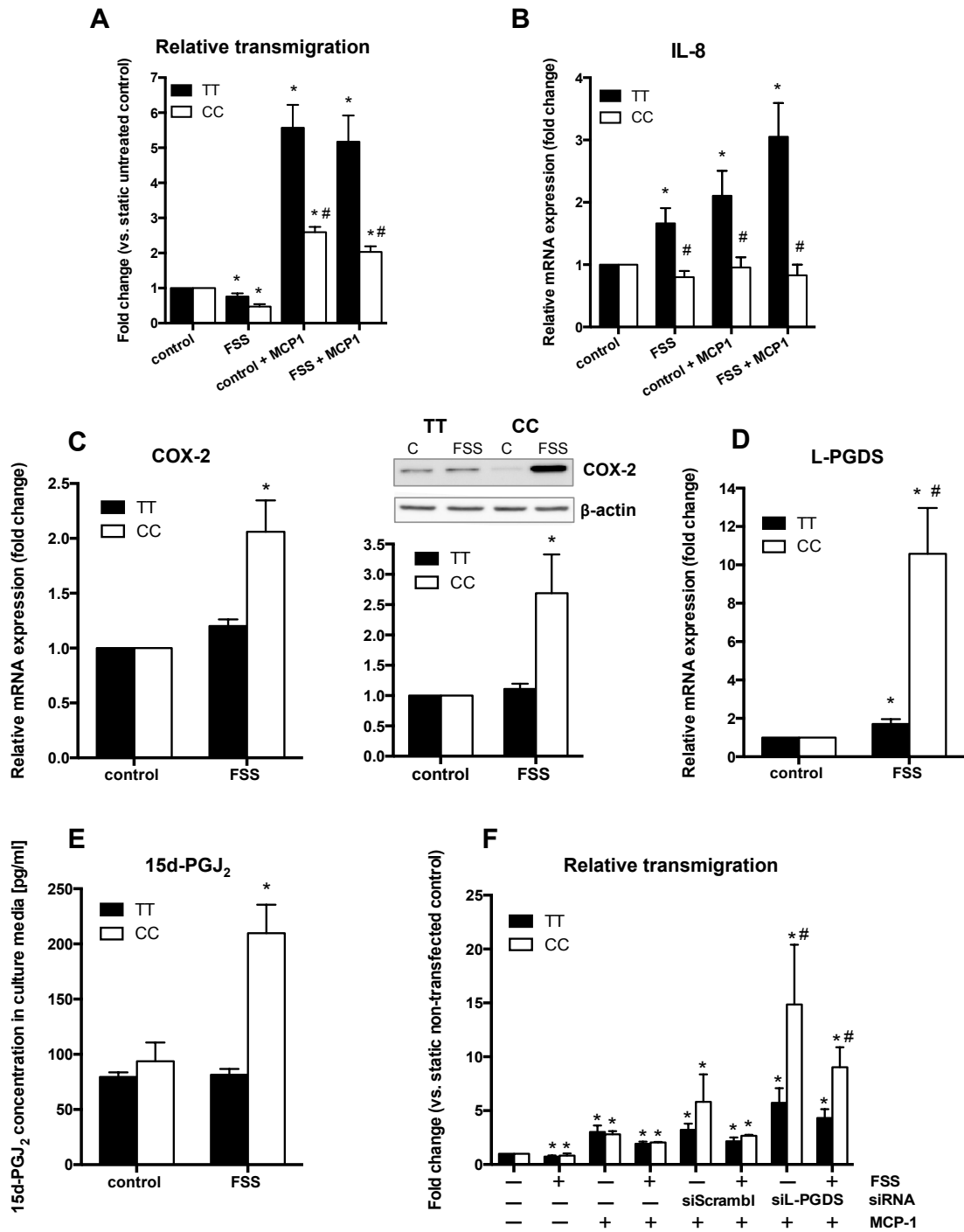
Pharmacological manipulation of NO levels in genotyped ECs failed to demonstrate a relationship between the capacity of ECs to synthesize NO and the observed phenotypic quiescence of THP-1 monocytes that had transmigrated through CC-genotype EC monolayers. Neither exposure of CC-genotype EC monolayers to the NO donor DETA NONO-ate nor the acute inhibition of NOS-3 in TT monolayers, altered the migratory capacity and pro-inflammatory gene expression of transmigrated THP-1 cells (data not shown). The fact that both these effects were independent of NO suggests that dysfunctional CC-genotype HUVECs have devised (an) alternative mechanism(s) to compensate for the relative lack of NOS-3-derived NO and its anti-inflammatory properties in homozygous carriers of the T-786C SNP of the *NOS3* gene.

4.1.2 COX-2 and L-PGDS are up-regulated in CC-genotype ECs upon FSS

Because NO levels are known to modulate the biosynthesis of prostanoids, and, prostanoids play pivotal roles in vascular biology and inflammation, we considered these bioactive lipid mediators as potential candidates to mediate the presumed compensatory mechanism. In Table 4.1, the relative transcript expression of AA-metabolizing enzymes is compared between HUVECs isolated from donors with both *NOS3* genotypes after exposure to unidirectional FSS. Among the nine AA-metabolizing enzymes present in ECs,

Figure 4.1 (facing page): Characterization of the 15d-PGJ₂-mediated compensatory mechanism in CC-genotype HUVECs. (A, B) CC-genotype HUVECs impede monocyte activation and migratory capacity. (A) Unidirectional FSS (~ 30 dyn/cm²) reduces the relative transmigration of THP-1 monocytic cells through both TT and CC-genotype HUVEC monolayers; $n=3-6 \pm$ SEM; * $p < 0.05$ vs. TT control; # $p < 0.05$ vs. TT/MCP-1/FSS. (B) Real-time qRT-PCR analysis of relative IL-8 mRNA expression in THP-1 cells that had transmigrated through monolayers of TT and CC-genotype HUVECs; $n=4 \pm$ SEM; * $p < 0.05$ vs. TT or CC control; # $p < 0.05$ vs. TT/FSS; data acquired with the help of Dr. Sviatlana Gehrman. (C, D) COX-2 and L-PGDS are up-regulated in CC but not in TT-genotype HUVECs upon exposure to FSS. (C) Real-time qRT-PCR and Western blot analyses (loading control: β -actin) of COX2 expression in TT and CC-genotype HUVECs 24 hours after exposure to FSS; $n=4-5$; * $p < 0.05$ vs. control. (D) Real-time qRT-PCR analysis of L-PGDS mRNA expression in TT and CC-genotype endothelial cells 24 hours after exposure to FSS; $n=5-7 \pm$ SEM; * $p < 0.05$ vs. control; # $p < 0.05$ vs. TT/FSS; data acquired with the help of Dr. Sviatlana Gehrman. (E) Enhanced release of 15d-PGJ₂ by CC-genotype HUVECs in response to FSS. 15d-PGJ₂ concentration in the culture supernatant was determined using an enzyme-immunoassay 24 hours after exposure to FSS; $n=3$ (CC); $n=4$ (TT); * $p < 0.02$ vs. control; data acquired with the help of Dr. Sviatlana Gehrman. (F) siRNA-based L-PGDS knockdown boosts the transmigration of THP-1 cells through CC-genotype HUVECs. Twenty-four hours post transfection HUVECs were exposed to FSS for another 24 hours and re-seeded on PET porous membranes. THP-1 cell transmigration was tested 24 hours later with THP-1 cells transmigrating through the HUVEC monolayers in the presence of MCP-1 (30 ng/ml) for 6 hours; $n=3 \pm$ SEM; * $p < 0.05$ vs. control; # $p < 0.05$ vs. TT control; data acquired with the help of Dr. Sviatlana Gehrman.

4.1. Characterization of a 15d-PGJ₂-mediated mechanism compensating for the relative lack of NO formation in endothelial cells (ECs) of individuals homozygous for the T-786C SNP of the *NOS3* gene



only COX-2 (Figure 4.1C), converting arachidonic acid to prostaglandin H₂ (PGH₂), and the lipocalin-type PGDS (L-PGDS), catalyzing the isomerization of PGH₂ to PGD₂, were markedly up-regulated by FSS solely in the CC-genotype HUVECs (Figure 4.1D). Furthermore, siRNA-mediated down-regulation of L-PGDS significantly boosted THP-1 cell transmigration through CC-genotype EC monolayers (Figure 4.1E), suggesting that PGD₂ or one of its metabolites may constitute the presumed mechanism compensating for the low availability of NO in these cells.

TABLE 4.1: Differences in arachidonic acid-metabolizing enzymes transcript levels in TT and CC-genotype ECs following exposure to FSS for 24 hours.

Arachidonic Acid-metabolizing enzyme		TT	CC
phospholipase A ₂	PLA ₂	→	↑
cyclooxygenase-1	COX-1	↑	↑
cyclooxygenase-2	COX-2	↑	↑↑↑
microsomal prostaglandin E synthase	mPGES	↑	→
cytosolic prostaglandin E synthase	cPGES	→	→
prostaglandin F synthase	PGFS	↑↑	↑
prostaglandin I synthase	PGIS	↑	↑
hematopoietic prostaglandin D synthase	H-PGDS	→	→
lipocalin-type prostaglandin D synthase	L-PGDS	↑	↑↑↑
prostaglandin I synthase	PGIS	↑	↑

In comparison to control "→" represents no or insignificant difference in mRNA levels, "↑↑↑" represents a very strong increase in mRNA expression.

4.1.3 CC-genotype HUVECs produce increased levels of 15d-PGJ₂, which has potent anti-migratory and anti-inflammatory activities *in vitro*

While many COX-2-derived prostanoids are generally pro-inflammatory mediators, cyclopentenone prostaglandins (CyPGs) by contrast have demonstrated pronounced anti-inflammatory activities. Interestingly, the terminal stable degradation product of PGD₂, the cyclopentenone 15d-PGJ₂, is known to act as an anti-inflammatory mediator in various cell types, including vascular and immune cells (for review, see Surh et al. (2011)), making it a promising candidate to maintain the quiescent phenotype of CC-genotype endothelial cells. In fact, we could further show that following exposure to FSS only CC-genotype HUVECs reveal an approximately 3-fold higher release of 15d-PGJ₂ into the supernatant as compared to the static control level, which was indistinguishable between both HUVEC genotypes (Figure 4.1E). Exogenously added 15d-PGJ₂ significantly attenuated the transmigration of THP-1 monocytes through TT-genotype HUVEC monolayers in a concentration-dependent manner (Figure 4.2A). Furthermore, 15d-PGJ₂ potently blocked the pro-inflammatory activation of THP-1 monocytes, as evidenced by its profound inhibitory effect on TNF- α -induced expression of IL-1 β and the co-stimulatory molecule, CD40, in these cells (Figure 4.2B, C).

4.1. Characterization of a 15d-PGJ₂-mediated mechanism compensating for the relative lack of NO formation in endothelial cells (ECs) of individuals homozygous for the T-786C SNP of the *NOS3* gene

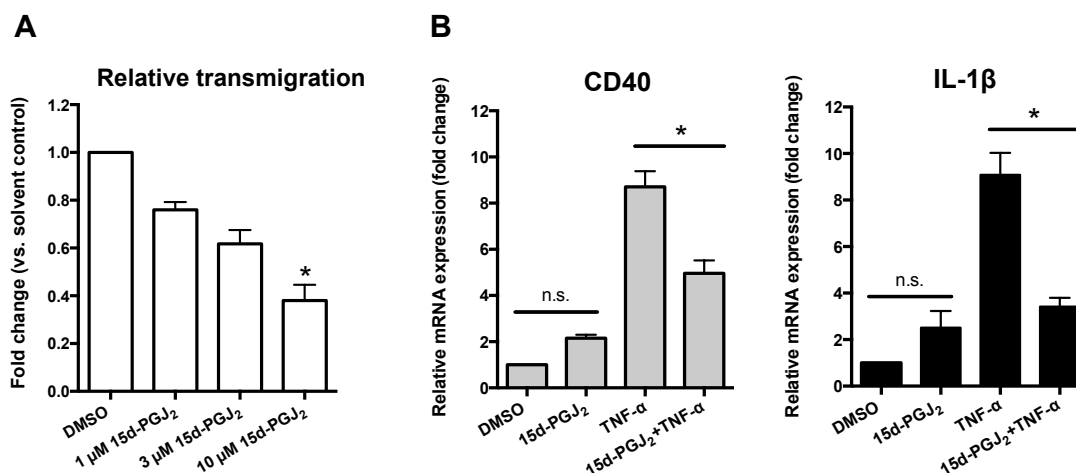


Figure 4.2: 15d-PGJ₂ inhibits the transmigration and pro-inflammatory activation of THP-1 monocytic cells. (A) Relative transmigration of THP-1 cells pulse-treated with 1 to 10 μM 15d-PGJ₂ or DMSO across TT-genotype HUVEC monolayers in the presence of 30 ng/ml MCP-1 for 6 hours; n=4; *p<0.05 vs. DMSO (set to 1.0); unpaired Student's t-test. (B) Real-time qPCR analysis of relative CD40 (left) and IL-1β (right) mRNA expression in THP-1 cells pre-treated for 1 hour with 10 μM 15d-PGJ₂ and subsequently stimulated for 6 hours with 1000 U/ml TNF-α; n=3-4 ± SEM; *p<0.05 vs. TNF-α-stimulation.

4.1.4 L-PGDS up-regulation in CC-genotype HUVECs is driven by the relative lack of NO

In order to examine whether the observed up-regulation of L-PGDS in CC-genotype HUVECs, challenged with FSS, is driven by the relative lack of NO, we treated both EC genotypes with the NOS-3 inhibitor, N ω -nitro-L-arginine, prior to a 24-hour exposure to FSS. This in fact resulted in a FSS-dependent increase in L-PGDS gene expression in TT-genotype ECs that was no longer discernible from that in CC-genotype ECs (Figure 4.3A), suggesting that the reduced availability of NO in these cells facilitates the FSS-dependent up-regulation of L-PGDS.

Analogous to the Egr1-dependent induction of NO-protecting SOD-2 expression in CC-genotype HUVECs (see section 1.5.1), the role of this TF in endothelial cell L-PGDS expression was investigated further. Initially, we performed an *in silico* analysis of the promoter of the human *PTGDS* gene and identified multiple binding motifs, closely resembling the consensus sequence for Egr1 binding. Egr1 is a shear stress-inducible TF whose expression and activity are highly dependent on endogenous NO levels (Chiu et al. (1999); for review, see Pagel and Deindl (2011)), making it an eligible candidate for mediating the observed genotype-dependent effect. To test this hypothesis we employed the decoy oligonucleotide (dODN) technique, in which short double-stranded DNA oligonucleotides, mimicking the putative Egr1 binding sites in the L-PGDS promoter, were used to neutralize Egr1 functionally.

In contrast to the scrambled control ODN (i.e., the scrambled version of the decoy sequence used as a control), pretreatment of CC-genotype HUVECs with the specific Egr1-neutralizing dODNs resulted in a clear reduction in L-PGDS transcript levels (Figure 4.3B), suggesting that Egr1, at least partially, accounts for the FSS-induced up-regulation of L-PGDS expression in NO-deficient ECs. The effects of the Egr1 dODNs on TT-genotype ECs were statistically insignificant.

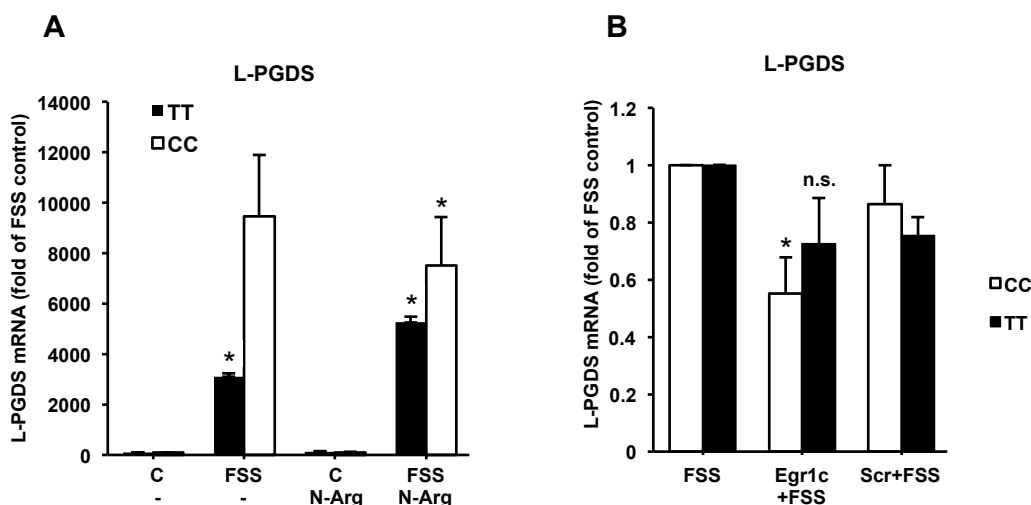


Figure 4.3: Relative lack of NO facilitates genotype-dependent differential L-PGDS expression. (A) NOS-3 inhibition in TT-genotype endothelial cells leads to increased L-PGDS mRNA expression. TT and CC-genotype HUVECs were treated for 3 hours with 100 μ M of *N* ω -nitro-L-arginine (N-Arg), prior to FSS application, or remained untreated. Real-time qRT-PCR analysis of relative L-PGDS mRNA expression was performed after 24-hour exposure to FSS; values represent the means \pm SEM of 3 independent experiments, each performed with cells derived from a different donor; * $p < 0.05$ vs. control or control+N-Arg, respectively. (B) Decoy ODN-mediated inhibition of Egr1 attenuates FSS-induced expression of L-PGDS mRNA in CC-genotype HUVECs. Real-time qRT-PCR analysis of L-PGDS mRNA levels in cultured CC or TT-genotype HUVECs. The decoy (Egr1) and scrambled control (Scr) oligonucleotides (3 μ M) were added 4 hours before exposure to unidirectional FSS. Values represent the means \pm SEM, $n = 3$; * $p < 0.05$ vs. FSS control; n.s., not significant.

4.2 Investigation of molecular mechanisms underlying the anti-inflammatory activity of 15d-PGJ₂ in human monocytes

In order to determine how 15d-PGJ₂ may exert these anti-inflammatory effects in the THP-1 cells, we looked at various signaling pathways modulated by this prostanoid. 15d-PGJ₂ may confer anti-inflammatory effects by three main mechanisms: (1) by activating the intranuclear receptor peroxisome proliferator-activated receptor- γ (PPAR- γ), (2) by suppressing inflammatory signaling and pro-inflammatory TF transactivation, and (3) by facilitating activation of the anti-oxidant TF Nrf2 (Figure 4.4A).

4.2. Investigation of molecular mechanisms underlying the anti-inflammatory activity of 15d-PGJ₂ in human monocytes

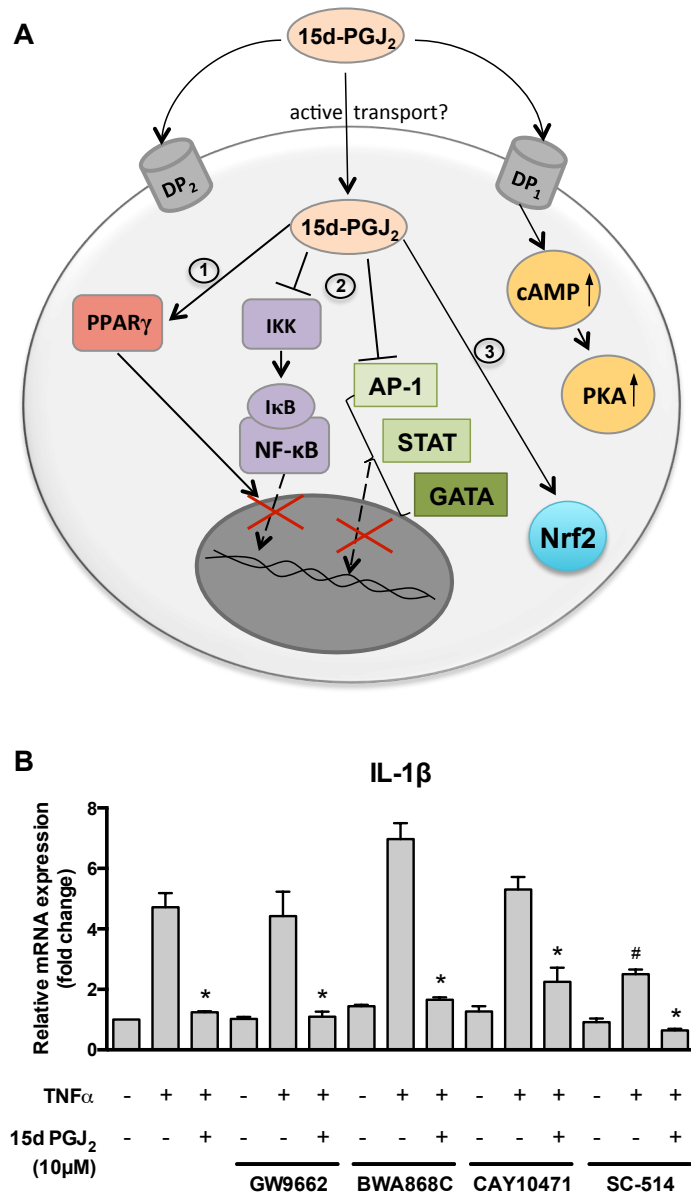


Figure 4.4: Inhibition of 15d-PGJ₂ effector signaling pathways in THP-1 monocytes. (A) Schematic representation of the anti-inflammatory effects mediated by 15d-PGJ₂. (B) Real-time qRT-PCR analysis of relative IL-1 β mRNA expression in THP-1 cells pre-treated for 1 hour with PPAR- γ antagonist GW9662 (10 μ M), DP-1 antagonist BWA969C (0.2 μ M), DP-2 antagonist CAY10471 (1 μ M) or IKK β inhibitor (50 μ M) followed by 2-hour incubation with 10 μ M 15d-PGJ₂ and stimulation with 100 U/ml TNF- α for 4 hours; data represent mean \pm SEM; n=3-5; *p<0.001 vs. TNF α -stimulated control; #p<0.05 vs. TNF α -stimulated control (data acquired with the help of Dr. Sviatlana Gehrman).

15d-PGJ₂ is one of the most extensively studied cyclopentenone prostaglandins because of its unique spectrum of biological activities. It is the first identified endogenous ligand for the orphan nuclear receptor PPAR- γ , a ligand-activated TF with pleiotropic effects on glucose homeostasis, adipocyte differentiation and lipid metabolism. Like all CyPGs, 15d-PGJ₂ possesses a α,β -unsaturated carbonyl moiety within the cyclopentenone ring that can participate in the Michael addition reaction with cellular nucleophils such as

free sulfhydryl (SH) groups of glutathione (GSH) and specific cysteine (Cys) residues of proteins (i.e., serving as redox-sensors), thus modulating their function.

15d-PGJ₂ suppresses the production of inflammatory mediators (i.e., cytokines and chemokines) and pro-inflammatory genes in numerous primary cell types and cell lines, including immune (dendritic cells, T cells, murine splenocytes) and inflammatory cells (activated monocytes/macrophages), vascular (ECs and SMCs) and mesenchymal cells (chondrocytes, fibroblast-like synoviocytes), both in a PPAR- γ -dependent and independent manner (for review, see Scher and Pillinger (2005); Scher and Pillinger (2009); Surh et al. (2011)). Ligation of PPAR- γ by 15d-PGJ₂ has been demonstrated to down-regulate pro-inflammatory responses in activated macrophages by preventing the expression of pro-inflammatory genes as well as the release of pro-inflammatory cytokines such as TNF- α , IL-1 β or IL-6 (Scher and Pillinger (2005); Scher and Pillinger (2009)). Mechanistically, 15d-PGJ₂ is thought to trigger PPAR- γ -dependent transrepression, i.e. interference with TF activation. 15d-PGJ₂ induces the interaction of PPAR- γ with co-activator complexes such as cAMP response element binding protein (CBP/p300, Varga and Nagy (2008)), which is indispensable for activation of pro-inflammatory TFs like NF- κ B, activator protein-1 (AP-1) or STAT-1. Co-activator deprivation consequently hampers expression of pro-inflammatory genes directed by these TFs (for review see Schmidt et al. (2010)).

Moreover, 15d-PGJ₂ has been shown to exert potent anti-inflammatory effects through inhibition of the NF- κ B pathway induced in response to pro-inflammatory cytokines, mitogens and viral infection. The principle mechanism through which 15d-PGJ₂ antagonizes this pathway involves a direct covalent modification and inactivation of the β -subunit of the IKK complex (Straus et al. (2000); Rossi et al. (2000); Castrillo et al. (2000)), as well as blockade of nuclear translocation and DNA binding of the NF- κ B p65/p50 heterodimer (Straus et al. (2000); Cernuda-Morollon et al. (2001)), thus abrogating expression of its target genes.

Likewise, 15d-PGJ₂ negatively regulates activity of the TF AP-1 (Perez-Sala et al. (2003)). Through alkylation of a conserved cysteine residue in the c-Jun DNA binding domain, 15d-PGJ₂ interferes directly with the transactivation by AP-1, thereby reducing the expression of various pro-inflammatory and proteolytic enzymes. In addition, phosphorylation of mitogen activated protein kinases (MAPK), such as p38 MAPK and JNK, essential for the activation of NF- κ B and AP-1 upon stress and various cytokines, is reduced in 15d-PGJ₂-pretreated human astrocytes (Zhao et al. (2004)).

Besides regulating the expression of genes involved in cell growth and survival, the Janus kinase (JAK)-STAT cascade is an essential pathway that mediates immune responses and inflammatory signaling. Suppressor of cytokine signaling (SOCS) proteins are negative feedback regulators of JAK-STAT signaling, the concomitant induction of expression of which appears to be an adaptive defensive response in a number of experimental models of chronic inflammation. Several studies have demonstrated reduced phosphorylation of

STAT1 and STAT3 as well as JAK1 and JAK2 upon exposure to 15d-PGJ₂, resulting in suppression of JAK-STAT-dependent pro-inflammatory responses (Park et al. (2003)). In various cell types, 15d-PGJ₂ has also been shown to rapidly induce expression of SOCS1 and SOCS3, thereby inhibiting the activity of JAKs (reviewed by Surh et al. (2011)).

Using a combination of specific pharmacological inhibitors, RNA interference and electrophoretic mobility shift assays we could effectively rule out a contribution by PPAR- γ , the TFs NF- κ B, AP-1 and STAT-1 (data for AP-1 and STAT-1 are not shown), as well as the cell surface receptors for PGD₂ and 15d-PGJ₂, DP1 and DP2, as the downstream effectors of 15d-PGJ₂ in human monocytic cells (Figure 4.4B). This essentially left the TF Nrf2 as the only feasible target of 15d-PGJ₂ to mediate its effects on inflammatory gene expression.

4.2.1 15d-PGJ₂ and Bardoxolone induce Nrf2 signaling in human THP-1 monocytes

15d-PGJ₂ exerts cytoprotective and anti-inflammatory activities through induction of the anti-oxidant response orchestrated by the Nrf2-Keap1 pathway. Nrf2 (NF-E2-related factor 2) is the master regulator of redox homeostasis, and as such it constitutes the major defensive mechanism of eukaryotic cells to counteract oxidative and environmental stresses (reviewed by Taguchi et al. (2011); Suzuki et al. (2013)). Nrf2 up-regulates the expression of a large number of cytoprotective enzymes, which in turn detoxify reactive chemical species and restore cellular redox homeostasis. It is noteworthy that many Nrf2-regulated cytoprotective genes, and in particular their anti-oxidant and detoxifying protein products (e.g., heme oxygenase1 (HO-1), peroxiredoxin I (PrxI), NADPH:quinone oxidoreductase 1 (NQO-1), etc.), have prominent anti-inflammatory effects themselves (for review, see Wakabayashi et al. (2010); Paine et al. (2010); Surh et al. (2011)), and have therefore been implicated in the regulation of inflammatory responses (Kisucka et al. (2008); Morse et al. (2009)).

Under physiologic conditions, Nrf2 is normally sequestered in the cytoplasm as an inactive complex with the repressor Kelch-like ECH-associated protein-1 (Keap-1), which targets it for proteasomal degradation to keep the cytosolic level of Nrf2 low. In the presence of oxidative or electrophilic stresses, Keap-1 is inactivated, enabling the translocation of Nrf2 to the nucleus. In the nucleus, Nrf2 dimerizes with small Maf proteins and activates the transcription of target genes encoding for various anti-oxidant and phase-2 detoxifying enzymes through binding to antioxidant response elements (ARE)/electrophile response elements (EpRE) in their promoters (Taguchi et al. (2011)).

Because of its highly electrophilic α,β -carbonyl moiety within the cyclopentenone ring, 15d-PGJ₂ forms covalent adducts with critical redox-sensitive cysteine residues in the

Keap-1 molecule (Kobayashi et al. (2009)). Electrophile modification of Keap-1 abrogates its ability to degrade Nrf2 (i.e., inhibits the Keap-1-mediated conjugation of ubiquitin to Nrf2), thereby provoking the opening of the Keap-1 “gate” and resulting in Nrf2 stabilization (for review, see Kansanen et al. (2009)). Western blot analysis of nuclear extracts from 15d-PGJ₂-treated THP-1 cells demonstrated that 15d-PGJ₂ actually induces the nuclear accumulation and thus activation of Nrf2 in these cells (Figure 4.6A). Similar results have been obtained when nuclear extracts of THP-1 cells were analyzed by electrophoretic mobility shift assay using an oligonucleotide probe specific for Nrf2 (Figure 4.5). Moreover, 15d-PGJ₂ strongly induced the expression of HO-1 and PrxI, both well-known Nrf2-target genes (Figure 4.6B, F).

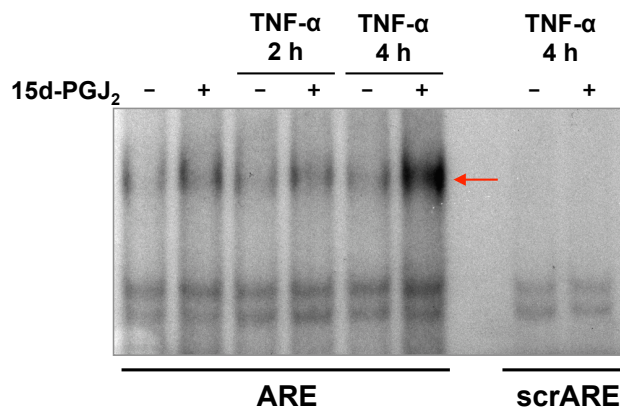


Figure 4.5: 15d-PGJ₂ induces Nrf2 DNA-binding activity in THP-1 monocytes. Electrophoretic mobility shift assay using ARE (Nrf2-binding) consensus sequence oligonucleotide (first six lines). THP-1 cells were pre-treated with 10 μ M 15d-PGJ₂ or not for 2 hours followed by stimulation with 100 U/ml TNF- α for the indicated times. Specificity was assured by scrambled ARE sequence oligonucleotide (last two lines). Representative assay of three experiments is shown (the assays were performed by PD Dr. Andreas Wagner, Institute of Physiology and Pathophysiology, Heidelberg University).

Given that 15d-PGJ₂ simultaneously targets multiple signaling pathways, and does not exert its biological effects merely by facilitating the nuclear translocation of Nrf2, we decided to use an alternative inducer of the Nrf2-Keap1 pathway, the synthetic triterpenoid Bardoxolone, which specifically activates Nrf2 without acting as a pro- or antioxidant in addition. Similar to 15d-PGJ₂, Bardoxolone induced a prominent nuclear translocation of Nrf2 in the THP-1 cells (Figure 4.6C). Moreover, it strongly up-regulated the expression of HO-1 mRNA and protein (Figure 4.6D, F), and at the same time repressed TNF- α -induced expression of IL-1 β in these cells (Figure 4.6E). Collectively, these data support the assumption that 15d-PGJ₂ confers its anti-inflammatory effect on monocytes through a mechanism that at least in part involves Nrf2 and its downstream target genes.

4.2. Investigation of molecular mechanisms underlying the anti-inflammatory activity of 15d-PGJ₂ in human monocytes

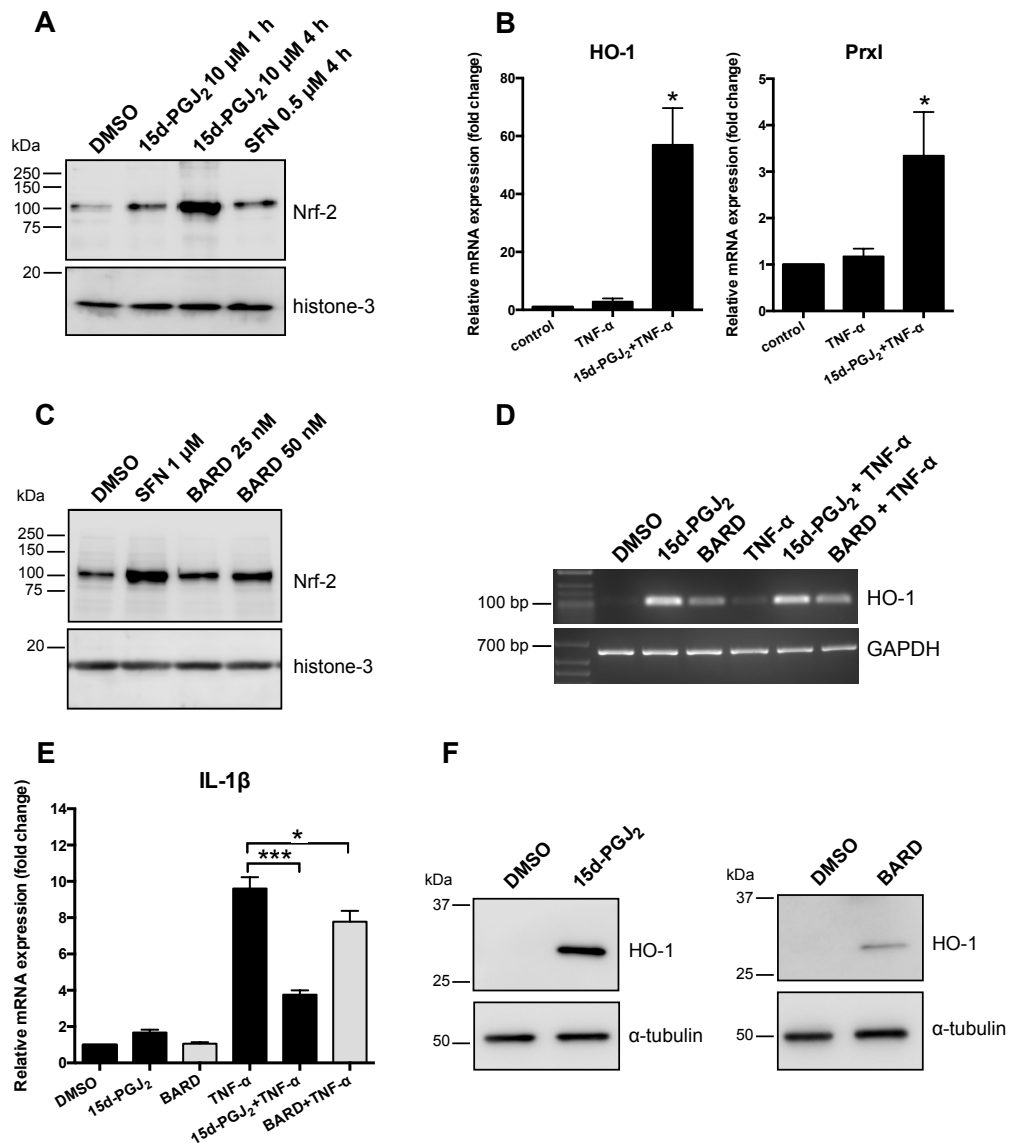


Figure 4.6: 15d-PGJ₂ and Nrf2 activator, Bardoxolone, induce nuclear accumulation and activation of Nrf2 in THP-1 cells. (A) Representative Western blot analysis of nuclear extracts from THP-1 cells stimulated with the indicated concentrations of either 15d-PGJ₂, or another Nrf2 activator, sulforaphane (SFN), for the indicated times. SFN was used as a positive control to activate the Nrf2-Keap1 pathway. Histone 3 served as a loading control. The Western blot shown is representative for 3 individual experiments performed. (B) Real-time qPCR analysis of relative Nrf2-dependent mRNA expression of HO-1 (left) and PrxI (right) in THP-1 cells pre-treated for 1 hour with 10 μM 15d-PGJ₂ and subsequently stimulated for 6 hours with 1000 U/ml TNF-α; n=4 ± SEM; *p<0.05 vs. TNF-α-stimulation. (C) Representative Western blot analysis (n=2) of nuclear extracts from THP-1 cells stimulated or not with the indicated concentrations of Bardoxolone-methyl (BARD) and SFN (positive control) for 4 hours. (D) Representative (n=4) semi-quantitative RT-PCR analysis of HO-1 mRNA expression in THP-1 cells pretreated or not for 1 hour with 10 μM 15d-PGJ₂ or 50 nM BARD followed by activation with 1000 U/ml TNF-α for 6 hours. GAPDH was used as a reference gene to normalize HO-1 mRNA levels. (E) Real-time qRT-PCR analysis of relative IL-1β mRNA expression in THP-1 cells pre-treated for 1 hour with either 10 μM 15d-PGJ₂ or 50 nM BARD and subsequently stimulated for 6 hours with 1000 U/ml TNF-α; n=3 ± SEM; *p<0.05, ***p<0.001 as indicated, one-way ANOVA with post-hoc Tukey's multiple comparison test. (F) Representative (n=2) Western blot analysis of HO-1 protein abundance in THP-1 whole cell lysates. Cells were stimulated or not with 10 μM 15d-PGJ₂ or 50 nM BARD for 4 hours, washed, placed in fresh media and harvested 4 hours later; α-tubulin served as a loading control.

4.2.2 15d-PGJ₂ and Bardoxolone cause the nuclear accumulation of *de novo* synthesized Nrf2

While it is well established that the nuclear abundance and activity of Nrf2 increases in response to oxidative and electrophilic stress, the exact mechanism leading to its accumulation in the nucleus is still incompletely understood. Previous research has revealed an alternative mechanism of Nrf2 activation involving nuclear translocation of newly synthesized Nrf2 rather than its liberation from Keap1 (Kobayashi et al. (2006)). Accordingly, we examined the effect of transcription and translation inhibitors, actinomycin D (ActD) and cycloheximide (CHX), on Nrf2 translocation to the nucleus of THP-1 monocytic cells. Pre-treatment with either ActD (Figure 4.7A, left) or CHX (Figure 4.7A, right) almost completely abrogated the ability of Nrf2 to translocate to the nucleus in response to 15d-PGJ₂, indicating that the *de novo* synthesis of both mRNA and protein is a prerequisite for Nrf2 to shuttle to the nucleus under conditions of electrophilic stress. The expression of inducible genes such as HO-1 naturally was blocked upon inhibition of transcription or translation. Bardoxolone-induced nuclear transport and activation of Nrf2 was sensitive to both inhibitors as well (Figure 4.7B).

4.2.3 Constitutive Nrf2 activation attenuates expression of IL-1 β

To prove the involvement of Nrf2 in the mechanism by which 15d-PGJ₂ confers its effects in monocytes, we began to use a siRNA-based loss-of-function approach. Because silencing of Nrf2 in THP-1 monocytes led to their apoptosis, this strategy turned out to be virtually impossible. Alternatively, we went on to manipulate the expression of Nrf2 in an indirect manner, by depleting its negative regulator, Keap-1. Using RNA interference we could achieve a significant ($\sim 80\%$) reduction in Keap-1 mRNA (Figure 4.8A) and a decrease in Keap-1 protein expression to less than 10% of control (Figure 4.8B). Compared to control cells transfected with non-silencing siRNAs, knockdown of Keap-1 in THP-1 monocytes substantially boosted basal expression of Nrf2 and enhanced its accumulation in the nucleus (Figure 4.8D). Consistent with constitutive stabilization of Nrf2, silencing of Keap-1 alone triggered the up-regulation of Nrf2-dependent genes, such as the inducible HO-1 (Figure 4.8C, D). In addition, similar to 15d-PGJ₂ and Bardoxolone, up-regulation of Nrf2 activity in Keap-1-depleted THP-1 cells attenuated the TNF- α -induced expression of IL-1 β (Figure 4.8E), further supporting the notion that Nrf2 is required to mediate the anti-inflammatory activity of 15d-PGJ₂ in monocytes, at least for this gene product.

4.2. Investigation of molecular mechanisms underlying the anti-inflammatory activity of 15d-PGJ₂ in human monocytes

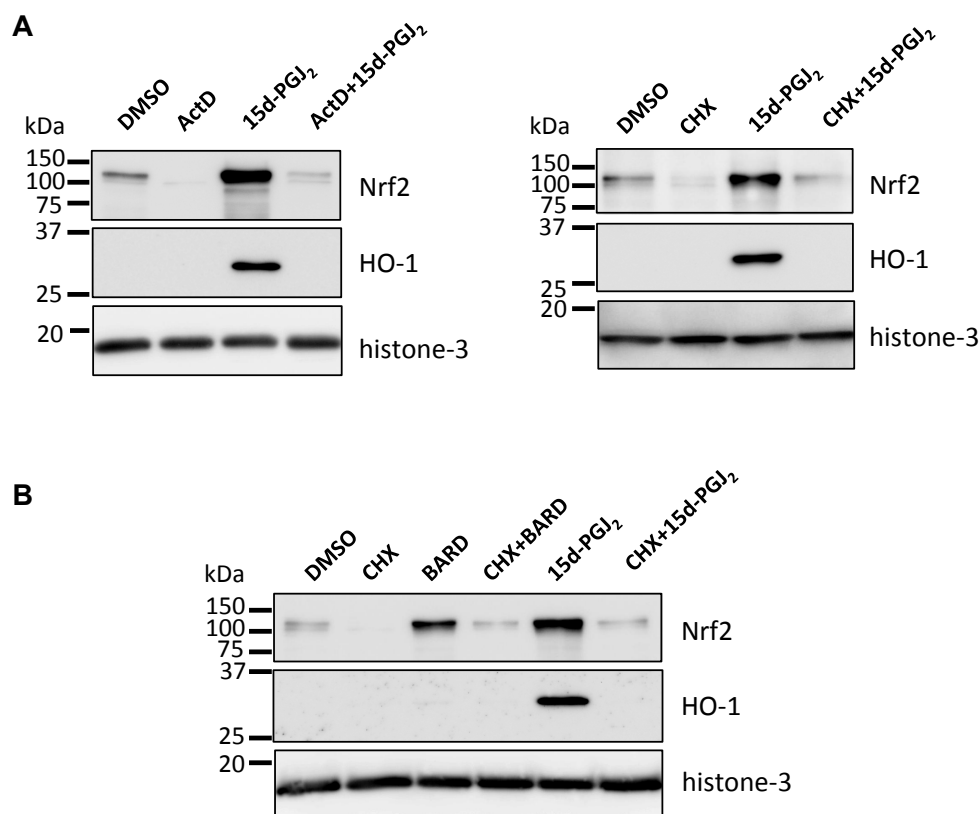


Figure 4.7: 15d-PGJ₂ and Bardoxolone induce accumulation of *de novo* synthesized Nrf2 in the nucleus. (A) THP-1 monocytes were pre-treated or not for 1 hour with transcription (left) or translation (right) inhibitors, actinomycin D (ActD; 0.3 μ M) or cycloheximide (CHX; 1 μ g/ml). Cells were subsequently incubated with 10 μ M 15d-PGJ₂ or DMSO (solvent control) for 4 hours. Nuclear extracts were prepared and subjected to Western blot analysis using anti-Nrf2 and anti-histone-3 antibodies. HO-1 was used as a read-out for inhibitory potential of ActD and CHX, respectively. Images are representative of five independent experiments. (B) THP-1 monocytes were pre-treated or not for 1 hour with CHX, and subsequently exposed to 10 μ M 15d-PGJ₂, 50 nM BARD or DMSO for another 4 hours. The image is representative of five independent experiments.

4.2.4 HO-1 is not a direct mediator of the anti-inflammatory activity of 15d-PGJ₂ in THP-1 monocytes

Because of its potent anti-inflammatory properties, 15d-PGJ₂ has been proposed as a promising therapeutic compound for treatment of inflammatory disorders. Understanding the molecular mechanism through which 15d-PGJ₂ exerts its protective action could therefore contribute to the development of anti-inflammatory therapies and further clarify the biological role of this prostaglandin. However, little is known regarding the molecular machinery that governs the anti-inflammatory activity of 15d-PGJ₂. Prompted by the intriguing finding that Nrf2 acts as a down-stream mediator of 15d-PGJ₂ signaling, we sought to elucidate the molecular mechanism through which 15d-PGJ₂-induced

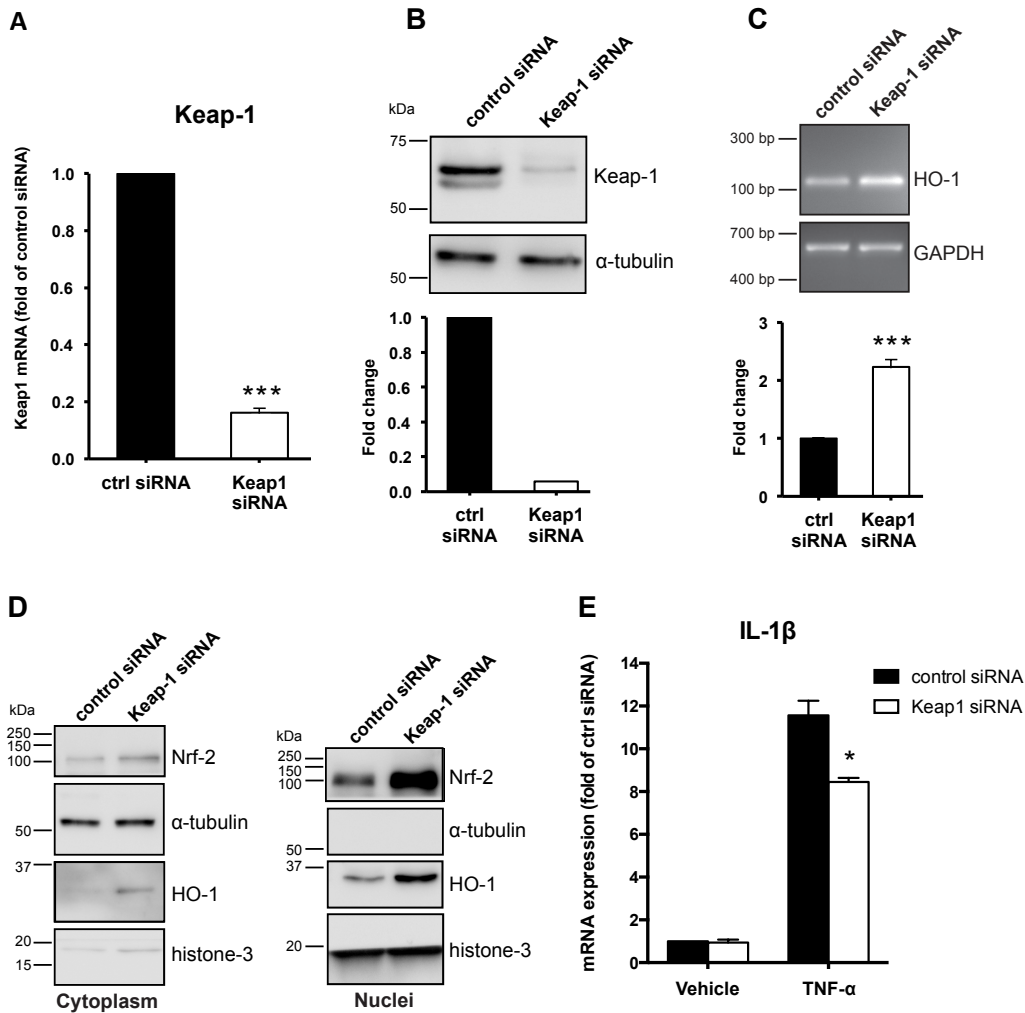


Figure 4.8: Knockdown of the negative Nrf2 regulator Keap-1 attenuates IL-1 β expression. (A) The relative expression levels of Keap-1 transcript were determined using real-time qRT-PCR 48 hours post transfection with either a non-silencing control siRNA or a Keap1-targeting siRNA; $n=3$, mean \pm SEM, *** $p<0.001$ vs. control siRNA; unpaired Student's t-test. (B) Representative ($n=3$) Western blot analysis of Keap-1 expression 48 hours post-transfection with the siRNAs. (C) Basal mRNA levels of HO-1 were examined using semi-quantitative RT-PCR 48 hours post transfection; $n=3$, mean \pm SEM, *** $p<0.001$ vs. control siRNA; unpaired Student's t-test. (D) Nuclear and cytoplasmic extracts from THP-1 cells with Keap1 knockdown were analyzed by Western blot for Nrf2 and HO-1; two blots representative for 3 individual experiments each are shown. (E) Real-time qRT-PCR analysis of IL-1 β mRNA abundance 48 hours post-transfection with Keap-1-targeting but not control siRNA, followed by a 6-hour stimulation with 1000 U/ml TNF- α , reveals a significant down-regulation; $n=3$, mean \pm SEM, * $p<0.05$ vs. TNF- α -stimulated control siRNA; unpaired Student's t-test.

Nrf2 represses the expression of *IL-1B* and possibly other pro-inflammatory genes in monocytes.

Whether Nrf2 inhibits the expression of IL-1 β by directly binding to an ARE response element in the *IL-1B* promoter, or indirectly, through an up-regulation of HO-1 and/or other Nrf2-dependent genes, remains unclear. In addition to its cytoprotective role, HO-1

4.2. Investigation of molecular mechanisms underlying the anti-inflammatory activity of 15d-PGJ₂ in human monocytes

and its reaction products, have been recently recognized to have major immunomodulatory and anti-inflammatory properties (for a review, see Paine et al. (2010)). Given that the suppressive activity of 15d-PGJ₂, as well as Bardoxolone, coincided with the induction of HO-1 expression in THP-1 cells, it is tempting to speculate that Nrf2 may inhibit IL-1 β expression indirectly through increasing abundance of this anti-oxidant enzyme (see model, Figure 4.9). Nonetheless, the time course of HO-1 induction upon exposure to 15d-PGJ₂ did not correlate with the time course of inhibition of *IL-1B* transactivation. A significant rise in HO-1 protein was first detected at 2 hours after the addition of 15d-PGJ₂ (i.e., 60 min post-stimulation with TNF- α), whereas the diminution in IL-1 β mRNA levels occurred earlier than that (i.e., within 30 min after TNF- α stimulation or 90 min after treatment with 15d-PGJ₂) (Figure 4.10A, left panel). Moreover, pharmacological blockade of HO-1 activity in THP-1 monocytes showed that the latter hypothesis may probably be incorrect (Figure 4.10C).

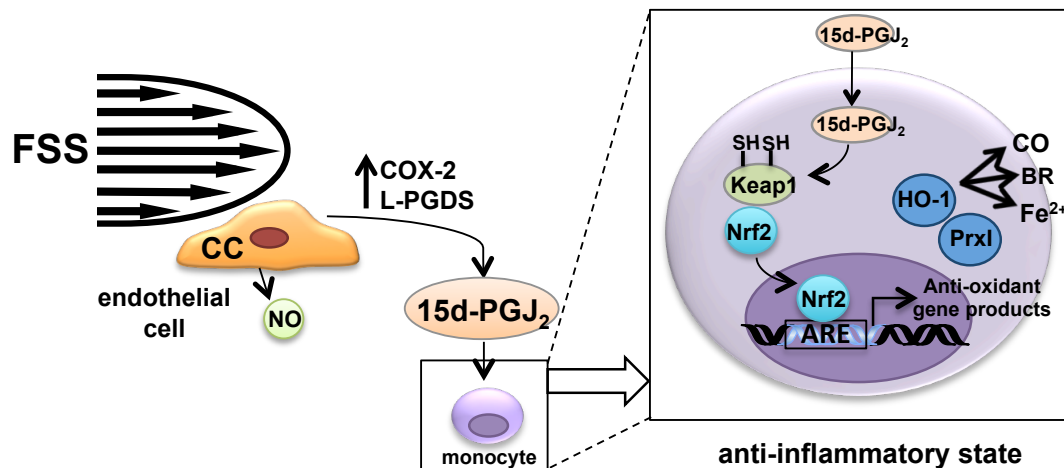


Figure 4.9: A model for compensatory anti-inflammatory mechanism in endothelial cells (ECs) with insufficient NO synthesis. In CC-genotype ECs, FSS causes a weak up-regulation of NOS-3 expression, resulting in a reduced NO synthesis capacity. To compensate for inadequate NO production, CC-genotype ECs up-regulate expression of COX-2 and L-PGDS in response to FSS, leading to an increased release of the anti-inflammatory prostanoid 15d-PGJ₂, which acts on circulating monocytes to prevent their endothelial adhesion and transmigration. EC-derived 15d-PGJ₂ maintains monocytes in an anti-inflammatory state by facilitating the nuclear accumulation and activation of the cytoprotective TF Nrf2. 15d-PGJ₂-Nrf2-mediated expression of anti-oxidant enzymes (e.g., HO-1 and its products carbon monoxide (CO), iron (II) (Fe²⁺), and bilirubin (BR)) promotes the quiescent phenotype and thus may be an adaptive mechanism to reinforce the anti-inflammatory capacity of ECs with compromised NO synthesis and protects against endothelial dysfunction.

Conversely, the time course of CD40 mRNA expression in TNF- α -stimulated THP-1 monocytes was very different from that of IL-1 β (Figure 4.10A, right panel). While stimulation with TNF- α caused a rapid induction of the *IL-1B* gene peaking at 1 hour, it induced a near linear increase in CD40 mRNA levels ($R^2=0.98$) over 6 hours. This

gradual increase in CD40 transcripts was similarly reduced by pretreatment with 15d-PGJ₂. In this context it was interesting to note that the rapid down-regulation of the CD40 gene by 15d-PGJ₂ coincided with the onset of HO-1 protein expression (Figure 4.10B). Therefore, activity of HO-1 could potentially contribute to the reduced expression of this co-stimulatory molecule in 15d-PGJ₂-treated THP-1 cells. The specific Nrf2 inducer Bardoxolone however did not exhibit an effect on CD40 transcript expression (Figure 4.10D), ruling out a major role of the Nrf2-Keap1 pathway in the inhibitory effect of 15d-PGJ₂ on transcription of the CD40 gene. Collectively, these data point to distinct mechanisms through which 15d-PGJ₂ modulates the expression of pro-inflammatory genes.

The fact that the inhibitory effect of 15d-PGJ₂ on IL-1 β expression commenced immediately after its addition points to the existence of a direct, rapid mechanism hampering up-regulation of transcription of the *IL-1B* gene in response to pro-inflammatory stimuli. Moreover, 15d-PGJ₂-activated Nrf2 had already begun to accumulate in the nucleus at the time when repression of the *IL-1B* gene became apparent. Hence, a direct 15d-PGJ₂-induced interplay between Nrf2 and pro-inflammatory TFs (such as AP-1 or NF- κ B) to prevent transcription of the *IL-1B* gene cannot be excluded at this point.

4.2. Investigation of molecular mechanisms underlying the anti-inflammatory activity of 15d-PGJ₂ in human monocytes

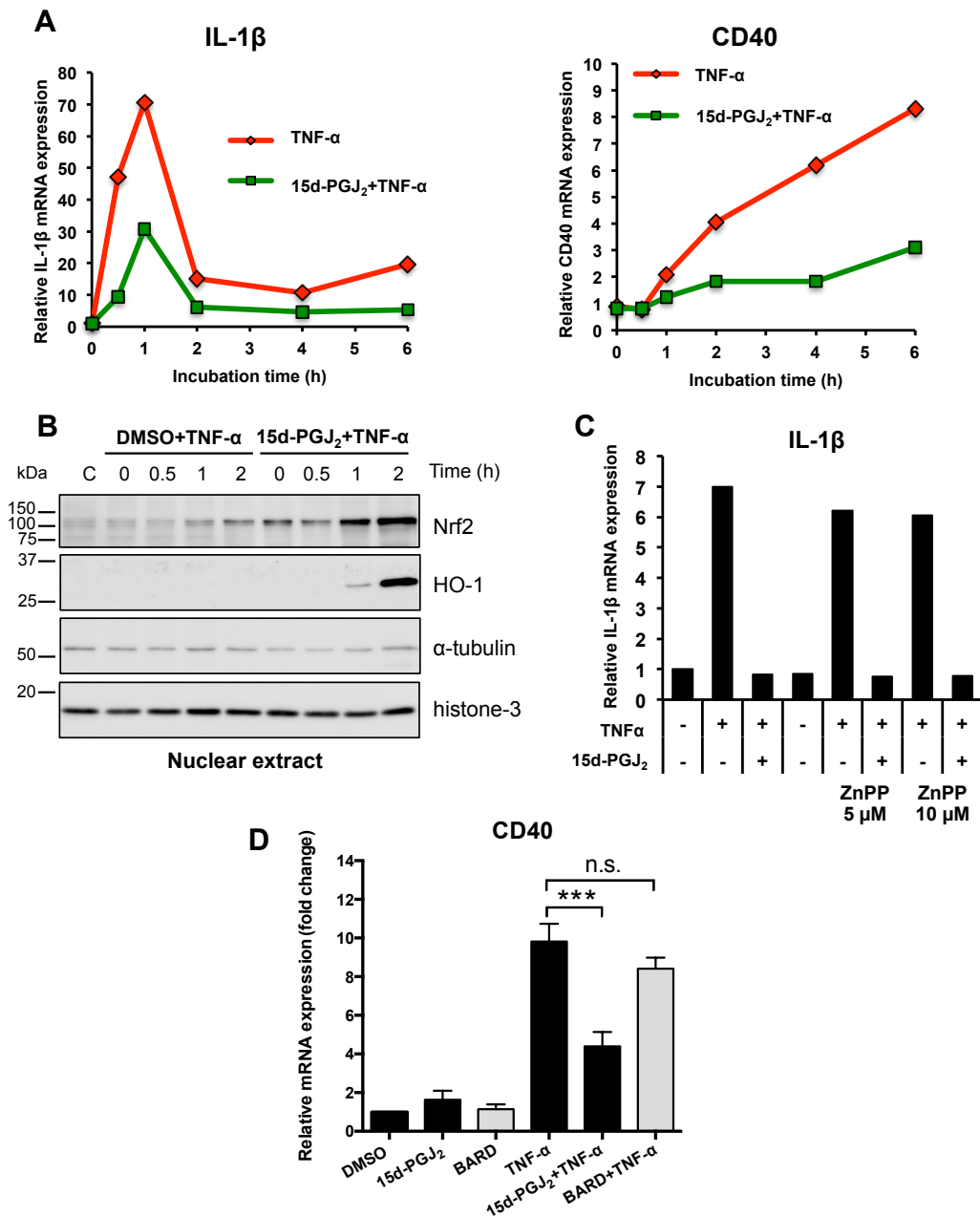


Figure 4.10: HO-1 inhibition does not abrogate the suppressor effect of 15d-PGJ₂ on *IL-1B* gene transcription. (A) Time course of changes in IL-1 β (left) and CD40 (right) mRNA levels in THP-1 monocytes following 1 hour pre-incubation with 15d-PGJ₂ (10 μ M, green) or DMSO (red), and subsequent addition of TNF- α (1000 U/ml) for the indicated times. (B) Representative Western blot analysis (n=2) of the time course of HO-1 expression, as well as the time course of accumulation of Nrf2 in the nucleus of THP-1 cells pre-incubated for 1 hour with DMSO or 15d-PGJ₂ and stimulated with TNF- α for the indicated times. “C” designates a non-treated control. (C) Relative mRNA expression of IL-1 β in THP-1 cells treated with the HO-1 inhibitor zinc protoporphyrin IX (ZnPP) at 5 and 10 μ M, respectively, for 1 hour followed by a 1-hour incubation with solvent or 15d-PGJ₂ (10 μ M) and 4-hour stimulation with TNF- α (1000 U/ml) (data acquired with the help of Dr. Sviatlana Gehrman). (D) Real-time qRT-PCR analysis of relative CD40 mRNA expression in THP-1 cells pre-treated for 1 hour with either 10 μ M 15d-PGJ₂ or 50 nM BARD and subsequently stimulated for 6 hours with 1000 U/ml TNF- α ; n=3 \pm SEM; ***p<0.001 TNF- α -stimulation vs. 15d-PGJ₂ + TNF- α , one-way ANOVA with post-hoc Tukey’s multiple comparison test; n.s., non-significant.

4.2.5 15d-PGJ₂ inhibits *IL-1B* gene expression at the transcriptional level

On the other hand, we identified three ARE-like sequence motifs (i.e., Nrf2-like binding sites) in the *IL-1B* gene promoter region (Figure 4.11B), suggesting that Nrf2 may act through an as yet unknown mechanism by which it directly interacts with the *IL-1B* promoter to repress transcription of the *IL-1B* gene (see model, Figure 4.11A). In fact, using chromatin immunoprecipitation (ChIP) we could demonstrate a 15d-PGJ₂-induced binding of Nrf2 to the region of the *IL-1B* gene promoter that harbors the three putative ARE-like sites (Figure 4.11C).

To assess the functional relevance of the detected Nrf2-*IL-1B* promoter interaction, we employed a luciferase reporter gene assay. For this purpose, we established a reporter assay system utilizing the easily transfectable HEK293 cell line and a DNA construct containing a 1.6-kb fragment of the human *IL-1B* gene promoter cloned in front of a luciferase reporter gene. Activity of the reporter gene construct was induced by stimulation with TNF- α . However, we observed a rather modest, though reproducible and statistically significant up-regulation of reporter gene expression in response to TNF- α , which we suspected is due to the absence of an essential enhancer region from the *IL-1B* promoter fragment inserted into the construct. At the same time, the reporter gene construct reproducibly revealed a rather high basal luciferase expression. In this experimental setting, exogenously added 15d-PGJ₂ completely abolished TNF- α -induced reporter gene expression (Figure 4.11D), demonstrating that the inhibitory Nrf2-mediated effect of this prostanoid on the *IL-1B* gene occurs on the level of transcription.

To verify the contribution of the identified ARE-like motifs to the observed inhibition of *IL-1B* promoter activity in response to 15d-PGJ₂, we deleted the core sequences of each of these DNA elements (Figure 4.12A), and subsequently analyzed the effect of 15d-PGJ₂ on the activity of the wild-type and mutant *IL-1B* promoter-reporter gene constructs. However, none of the deletion mutants was capable of attenuating the potent suppressor activity of 15d-PGJ₂ on the *IL-1B* promoter (Figure 4.12B).

Similarly, the specific Nrf2 inducer, Bardoxolone, effectively suppressed the *IL-1B* promoter activity both in the presence and absence of the intact ARE motifs (Figure 4.12C).

4.2. Investigation of molecular mechanisms underlying the anti-inflammatory activity of 15d-PGJ₂ in human monocytes

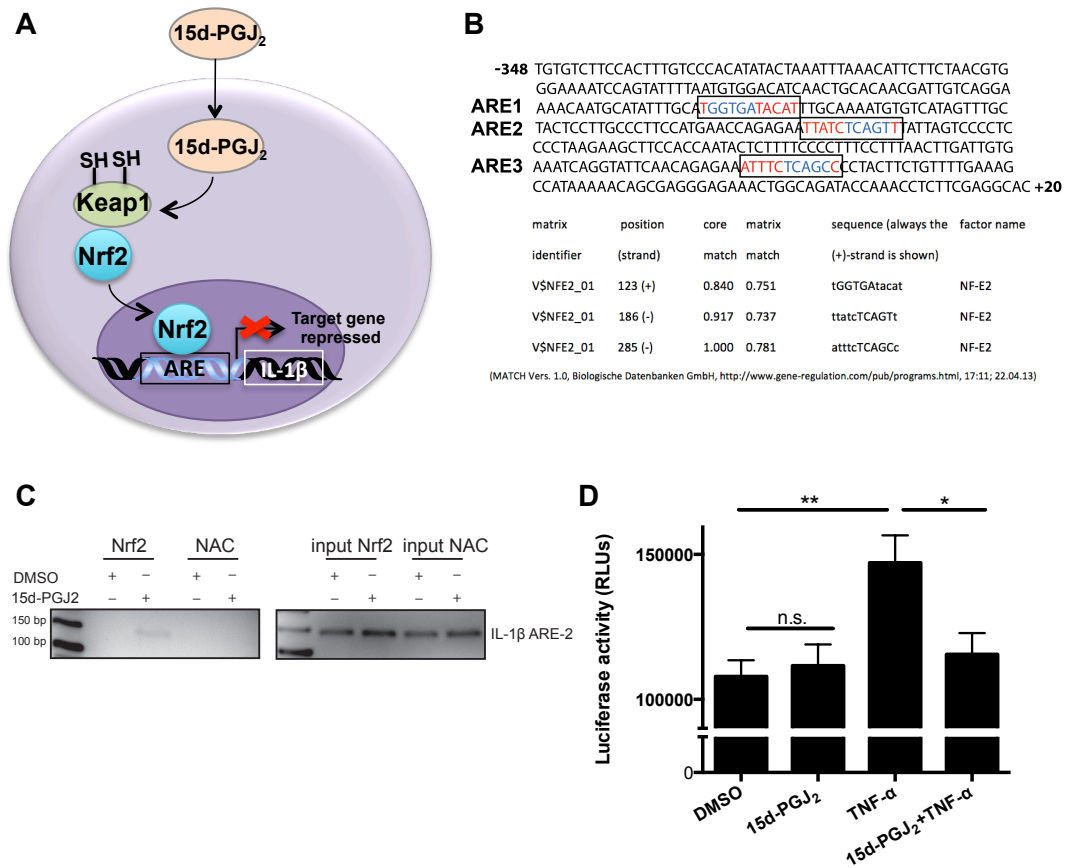


Figure 4.11: 15d-PGJ₂ inhibits the expression of the *IL-1B* gene at the transcriptional level. (A) 15d-PGJ₂-Nrf2-mediated direct transcriptional repression could be a potential mechanism to inhibit *IL-1β* expression. (B) Putative Nrf2 consensus binding sites (AREs) in the proximal promoter of the human *IL-1B* gene were identified using the MatInspector software (in collaboration with PD Dr. Andreas Wagner; Institute of Physiology and Pathophysiology, Heidelberg University). The ARE-like motifs are highlighted in red with their core sequences in blue. The strand positions, similarity scores and sequences of each binding site are indicated. (C) 15d-PGJ₂ induces binding of Nrf2 to the human *IL-1B* promoter. Chromatin from THP-1 cells, treated with 10 μM 15d-PGJ₂ for 4 hours, was immunoprecipitated or not (no antibody control, NAC) with an anti-Nrf2 antibody, and Nrf2 binding analyzed by PCR with specific primers for the ARE-2 region of the *IL-1B* promoter (product size: 136 bp). The ARE-2 region was amplified from 5 μl of purified soluble chromatin before immunoprecipitation to show input DNA; representative PCR analysis of 3 independent experiments (D) HEK293 cells were transfected with human *IL-1B* promoter-luciferase reporter gene construct. Twenty-four hours following transfection, cells were pre-treated with 10 μM 15d-PGJ₂ for 1 hour prior to induction of reporter gene expression with 1000 U/ml TNF-α. Eighteen hours post stimulation, activity of the secreted *Gaussia* luciferase was assessed in the cell culture supernatant; n=4; error bars represent means ± SEM; one-way ANOVA with post-hoc Tukey's multiple comparison test; *p<0.05, **p<0.01.

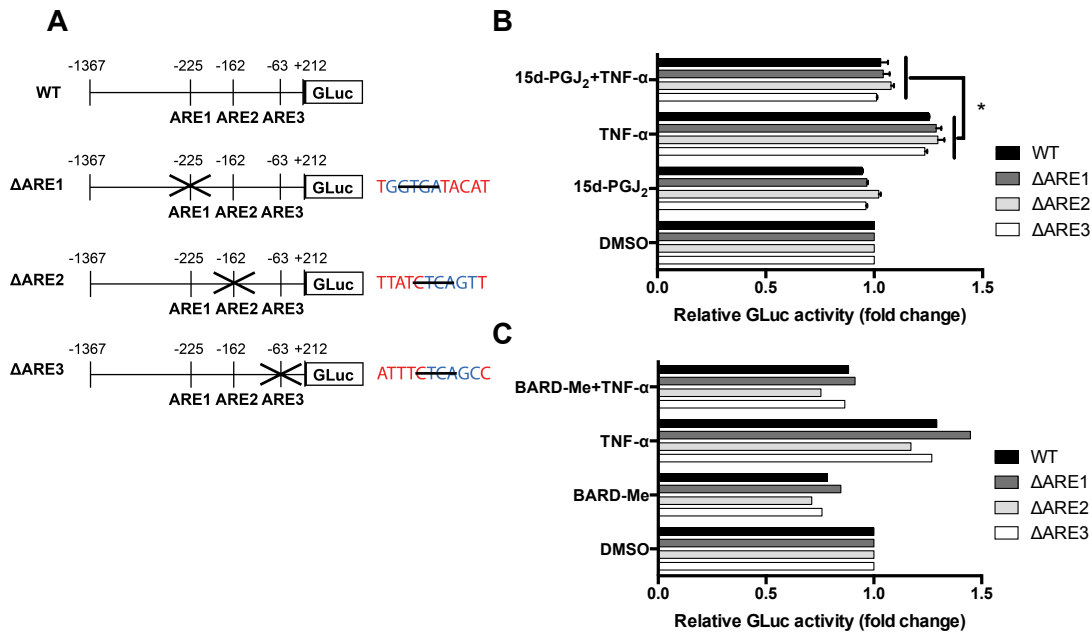


Figure 4.12: Deletion of ARE-like Nrf2-binding sites in the *IL-1B* promoter does not alter the transcriptional repressor activity of 15d-PGJ₂. (A) Schematic representation of the wild type and deletion *IL-1B* promoter-reporter constructs. The core sequences of each of the 3 ARE-like motifs were disrupted using site-directed mutagenesis. One ARE was targeted per construct (the deleted sequences are shown on the right), whereas the other 2 were left intact. (B) Twenty-four hours following transfection with wild-type or deletion mutant reporter gene constructs, cells were pre-treated with 10 μ M 15d-PGJ₂ for 1 hour prior to an induction of the promoter-reporter activity with 1000 U/ml TNF- α . Eighteen hours post stimulation, activity of the secreted *Gaussia* luciferase was assessed in cell supernatants. Luciferase activity was calculated relative to the DMSO control of each of the respective types of reporter gene constructs; n=3; mean \pm SEM; one-way ANOVA with post-hoc Tukey's multiple comparisons test; *p<0.05 vs. TNF- α stimulation. (C) Twenty-four hours post-transfection, cells were pre-treated with 50 nM BARD-Me for 1 hour prior to an induction of the promoter-reporter activity with 1000 U/ml TNF- α . Luciferase activity was assessed eighteen hours post stimulation as described before.

4.2.6 Silencing of Nrf2 does not abrogate the transcriptional repressor activity of 15d-PGJ₂

To exclude a contribution of the non-mutated ARE motif as well as the potential cooperative interaction of Nrf2 with other TFs, which may obscure the effect of deleting only a single ARE motif on *IL-1B* promoter-reporter gene activity, we went on to transiently silence expression of Nrf2 in the HEK293 cells. Unlike in THP-1 monocytes, siRNA-mediated depletion of Nrf2 in these cells turned out to be feasible. We could successfully knockdown Nrf2 on the mRNA level (Figure 4.13A), and inhibit its activity, as evidenced by the reduced expression of Nrf2-dependent genes such as HO-1 as well as the inability of Nrf2 to translocate to the nucleus in response to Bardoxolone treatment (Figure 4.13B). This pronounced drop in nuclear Nrf2 protein following siRNA-based knockdown further

corroborates our finding that it is primarily the newly synthesized Nrf2, which translocates to the nucleus upon induction of the Keap1-Nrf2 pathway. Using this approach, we next re-examined the effects of 15d-PGJ₂ on transactivation of the non-mutated *IL-1B* promoter in the absence of Nrf2. Down-regulation of Nrf2 expression ($80 \pm 2\%$ reduction in Nrf2 mRNA expression; Figure 4.13C) attenuated the relative induction of the *IL-1B* promoter-reporter gene construct in response to TNF- α , so that there was no longer a significant difference between stimulated and basal promoter-reporter gene activity (Figure 4.13D). Nonetheless, even when Nrf2 was nearly completely silenced, 15d-PGJ₂ was still able to significantly down-regulate TNF- α -induced expression of the *IL-1B* promoter-reporter gene construct (Figure 4.13D).

4.2.7 Deletion of ARE-like motifs 2 and 3 in the *IL-1B* promoter may attenuate the transcriptional repressor activity of 15d-PGJ₂

Given that the high basal activity of the promoter-reporter gene construct in the HEK293 cells might mask weak stimulatory or inhibitory effects on the *IL-1B* promoter, and thus obscure the impact of Nrf2 silencing, we aimed at increasing the signal-to-noise ratio of the reporter gene assay. For this purpose, we cloned the full-length *IL-1B* promoter into the luciferase reporter vector comprising all *cis*-regulatory sequences necessary to direct expression of the *IL-1B* gene. Contrary to our assumption, the full-length promoter did not potentiate TNF- α -stimulated reporter gene activity, but much like the truncated promoter, maintained a high basal and low inducible promoter activity (Figure 4.14A, B left panels), pointing towards a purely vector-driven unspecific expression of the reporter gene. To improve specific TNF- α -dependent expression of the reporter gene, we reduced the amount of reporter gene construct transfected per cell, and thus minimize cellular saturation by too high concentrations of the vector. Indeed, lowering activity (i.e., bioluminescence) of the reporter gene product down to levels just above background bioluminescence led to an approximately 2-fold increase over baseline in expression of the reporter gene construct (Figure 4.14A, B right panels).

Using this improved reporter gene assay, we re-evaluated the impact of 15d-PGJ₂ on expression of the wild-type and mutant *IL-1B* promoter-reporter gene constructs in the HEK293 cells. As compared with the wild-type promoter, deletion of the ARE2 or ARE3 but not the ARE1 motif reduced the stimulatory potency of TNF- α and concomitantly weakened the inhibitory effect of 15d-PGJ₂, which was no longer significantly different (Figure 4.15). This experiment was done four times so that its outcome has to be interpreted with some caution. Nonetheless, it suggests that the Nrf2-binding ARE-like motifs 2 and 3 in the human *IL-1B* promoter are associated with the transcriptional repressor activity of 15d-PGJ₂, and therefore may be interpreted as evidence for a direct repression of transcription of the *IL-1B* gene by Nrf2.

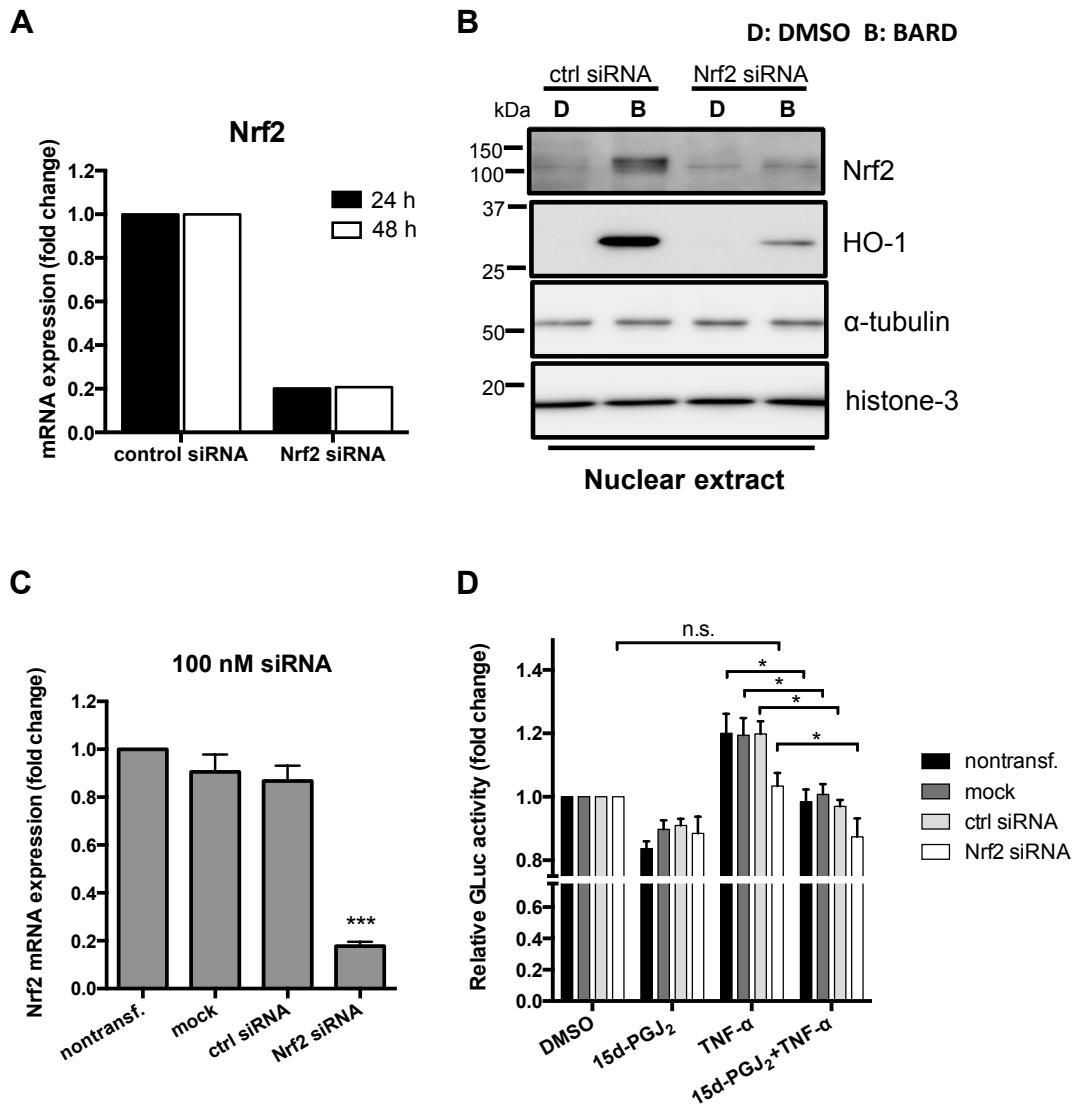


Figure 4.13: Knockdown of Nrf2 does not abrogate the transcriptional repressor activity of 15d-PGJ₂ on the *IL-1B* promoter-reporter gene construct. (A) The expression levels of Nrf2 transcript in HEK293 cells were determined using real-time qRT-PCR, 24 and 48 hours post transfection with either a non-silencing control siRNA pool or an Nrf2-targeting siRNA pool. Data is representative of 2 experiments. (B) Representative (n=3) Western blot analysis of nuclear extracts from control siRNA or Nrf2 siRNA-transfected cells. Thirty hours post-transfection with the respective siRNAs, cells were treated with DMSO or BARD 50 nM for additional 8 hours and subjected to cellular fractionation. Nuclear extracts were assessed for Nrf2 and HO-1 protein abundance. (C) Real-time qRT-PCR analysis of Nrf2 mRNA levels in HEK293 cells transfected with the wild-type *IL-1B* promoter-luciferase gene construct and subsequently subjected to siRNA-mediated Nrf2 knockdown (for transfection and treatment conditions, see sections 3.1.10 and 3.2.10); n=5, mean \pm SEM; ***p<0.001 vs. control siRNA-transfected cells; unpaired Student's t-test. (D) HEK293 cells were transfected with Nrf2-targeting siRNAs 24 hours after transfection with the wild-type *IL-1B* promoter-luciferase gene construct. After an additional 24 hours, cells were pre-treated with 10 μ M 15d-PGJ₂ for 1 hour prior to up-regulation of promoter-reporter gene construct expression with 1000 U/ml TNF- α and subsequent assessment of secreted luciferase activity; n=5, mean \pm SEM; *p<0.05 as indicated; n.s., not significant.

4.2. Investigation of molecular mechanisms underlying the anti-inflammatory activity of 15d-PGJ₂ in human monocytes

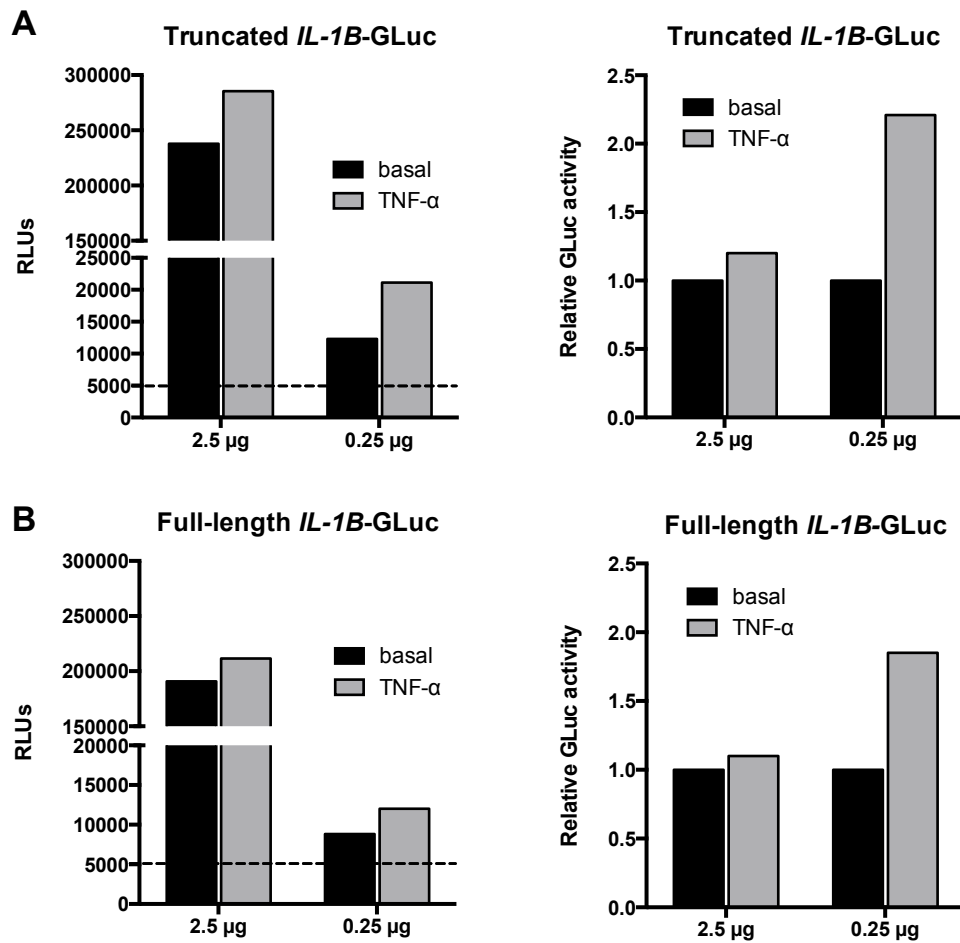


Figure 4.14: Length of the *IL-1B* promoter insert does not influence the basal and TNF- α -induced expression of the luciferase reporter construct. HEK293 cells were transfected with luciferase reporter constructs comprising different length of the human *IL-1B* promoter: (A) “truncated” and (B) “full-length” (see section 3.2.8). Induction of the two promoters was compared at two different concentrations of the respective reporter gene construct per cell, i.e., 2.5 μ g vs. 0.25 μ g per 1×10^6 cells. Twenty-four hours following transfection, the promoters were induced with 1000 U/ml of TNF- α and the activity of the secreted luciferase was subsequently determined as described before. Absolute (RLUs: A, B left) and relative (fold-change over basal expression: A, B right) numbers of *Gaussia* luciferase activity are presented as the mean of two technical replicates from 1 exemplary experiment. Dashed lines designate the background bioluminescence levels of mock-transfected cells.

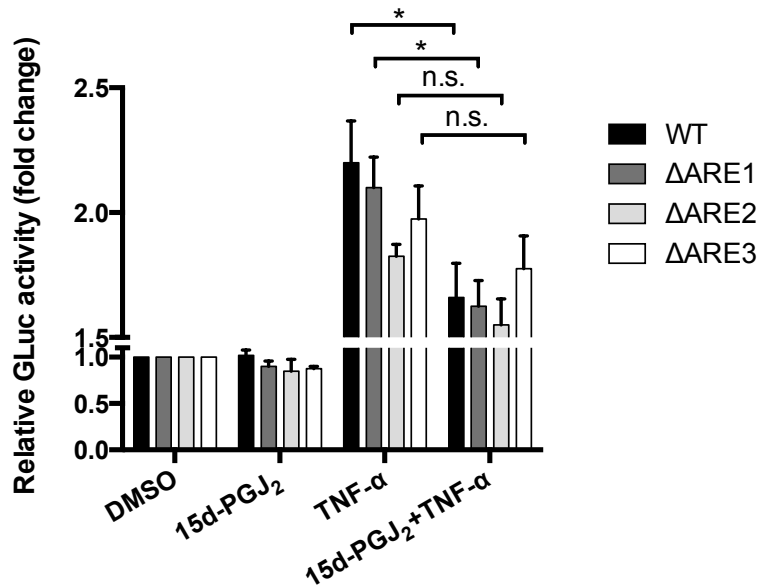


Figure 4.15: Disruption of DNA sequence motifs ARE2 and ARE3 attenuates the inhibitory effect of 15d-PGJ₂ in an improved *IL-1B* promoter-reporter gene assay. Cells were transfected with wild-type *IL-1B* or ARE-deletion mutant *IL-1B* promoter-luciferase constructs (0.25 μ g instead of 2.5 μ g from each construct per 1×10^6 HEK293 cells). Twenty-four hours post transfection, cells were pre-treated with 10 μ M 15d-PGJ₂ for 1 hour prior to exposure to 1000 U/ml TNF- α for 18 hours, followed by determination of activity of the secreted *Gaussia* luciferase in cell supernatants as described before; n=4; mean \pm SEM; one-way ANOVA with post-hoc Tukey's multiple comparison test; *p<0.05 as indicated; n.s., not significant.

4.2.8 Bach1 knockdown does not affect the suppressive activity of 15d-PGJ₂ on the *IL-1B* gene

It is known that Nrf2 requires small Maf proteins (sMaf) as obligatory dimerization partners for their function as transcriptional regulators (for review see Kannan et al. (2012)). The ARE enhancer motif is one form of the Maf response element (MARE), harboring a consensus sequence closely resembling the MARE and a conserved GC flanking element that mediates the specificity of Nrf2 recognition. It is, therefore, critical for the induction of genes by Nrf2 in response to oxidative stimuli. Some variations of the ARE motif can be recognized by other regulatory factors, in addition to Nrf2, including other members of the Cap 'n' Collar (CNC) TF family such as Nrf1 (Venugopal and Jaiswal (1996)), Nrf3 (Sankaranarayanan and Jaiswal (2004)) and Bach1 (BTB and CNC homolog 1) (Oyake et al. (1996)). Variation of ARE motif sequences may therefore contribute to overlapping DNA binding by factors that compete with Nrf2 for the ARE. Such interplay of DNA-binding proteins exists between Nrf2 and Bach1 (Dhakshinamoorthy et al. (2005)).

Bach1 is a transcriptional repressor with poorly characterized function in gene regulation. Like Nrf2, Bach1 forms a heterodimer with sMaf proteins in order to bind DNA. As a repressive TF, Bach1 allows gene induction upon its dissociation from ARE enhancer

motifs (Sun et al. (2004)). In this regard, the nuclear export of this protein in response to stimuli precedes its inactivation and proteasomal degradation in the cytoplasm.

The effects of 15d-PGJ₂ on Bach1 activity and function have not yet been elucidated. Due to the lack of a specific anti-Bach1 antibody, we were unable to assess the sub-cellular localization of Bach1 protein after treatment with 15d-PGJ₂, which similar to Nrf2 reflects its activity. Hence, elimination of Bach1 from our genetic reporter system turned out to be the best alternative to study its impact on *IL-1B* gene expression. We could achieve a 60% reduction of Bach1 mRNA expression (Figure 4.16A) in transiently siRNA-transfected HEK293 cells. Because antibody-based confirmation of the knockdown was impossible, we analyzed the expression of HO-1, a gene also regulated by Bach1, as a functional readout for the diminished function of this transcriptional repressor. Consistent with previous reports, silencing of Bach1 triggered induction of the HO-1 gene (Figure 4.16B). Finally, we analyzed the effect of Bach1 knockdown on the expression of the wild-type and mutant *IL-1B* promoter-reporter gene constructs. Despite reduced function of Bach1, the potent inhibitory effect of 15d-PGJ₂ on the wild-type and all ARE-mutated constructs remained unaltered (Figure 4.16C), thus excluding Bach1 as a potential repressor of the *IL-1B* gene downstream of 15d-PGJ₂.

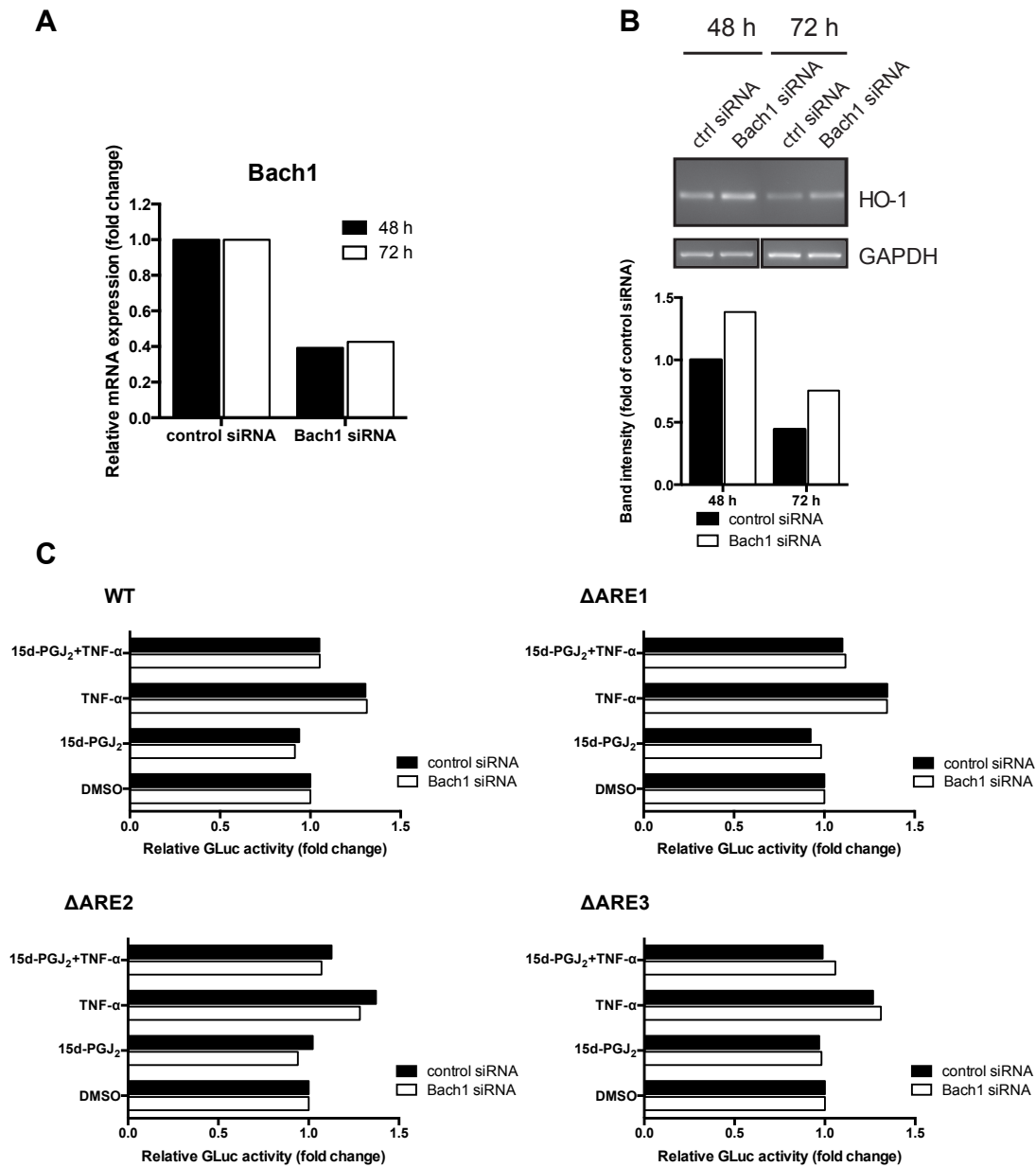


Figure 4.16: Bach1 knockdown does not affect the repressor activity of 15d-PGJ₂ on the *IL-1B* gene. (A) Bach1 transcript (mRNA) levels were determined using real-time qRT-PCR 48 and 72 hours post transfection with either a non-silencing control siRNA or a Bach1-targeting siRNA. Relative mRNA expression was expressed as fold-change over control siRNA-transfected cells; n=2. (B) Representative RT-PCR analysis (n=2) of basal HO-1 mRNA expression in HEK293 cells transfected with either a non-silencing control siRNA or Bach1-targeting a siRNA. HO-1 transcript levels were determined 48 and 72 hours post-transfection. Band intensities were quantified using ImageJ densitometry software. (C) An exemplary experiment showing the effect of Bach1 silencing on the *IL-1B* promoter-reporter gene construct expression. Twenty-four hours after transfection with either a non-silencing control siRNA or a Bach1-targeting siRNA, HEK293 cells were transfected with wild-type *IL-1B* or ARE-deletion mutant *IL-1B* promoter-reporter gene constructs. After an additional 24 hours, cells were pre-treated with 10 μ M 15d-PGJ₂ for 1 hour prior to up-regulation of promoter-reporter gene expression with 1000 U/ml TNF- α for 18 hours, followed by determining activity of the secreted *Gaussia* luciferase in cell supernatants as described before.

4.2.9 Inhibition of histone deacetylase and p300/CBP histone acetyltransferase activities does not reverse the repressor effect of 15d-PGJ₂ on the *IL-1B* promoter transcriptional activity

Histone acetylation is an epigenetic mechanism considered to be of great relevance for gene regulation. Acetylation of histone-3 (H3), e.g. at lysyl residue 27, and 4 (H4), in particular, relaxes the chromatin structure (unwinds 146 bp of DNA from the histones) and allows access of gene regulatory proteins such as TFs and components of the general transcriptional machinery to target this stretch of the promoter of a gene, which is commonly referred to as nucleosome. Conversely, histone deacetylation leads to transcriptional repression through localized chromatin compaction whereby the nucleosome is wrapped around the core histones. The dynamic state of histone acetylation and deacetylation is maintained through the physical and functional interplay between co-activators and histone acetyltransferases (HATs) or histone deacetylases (HDACs) (for review, see Haberland et al. (2009); Dancy and Cole (2015)). Transcriptional activation of a number of pro-inflammatory genes has been found to depend on the increase in acetylation of H3 and H4 (Park et al. (2004); Miao et al. (2004)), whereas repression correlates with deacetylation of these histones (Ito et al. (2000); Ito et al. (2002)). 15d-PGJ₂ has been shown to suppress genes encoding pro-inflammatory cytokines by modulating the activity and/or interfering with the recruitment of histone-modifying enzymes such as the HATs p300/CBP or HDACs (Farrajota et al. (2005); Engdahl et al. (2007)). Therefore we investigated the ability of 15d-PGJ₂ to affect expression of the *IL-1B* gene through mechanisms involving HDACs or p300/CBP.

The effect of 15d-PGJ₂ on histone acetylation at the *IL-1B* gene promoter was explored using Trichostatin A (TSA), a broad spectrum HDAC inhibitor acting on class I and II HDACs, and the p300/CBP HAT-specific inhibitor, C646. TSA pre-treatment significantly up-regulated basal expression of the full-length *IL-1B* promoter-reporter gene construct in the HEK293 cells and, in addition, markedly potentiated the stimulatory effect of TNF- α on expression of the reporter gene (Figure 4.17A, left and right), implying the existence of a HDAC-dependent inhibitory element in our reporter gene assay. Conversely, inhibition of p300/CBP HATs albeit not significantly reduced basal but not TNF- α -induced expression of the reporter gene construct (Figure 4.17B, left and right panel). While TSA clearly failed to overcome the inhibitory effect of 15d-PGJ₂ on *IL-1B* reporter gene activity (Figure 4.17A, left panel) and IL-1 β expression in THP-1 cells (Figure 4.17A right panel), C646 at first seemed to somewhat attenuate the inhibitory effect of 15d-PGJ₂ in the reporter gene assay (Figure 4.17B, left panel) but was then attributed to dilution of the inhibitory capacity 15d-PGJ₂ in the modified reporter gene assay (Figure 4.17B, right panel).

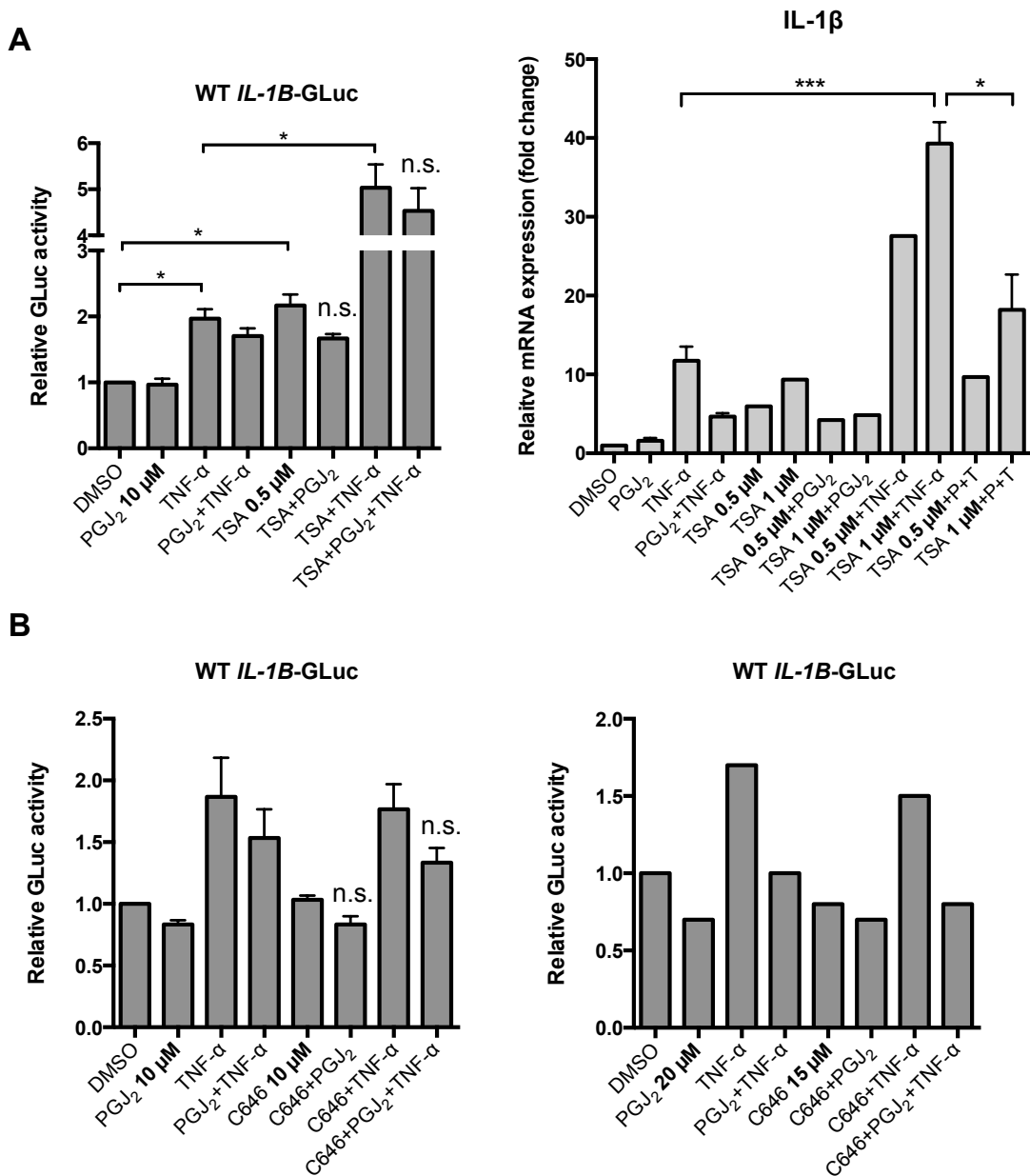


Figure 4.17: Inhibition of HDACs and p300/CBP HATs does not reverse the repressor activity of 15d-PGJ₂ on the *IL-1B* gene. (A, left panel) Twenty-four hours following transfection with wild-type *IL-1B* promoter-luciferase reporter gene construct HEK293 cells were pre-treated with 0.5 μM TSA for 1 hour, followed by 1-hour pre-incubation with 10 μM 15d-PGJ₂ and exposure to 1000 U/ml TNF-α for another 18 hours after which activity of the secreted *Gaussia* luciferase was assessed in the cell supernatants as described before; n=3, means ± SEM; *p<0.05 as indicated; n.s., not significant. (A, right panel) Real-time qRT-PCR analysis of relative *IL-1β* mRNA expression in THP-1 cells pre-treated for 1 hour with either 0.5 μM or 1 μM TSA, followed by 1 hour pre-incubation with 10 μM 15d-PGJ₂ and 4 hours exposure to 1000 U/ml TNF-α; n=2-3 ± SEM (when n=3); *p<0.05, ***p<0.001 as indicated. (B) HEK293 cells were transfected with the wild-type *IL-1B* promoter-luciferase reporter gene construct as described above. Pre-treatment with 10 μM (left panel) or 15 μM (right panel) C646 for 1 hour was followed by an incubation with 10 μM (left panel) or 20 μM (right panel) 15d-PGJ₂ for an additional 1 hour and subsequent exposure to 1000 U/ml TNF-α for 18 hours. Luciferase activities were assayed as described before; n=3 (left panel), n=1 (right panel); n.s., not significant; PGJ₂ - 15d-PGJ₂; T - TNF-α; P - 15d-PGJ₂.

4.3 Increased 15d-PGJ₂ plasma levels in patients suffering from coronary heart disease

Given its immune-modulatory properties, 15d-PGJ₂ may exert potent anti-inflammatory activities that modulate vascular inflammation as well as atherogenesis in affected individuals. To evaluate its relevance as a (prognostic) marker and possibly also as a maker, we compared 15d-PGJ₂ plasma levels, in patients with coronary heart disease (CHD) and age-matched controls (in collaboration with Dres. Florian Leuschner, Maik Brune and Thomas Fleming, all University Hospital Heidelberg).

After genotyping patients and controls for the T-786C SNP of the *NOS3* gene, we observed comparable allele frequencies as previously published (Cattaruzza et al. (2004)) with a slightly higher percentage of CC-genotype carriers in the CHD patient group who all suffered from severe, i.e., multivessel CHD (Figure 4.18).

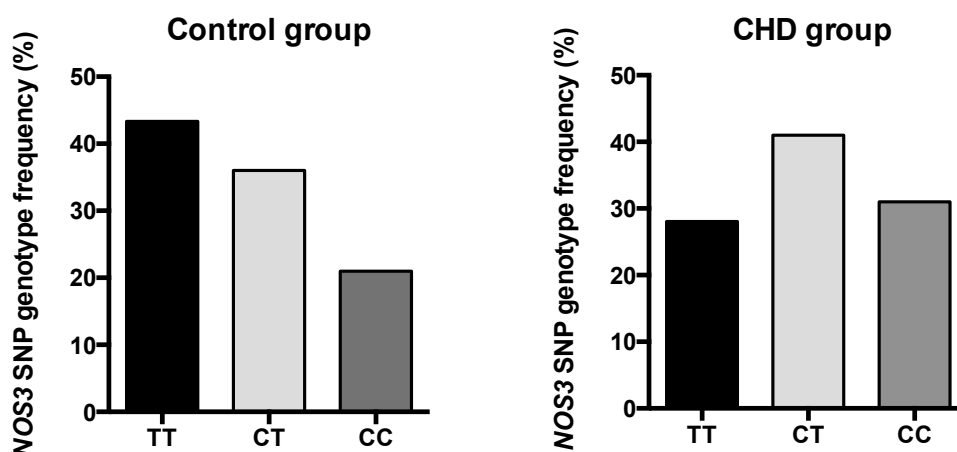


Figure 4.18: Prevalence of the -786C-allele is greater in patients suffering from CHD. T-786C *NOS3* SNP genotype frequencies were analyzed in the control (n=108) and the CHD group (n=32), respectively. Odd ratios (OR) of CHD patients vs. control (CHD-negative) patients: CC, OR = 2.17, p<0.140; CT, OR = 1.63, p<0.317; TT, OR = 0.46, p<0.140

We found that the levels of 15d-PGJ₂ were markedly increased in the CHD group (about 6-fold) as compared to the age-matched controls (Figure 4.19A), suggesting that 15d-PGJ₂ may constitute a general defence mechanism to counteract the ongoing chronic inflammatory process even in patients that are not affected by the T-786C SNP of the *NOS3* gene. Therefore, we next compared the plasma levels of 15d-PGJ₂ among CHD patients who were homozygous for T- or C-allele or heterozygous (Figure 4.19B). In fact, there were no appreciable differences in plasma concentrations of 15d-PGJ₂ among CHD patients with the three *NOS3* SNP genotypes, however, at present the cohort sizes must be considered too small to perform an unambiguous subgroup analysis and detect a genuine relationship between 15d-PGJ₂ plasma levels and presence of the 3 different

allele combinations. We are therefore continuously acquiring additional samples from patients with CHD and age-matched “healthy” controls.

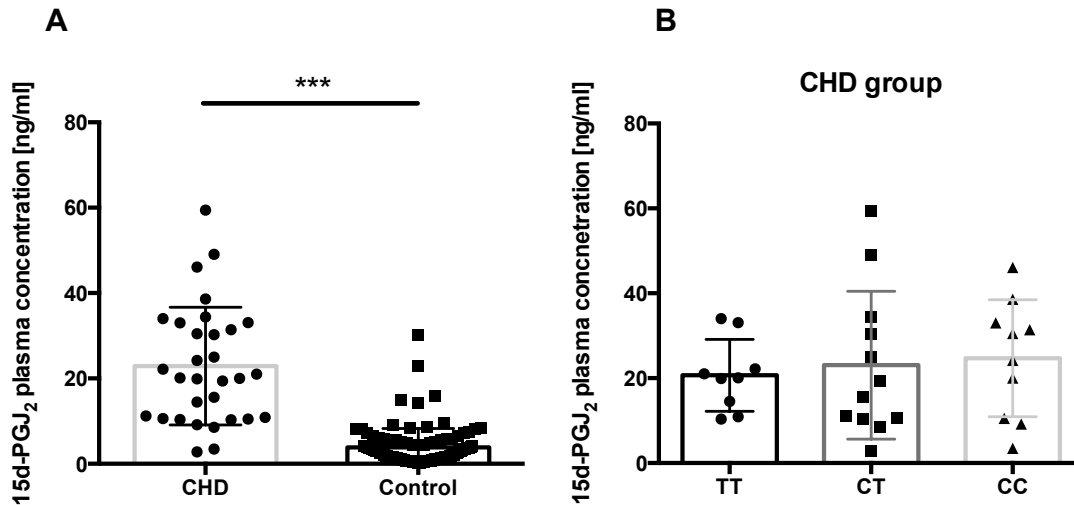


Figure 4.19: Increased 15d-PGJ₂ plasma levels in patients suffering from CHD. (A) Plasma 15d-PGJ₂ concentration was quantified in patients with CHD and in age-matched controls using ultra performance liquid chromatography-tandem mass spectrometry; n=32 (CHD); n=108 (controls); mean \pm SD; unpaired Student’s t-test; ***p<0.001. (B) Plasma 15d-PGJ₂ concentrations in the CHD patient group according to distribution of the genotype for the T-786C SNP of the *NOS3* gene.

4.4 Implications of the T-786C *NOS3* SNP for T helper cell-endothelial cell interactions

4.4.1 Isolation and expansion of human T helper cells

Given the detrimental contribution of T helper 1 cell-driven responses to the process of atherosclerotic as well as all kinds of chronic inflammatory disorders, we have begun to analyze the effect of the T-786C SNP of the *NOS3* gene on the interaction between ECs and Th1 cells *in vitro*. As mentioned before, ECs isolated from individuals homozygous for either the T- or C-allele provide us with a pathophysiologically relevant model for endothelial dysfunction in humans, as well as a well-characterized experimental system to study interactions between dysfunctional endothelial cells and components of the immune system *in vitro*. Using this system, we were able to address for the first time the possible impact of a genetically imprinted endothelial dysfunction on EC-Th1 cell interactions in atherosclerosis. For this purpose, we have begun to isolate and expand naïve CD4⁺ T cells from human blood samples (buffy coats) using commercially available cell isolation kits. Human CD4⁺ T cells can be divided into two subsets based on the expression of different isoforms of CD45 on their surface. CD4⁺ CD45RA⁺ cells represent

the naïve cell population, whereas CD4⁺ CD45RO⁺ cells represent the effector/memory population (Michie et al. (1992)). Naïve CD4⁺ CD45RA⁺ T cells were isolated from peripheral blood mononuclear cells by depleting non-T helper and memory CD45RO⁺ T cells, and subsequently subjected to a phenotypic characterization. Flow cytometric analyses of suitable cell surface markers within the enriched cell population consistently revealed 80-85% pure naïve Th cells (Figure 4.20A).

Next, to drive their expansion, isolated naïve cells were activated through the T cell receptor-CD3 complex and simultaneously exposed to exogenous IL-2. Clonal expansion *in vitro* was monitored using the intracellular fluorescent dye, CFSE. Generally, CFSE has the ability to stably label molecules within cells and thereby it allows to detect cell division and determine the number of divisions a cell has undergone under the given experimental conditions. Using this approach, 3 days after exposure to activating stimuli, we could detect an active cell proliferation represented by the reduction of CFSE fluorescence with each cell division (Figure 4.20B).

4.4.2 15d-PGJ₂ inhibits the transmigration of Th1 lymphocytes

Activated Th cells were further differentiated *in vitro* to Th1 cells in the presence of IL-12 and anti-IL-4 antibodies (Figure 4.21A). We have established an intracellular cytokine staining protocol to monitor cell differentiation status under Th1-skewing conditions characterized by the expression of specific signature cytokines, i.e. IFN- γ (Th1) and IL-4 (Th2) (in collaboration with Philipp Rößner, DKFZ, Heidelberg). Furthermore, we evaluated the impact of 15d-PGJ₂ on the transendothelial migration of differentiated Th1 cells *in vitro*. The effect of 15d-PGJ₂ on the migratory capacity of the Th1 cells was assessed in a Transwell[®] transmigration assay (see section 3.1.7), wherein Th1-skewed cells were allowed to transmigrate across monolayers of orbital shear stress-preconditioned HUVECs (TT-genotype) in the presence of chemoattractant gradients, i.e. CCL-5 or MCP-1.

Similar to THP-1 monocytes, pre-treatment with 15d-PGJ₂ potently impeded the capacity of the Th1 cells to migrate along the chemotactic gradient irrespective of the chemoattractant used (Figure 4.21B). In addition, 15d-PGJ₂ reduced the mean size (i.e., 10.7 μ m mean cell size distribution in the presence of DMSO vs. 9.5 μ m in the presence of 15d-PGJ₂) and volume (i.e., mean cell volume distribution of 0.650 pl in the presence DMSO vs. 0.450 pl in the presence of 15d-PGJ₂; both cell size and volume values represent means of two measurements from one exemplary experiment) of the transmigrated Th1 cells, indicating an alteration in cellular morphology in the presence of this prostanoid.

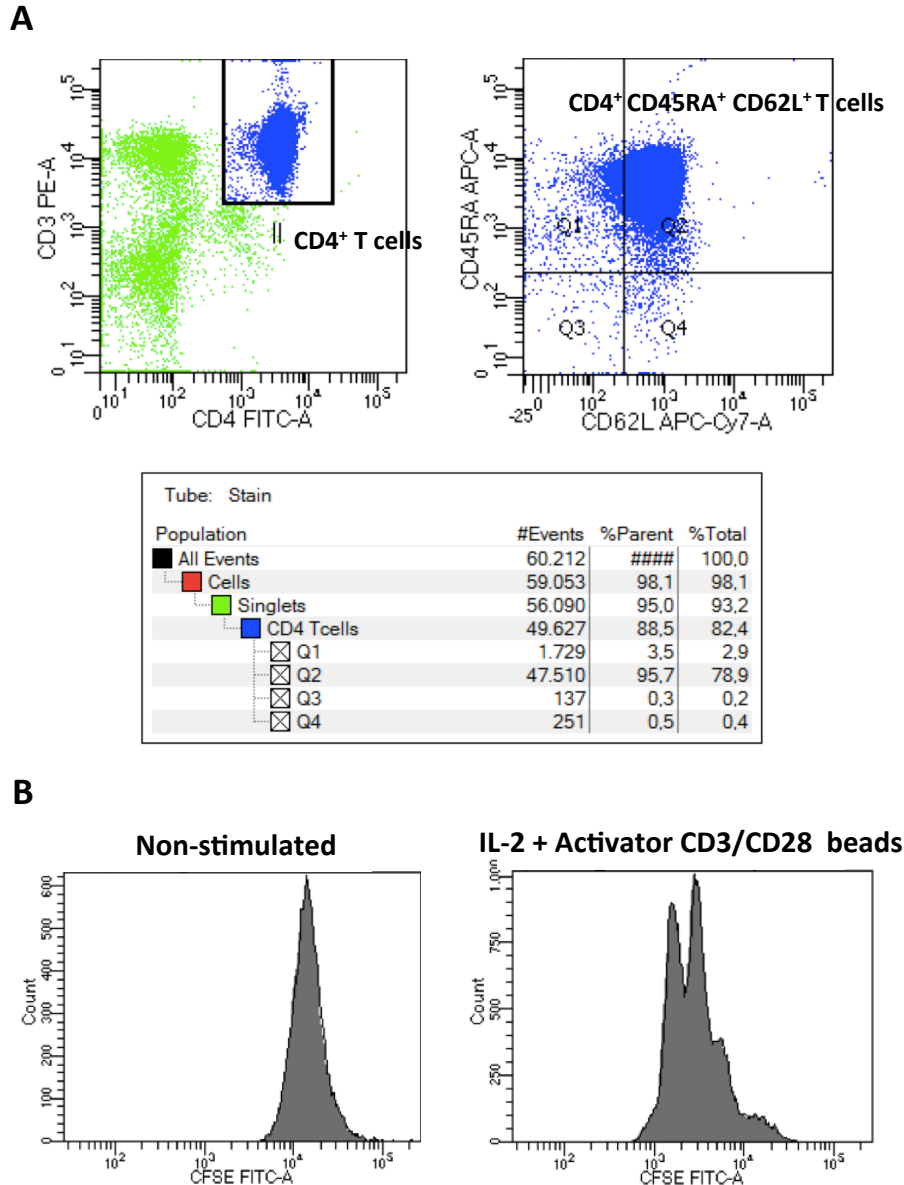


Figure 4.20: Isolation and expansion of human T helper cells. (A) Surface markers of naïve T helper cells were assessed by flow cytometry. The figure depicts a representative flow cytometric analysis of the purity of isolated cell populations (flow cytometric data acquisition and analysis were performed with the help of Philipp Rößner). The purity of the isolated cell population was determined by the relative abundance of the naïve T cell markers CD4, CD45RA and CD62L. The percentage of each cell subset is indicated in the statistical analysis displayed in the table below. (B) Histogram plots of CFSE fluorescence of naïve (left) or activated with anti-CD3/CD28 T cell activator Dynabeads® and IL-2 (right) T helper cells, 4 days post-stimulation. The 4 CFSE peaks in the right panel indicate that the cells have undergone up to 3 divisions upon activation.

4.4. Implications of the T-786C *NOS3* SNP for T helper cell-endothelial cell interactions

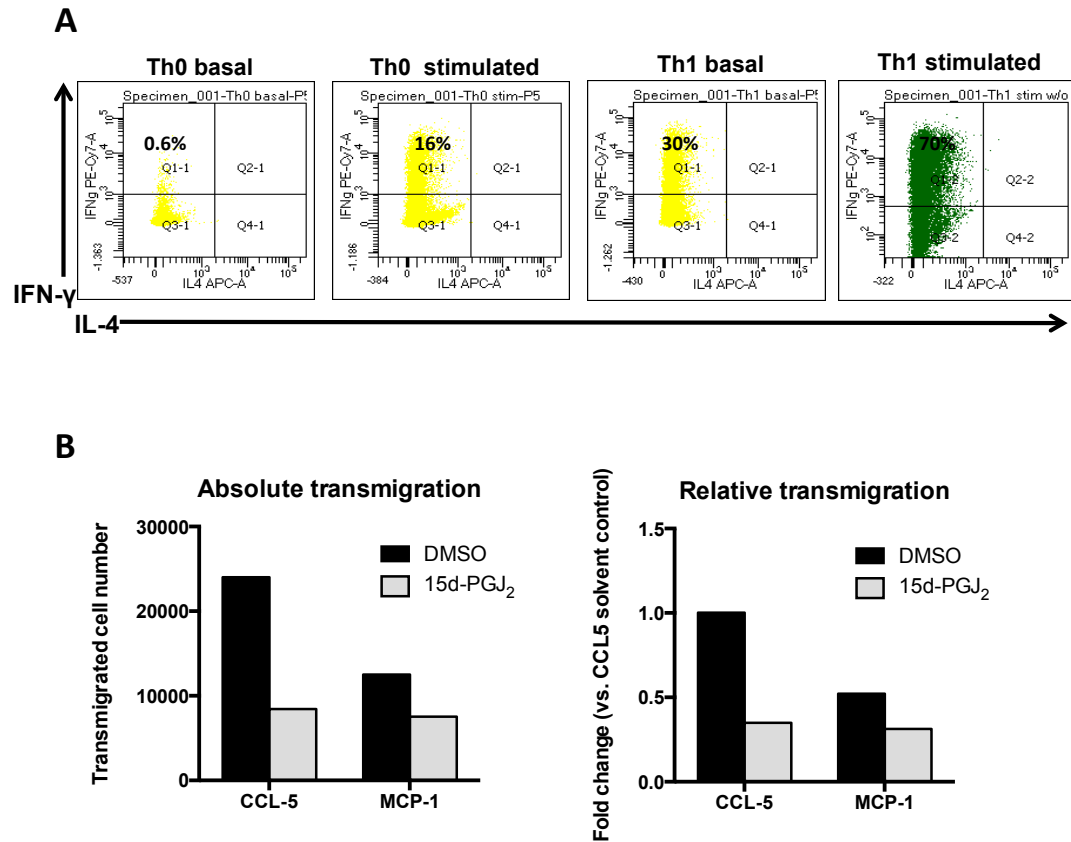


Figure 4.21: 15d-PGJ₂ impedes the transendothelial migration of *in vitro* differentiated Th1 cells. (A) Polarization of naïve human CD4⁺ T helper cells towards the Th1 phenotype. Nave CD4⁺ CD45RA⁺ T cells were either stimulated with anti-CD3/CD28 T cell activator Dynabeads[®] and IL-2 (Th0) or stimulated and cultured in the presence of IL-12 and IL-4 neutralizing antibodies (Th1) to differentiate them into Th1 cells. After 4 days the cells were expanded and cultured under the same conditions in the absence of anti-CD3/CD28 T cell activator beads. At day 7, cells were assessed for their ability to express prototypic Th1 (IFN- γ) and Th2 (IL-4) phenotype markers by intracellular cytokine staining. Resting cells were either left untreated (basal) or activated for 5 hours with anti-CD3/CD28 T cell activator beads (stimulated) prior incubation with PE-Cy7-conjugated anti-IFN- γ and APC-conjugated anti-IL-4 antibodies. Dead cells were excluded from the analyses using fixable viability dye eFluor[®] 780. Numbers represent the IFN- γ ⁺ cell population frequencies (%). The data shown are representative of 3 experiments from different donors (flow cytometric data acquisition and analysis were performed with the help of Philipp Rößner). (B) Seven days post-exposure to Th1 skewing stimuli, IFN- γ -expressing Th1 cells were pulse-treated for 1 hour with either solvent or 10 μ M 15d-PGJ₂, washed and loaded (1×10^6 /ml) on PET Transwell[®] inserts (8 μ m-pore size), which had been pre-seeded with TT-genotype HUVECs. HUVECs were pre-conditioned with orbital shear stress (shaking speed 100 rpm) for 24 hours prior to the transmigration assay. Th1 cells were allowed to transmigrate across the HUVEC monolayers for 6 hours in the presence of either CCL-5 (100 ng/ml) or MCP-1 (100 ng/ml) added to the bottom chamber. Absolute (left) and relative (right) numbers of transmigrated Th1 cells are presented as the mean of 2 independent experiments.

Atherosclerosis is caused by the complex interaction between genes and environment. Genetic susceptibility to atherosclerosis and CHD is largely determined by the presence of common inherited genetic variants (i.e., polymorphisms or SNPs) present in different genes, usually acting additively to shape the individual's risk of developing the disease. The Human Genome Project and the International HapMap project led to identification of many of the common SNPs in the world populations (Lusis (2012)). These consortia, together with the development of advanced array technologies, made possible the realisation of genome-wide association studies of common and rare genetic variants for complex traits, diseases and disease risk factors. GWAS from the last several years have provided the first unbiased knowledge on genetic variants associated with the risk for atherosclerosis (and CHD) and have largely contributed to explaining the heritability of this frequent disease. Despite a reasonable number of common and rare genetic variants covered by the latest GWAS (48 genomic loci by The CARDIoGRAMplusC4D Consortium in 2015; Nikpay et al. (2015)), most genetic determinants of atherosclerosis still remain undiscovered. Moreover, for most of the genetic variants identified thus far it is not clear what their functional impact in the context of atherosclerosis actually is.

Several SNPs in the human *NOS3* gene have demonstrated such functional consequences (i.e., to affect NOS-3 expression and/or activity) and therefore may have clinical implications. Amongst these, the T>C variance at position -786 in the *NOS3* promoter has been proven by us and others to be an independent predictor for CHD and rheumatic diseases in conventional association studies. This and other clinically relevant *NOS3* polymorphisms, however, have long failed to reach a genome-wide significance in GWAS for CHD, likely because of their relatively modest effects and interethnic differences in linkage disequilibrium with other genetic variants. In fact, a genetic variant that is associated with a disease in one population may be only weakly associated with the disease in other ethnic groups. Therefore, mixing people with different ancestries, e.g. in a meta-analysis for a certain disease entity may confound or even invalidate identification

of such causative genetic variants. On the other hand, the effect of any polymorphism may be minimized by compensatory mechanisms that keep the affected pathway, cell or organ function balanced.

This concept is exemplified by the compensatory shear stress-dependent up-regulation of the anti-oxidant enzyme, SOD-2, which we found in homozygous carriers of the C allele of the T-786C SNP of the *NOS3* gene (Asif et al. (2009a)). We have demonstrated that enhanced SOD-2-mediated anti-oxidant capacity is an adaptive mechanism in response to the reduced bioavailability of endothelial NO present in these individuals, aiming at its better protection from neutralization by excess superoxide anions. In the present work, we investigated a second compensatory mechanism, which stabilizes the anti-inflammatory phenotype of CC-genotype endothelial cells and thus may reduce the risk for premature atherosclerosis and CHD associated with this genetic defect in affected individuals. In these cells, we found an enhanced shear stress-dependent formation and release of the anti-inflammatory prostanoid, 15d-PGJ₂, compensating for the insufficient production of NO and its leukocyte-inhibiting properties.

In this context, the modulatory effects of 15d-PGJ₂ on diapedesis and activity of different leukocyte subsets were examined in detail. Although considerable effort has been devoted to elucidate the various biological roles of this autacoid, a general mechanism for its anti-inflammatory activity has not yet been identified. Using a combination of *in vitro* tools, we explored the molecular mechanisms underlying the anti-inflammatory action of 15d-PGJ₂ in monocytes. Additionally, this work addressed for the first time the relevance of 15d-PGJ₂ as a prognostic biomarker in patients with CHD.

5.1 Characterization of the 15d-PGJ₂-mediated compensatory mechanism in CC-genotype carriers

Insufficient shear stress-dependent maintenance of NOS-3 expression *in vivo* is a decisive factor in the development of endothelial dysfunction and cardiovascular complications (Cattaruzza et al. (2004)). The resulting enhanced basal production of NO is known to maintain quiescence of the resting endothelium under through several mechanisms, including inhibition of endothelial pro-inflammatory gene expression - NO contributes to suppressing the expression cell adhesion molecules such as VCAM-1, ICAM-1 and E-selectin - inhibition of Weibel-Palade body fusion and release of pro-inflammatory and pro-thrombotic mediators such as angiopoietin-2, IL-8, von Willebrand factor and P-selectin as well as inhibition of leukocyte recruitment and activation (Pofer and Sessa (2007)). The impaired expression of NOS-3 and hence endothelial NO production in individuals homozygous for the C-allele of the T-786C SNP may therefore compromise these anti-inflammatory activities and thus promote endothelial dysfunction and atherogenesis.

To address this hypothesis, we used clonally expanded ECs from individuals with CC-genotype, which herein served as a unique *in vitro* model for a genetically determined endothelial dysfunction without the necessity to use confounding stimuli such as, e.g. pro-inflammatory cytokines. The prolonged exposure of ECs to unidirectional FSS (≥ 24 hours) closely approximates the *in vivo* flow conditions. Pre-conditioning of isolated ECs with physiological levels of unidirectional FSS (~ 30 dyn/cm² for 24 hours) therefore aimed at restoring shear stress-responsive gene expression, including that of NOS-3, in the cultured ECs, thereby eliciting a mostly atheroprotective phenotype. In this experimental setting we could discern the impact of the different genotypes the phenotype of the ECs in a physiological environment reproducing the regions of undisturbed uniform blood flow (i.e., in a straight artery).

To mimic *in vitro* the diapedesis (i.e., extravasation) of leukocytes recruited to the vessel wall, we used the human monocytic cell line, THP-1, that resembles many features of primary monocytes/macrophages (for a review, see Qin (2012)). In our setup, the THP-1 cells transmigrated through a monolayer of TT- or CC-genotype human ECs along a chemotactic gradient composed of MCP-1 (CCL-2). Contrary to expectation not only transmigration of the THP-1 cells through the CC-genotype EC monolayer was strongly impeded as compared to the TT-genotype EC monolayer, but also expression of the pro-inflammatory chemokine IL-8, which is known to promote subsequent extravasation of polymorphonuclear leukocytes and lymphocytes (Takahashi et al. (1997)), was virtually abrogated in the THP-1 cells that had migrated through the CC-genotype EC monolayer. Using NOS-3 inhibitors and NO donors, both of these phenomena seemed to occur independently of the NO-synthesizing capacity of the ECs, arguing for the existence of (an) alternative mediator(s) capable of restraining the transmigration and pro-inflammatory activation of leukocytes and thus reinforcing the anti-inflammatory capacity of ECs under conditions of insufficient NO synthesis.

NO *inter alia* modulates intracellular calcium homeostasis in ECs and thus the synthesis and release of arachidonic acid (AA) metabolites in response to various agonists. For the liberation of AA from membrane phospholipids activation of phospholipase A₂ (PLA₂) enzymes is required, the majority of which is active only following an increase in intracellular calcium (Jain and Berg (1989)). NO through secondary cGMP formation and activation of protein kinase G suppresses the influx of extracellular calcium and enhances its sequestration into intracellular stores hence causing a decrease in intracellular calcium and in turn a decline in PLA₂ activity. Therefore an alteration in prostanoid levels and profile in NO-deficient CC-genotype ECs seemed conceivable.

Analysing the expression of all major enzymes contributing to prostaglandin biosynthesis in fact revealed a pronounced shear stress-dependent up-regulation of COX-2 and the lipocalin-type PGDS (L-PGDS), solely in CC-genotype ECs. COX-2 has long been regarded as the cyclooxygenase isoform the expression of which is induced exclusively

by pro-inflammatory mediators such as, e.g. cytokines. Now, it is known that COX-2 is not only an inducible enzyme but can also be constitutively expressed in several organs (e.g., kidney, gastrointestinal tract) where it participates in maintaining local homeostasis (Laufer et al. (2003)). On the other hand, L-PGDS is constitutively expressed in the vascular endothelium and its expression is maintained by unidirectional shear stress (Taba et al. (2000)). In fact, L-PGDS and its downstream products (i.e., PGD₂ and J₂ series of prostaglandins) have been proposed to contribute to the shear stress-mediated prevention of atherosclerosis, by facilitating the anti-inflammatory and thus atheroprotective phenotype of the vessel wall (Tanaka et al. (2009)).

Herein, we found that differential expression of L-PGDS in TT- and CC-genotype ECs is associated with their relative to synthesize NO. Acute inhibition of NOS-3 activity in TT-genotype ECs markedly up-regulated shear stress-dependent L-PGDS, suggesting that it is the relative lack of NO that facilitates up-regulation of this enzyme in CC-genotype ECs. In addition, siRNA-mediated knockdown of L-PGDS significantly potentiated THP-1 cell transmigration through CC-genotype EC monolayers, suggesting that one of its products must constitute the compensatory mechanism, which maintains the anti-inflammatory phenotype of these ECs. In fact, as compared to TT-genotype ECs exposure of these cells to unidirectional FSS increased the concentration of the anti-inflammatory prostanoid 15d-PGJ₂ in the cell supernatant.

15d-PGJ₂ has in fact been proposed to act as an atheroprotective autacoid released by the endothelium in response to shear stress to restrain vascular inflammation and protect arterial blood vessels from harmful stimuli (Taba et al. (2000); Sasaguri and Miwa (2004)). Consistently, intraperitoneal administration of 15d-PGJ₂ inhibited the expression of MCP-1, TNF- α and MMP-9, and significantly reduced the number of infiltrated monocytes/macrophages in aortic root plaques in atherosclerosis-prone ApoE-deficient mice (Seno et al. (2011)). Moreover, 15d-PGJ₂ has been implicated in the resolution of inflammation *in vivo*. By controlling the balance of cytokines and chemokines, 15d-PGJ₂ as well as its precursor PGD₂ regulate the trafficking of leukocytes during acute inflammation as well as the efflux of macrophages to draining lymphatics, promoting resolution of the acute inflammatory response (Rajakariar et al. (2007)).

A key step in inflammation is the recruitment of pro-inflammatory leukocytes from the circulation to the site of inflammation or injury. Herein, we demonstrate that exogenous 15d-PGJ₂ at micromolar concentrations exerts a potent anti-migratory effect on activated THP-1 monocytes in an *in vitro* transmigration assay. In our assay system, EC monolayers are pre-conditioned with orbital shear stress closely mimicking the non-uniform flow conditions encountered at predilection sites of atherosclerosis. 15d-PGJ₂, therefore, has the capacity to suppress transendothelial migration of monocytic cells in a pathophysiologically relevant setting. In a mouse model of peritonitis 15d-PGJ₂ has been shown to attenuate carrageenan-induced neutrophil migration to mesenteric tissues by inhibiting actin dynamics in the neutrophils during chemotaxis (Napimoga

et al. (2008)). In addition, attenuation of EC adhesion molecule expression in response to inflammatory stimuli may contribute to the anti-inflammatory effect of 15d-PGJ₂. For example, in the aforementioned peritonitis model ICAM-1 expression in the endothelium of mesenteric microvessels was significantly decreased by pretreating the mice with 15d-PGJ₂ (Napimoga et al. (2008)). Further investigations are required to show that these mechanisms are also involved in the observed inhibitory effect of 15d-PGJ₂ on THP-1 cell, i.e. monocyte extravasation.

Apart from its anti-migratory capacity, 15d-PGJ₂ also exhibited a strong inhibitory effect on TNF- α -stimulated expression of IL-1 β and CD40 in the THP-1 cells. Similarly, 15d-PGJ₂ has been shown to inhibit the release of a wide range of pro-inflammatory cytokines (e.g., IL-1 β , IL-6, IL-12 and TNF- α) from activated macrophages and to down-regulate expression of multiple pro-inflammatory genes (e.g., *iNOS*, *VCAM1*, *MMP9* and *MMP13*) in both vascular and inflammatory cells (reviewed by Scher and Pillinger (2009); Surh et al. (2011)). Recent data suggest that 15d-PGJ₂ inhibits the NLR family leucine-rich repeat protein (NLRP)1 and NLRP3 inflammasomes, i.e. cytosolic protein complexes that detect stress and pathogen-associated molecular patterns, and hence the maturation and release of IL-1 β both *in vitro* and *in vivo* (Maier et al. (2015)). Inhibition of inflammasome components may in fact constitute a novel mechanism underlying the anti-inflammatory properties of this prostanoid and one of its modes of action to inhibit the expression of IL-1 β (see below).

CD40 is a co-stimulatory molecule expressed by antigen-presenting cells as well as various non-immune cells the ligation of which is crucial for both adaptive and innate immunity. In our hands, pre-incubation of THP-1 cells with 15d-PGJ₂ strongly attenuated the *de novo* expression of CD40 in response to TNF- α stimulation. In line with this finding, 15d-PGJ₂ has been shown to abrogate expression of CD40 as well as CD40-mediated production of the chemokine CCL-5 (also known as RANTES) in cultured renal tubular epithelial cells upon concomitant exposure to IFN- γ and TNF- α (Zhang et al. (2006)). In addition, 15d-PGJ₂ inhibits expression of CD40 on rodent microglial cells and by that it has been demonstrated to modulate the differentiation of CD4⁺ encephalitogenic T cells as a part of the effector pathways in experimental autoimmune encephalomyelitis, i.e., a murine model of human multiple sclerosis (Diab et al. (2002)).

Collectively, these data corroborate 15d-PGJ₂ as an anti-inflammatory mediator capable of compensating for the anti-inflammatory properties of NO and thus balancing the insufficient endothelial NO synthesis associated with homozygosity for the C-allele of the T-786C SNP of the *NOS3* gene.

5.2 Investigation of molecular mechanisms underlying the anti-inflammatory activity of 15d-PGJ₂

A growing body of research has been devoted to elucidating the mechanisms underlying the immunomodulatory activities of 15d-PGJ₂. The pleiotropic roles of this bioactive lipid, however, have hampered the clarification of its functions. The ability of this highly electrophilic prostanoid to covalently modify cellular proteins is considered to be the major mechanism for most of its biological effects. By modulating the activity of redox-sensitive TFs as well as co-factors required for transcriptional activation by these TFs, 15d-PGJ₂ has been shown to directly influence the stability of DNA regulatory complexes and thus to control transcription of multiple genes. Given that 15d-PGJ₂ is able to regulate the course of inflammatory responses, suppression of pro-inflammatory gene expression as one mode of its anti-inflammatory action has been proposed. Herein, we showed that 15d-PGJ₂ represses transcription of the *IL-1B* gene in TNF- α -stimulated THP-1 cells. This finding is in accordance with the inhibitory effects that 15d-PGJ₂ has on the promoters of multiple pro-inflammatory genes. For example, in T cells 15d-PGJ₂ inhibits transactivation of the *FASL* gene encoding Fas ligand by interfering with the expression and/or transcriptional activity of several transcription factors such as Egr1, NF- κ B or AP-1 (Cippitelli et al. (2003)). Given that the Fas/Fas-L dyad is deregulated in diseases affecting lymphocyte homeostasis (Takahashi et al. (1994)), modulation of *FASL* gene expression by 15d-PGJ₂ in T cells may thus spur to the development of therapies for immune disorders.

Moreover, 15d-PGJ₂ has been shown to inhibit c-Myc, Sp1 or the estrogen receptor, which results in repression of the human telomerase reverse transcriptase gene (*hTERT*) in colon cancer cells (Moriai et al. (2009)). In fact, the pro-apoptotic properties of 15d-PGJ₂ in cancer cells of various origins have been attributed to its transcriptional repression of the *hTERT* gene, substantiating its anti-tumour potential (Kondoh et al. (2007); Toaldo et al. (2009)). Furthermore, 15d-PGJ₂ inhibits transactivation of the *COX2* promoter (Farrajota et al. (2005)) as well as COX-2 expression (Tsubouchi et al. (2001)) in human synovial fibroblasts. Hence, 15d-PGJ₂ has been implicated in a negative feedback loop controlling COX-2-dependent formation of pro-inflammatory prostaglandins such as PGE₂, thereby protecting against chronic inflammation in rheumatoid arthritis (Tsubouchi et al. (2001); Farrajota et al. (2005)). Based on these findings, it is plausible that transcriptional modulation of gene expression, and in particular, transcriptional repression, is a general mechanism underlying the anti-inflammatory actions of 15d-PGJ₂.

5.2.1 The Nrf2-Keap-1 pathway as a mediator of the anti-inflammatory activities of 15d-PGJ₂

Apart from direct inhibition of pro-inflammatory gene transcription, 15d-PGJ₂ can attenuate inflammation by modulating up-stream signaling as well as activating and/or inducing the expression of proteins with anti-inflammatory effects. For example, 15d-PGJ₂ interacts with a broad but specific set of signaling proteins, thereby modulating cellular functions. Based on the fact that 15d-PGJ₂ acts as a ligand for the TF PPAR- γ , which is known to have potent anti-inflammatory properties, we have explored the possibility that activation of this nuclear receptor mediates the observed anti-inflammatory activity of 15d-PGJ₂ in THP-1 monocytes. In fact, many of the protective effects of 15d-PGJ₂ in both cellular and animal models of inflammation have been attributed to the ligation of PPAR- γ (for a review, see Scher and Pillinger (2005); Scher and Pillinger (2009)). In our *in vitro* model, pharmacological inhibition of PPAR- γ failed to abrogate the inhibitory effect of 15d-PGJ₂ on pro-inflammatory gene expression, in particular, TNF- α -induced expression of the *IL-1B* gene.

Inhibition of pro-inflammatory gene expression by 15d-PGJ₂, e.g., in activated monocytes/macrophages and other cell types, has primarily been ascribed to the suppression of pro-inflammatory TFs such as NF- κ B or AP-1 both in a PPAR- γ -dependent and independent manner (reviewed, by Scher and Pillinger (2009); Surh et al. (2011)). Nonetheless, in our hands the DNA-binding activity of these and other gene regulatory proteins (e.g., STAT-1, GATA) remained unaltered in THP-1 monocytes exposed to 15d-PGJ₂. Another signaling mechanism involving 15d-PGJ₂ concerns activation of the PGD₂ receptors DP1 and DP2/CRTH2 for both of which 15d-PGJ₂ is a weak agonist (Wright et al. (1998); Vaidya et al. (1999)). While interaction with the DP1 receptor causes a rise in intracellular cAMP and subsequent activation of PKA, and therefore has been implicated in the anti-inflammatory activities of PGD₂ and 15d-PGJ₂, the effects of 15d-PGJ₂ mediated via DP2 remain incompletely understood but may involve induction of apoptosis in pro-inflammatory leukocytes. However, pharmacological blockade of both of these PGD₂ receptors did not affect the inhibitory effect of 15d-PGJ₂ on pro-inflammatory gene expression in the human monocytic cells. This left us with the Nrf2-Keap-1 pathway as the most promising transcriptional effector pathway activated by 15d-PGJ₂.

Upon exposure to oxidative or electrophilic stresses, the Nrf2-Keap-1 cellular defense pathway, also known as the Nrf2 antioxidant stress response, is activated by releasing the TF Nrf2 from its repressor Keap-1 in the cytoplasm. The de-repressed Nrf2 in turn shuttles to the nucleus where it transactivates the transcription of a number of detoxifying/antioxidant genes to protect cells from intrinsically and extrinsically generated stress factors (Taguchi et al. (2011); Suzuki et al. (2013)). 15d-PGJ₂ is a potent inducer of Nrf2 signaling owing to its highly electrophilic cyclopentenone moiety (Kobayashi et al. (2009)). Accordingly, 15d-PGJ₂ has been shown to induce nuclear translocation of

Nrf2 in a vast number of cell types including vascular cells, activated macrophages and lymphocytes where it elicits cytoprotection (reviewed by Surh et al. (2011)). In a similar manner, micromolar concentrations of 15d-PGJ₂ used in this work caused a pronounced nuclear accumulation of Nrf2, binding to the ARE and expression of Nrf2-dependent genes in THP-1 monocytes.

Because numerous studies have documented beneficial effects of Nrf2 activation in various diseases, including cardiovascular, neurodegenerative, autoimmune and inflammatory disorders, compounds that manipulate the Nrf2-Keap-1 pathway – both naturally occurring and synthetic ones – have become of therapeutic interest (reviewed by Suzuki et al. (2013)). As an alternative inducer of the pathway, we employed one such synthetic compound, Bardoxolone methyl (originally developed as the first disease-modifying treatment for chronic kidney disease), which specifically activates Nrf2 and unlike 15d-PGJ₂ does not alter the intracellular redox state. The fact that specific activation of Nrf2 with Bardoxolone significantly reduced TNF- α -induced IL-1 β expression in the THP-1 cells confirmed involvement of the Nrf2-Keap-1 pathway downstream of 15d-PGJ₂.

Kobayashi et al. showed for the first time that oxidative/electrophilic stress, which was induced with the Nrf2-activating chemical, *tert*-butylhydroquinone, provokes the nuclear accumulation of *de novo* synthesized Nrf2 and not, as initially thought, of Nrf2 freed from the cytoplasmic Keap-1 repressor complex (Kobayashi et al. (2006)). Using transcription and translation inhibitors, we could demonstrate herein that the mechanism of Nrf2 translocation to the nucleus of the THP-1 cells, induced by both 15d-PGJ₂ and Bardoxolone, likewise relies on bypassing the Keap-1 "trap" in the cytoplasm by the newly synthesized protein, which in turn accumulates in the nucleus (Figure 5.1.)

5.2.2 Verifying a role for the Nrf2-Keap-1 pathway in THP-1 monocytes

To confirm our hypothesis that Nrf2 mediates the anti-inflammatory effects of 15d-PGJ₂ in the THP-1 cells, we used a combination of *in vitro* tools to mimic either a loss or a gain of function of the Nrf2-Keap-1 pathway. Deficiency/silencing of Nrf2 has been shown to enhance pro-inflammatory responses in human (Rushworth et al. (2008)) and murine monocytes/macrophages (Lin et al. (2008)), as well as in *in vivo* mouse models of inflammation (Thimmulappa et al. (2006)) and injury (Jin et al. (2008)). Conversely, overexpression of Nrf2 (Narasimhan et al. (2011)) or Nrf2-dependent cytoprotective, namely antioxidant enzymes (Lee et al. (2009b)), has been shown to confer protection against experimentally induced cellular injury and inflammation. At first, we undertook a siRNA-mediated approach to down-regulate Nrf2 in the THP-1 cells, thereby aiming at exploring its involvement downstream of 15d-PGJ₂ that primarily acts on Keap-1. Effective knockdown of Nrf2 in the THP-1 cells caused them to undergo apoptosis,

5.2. Investigation of molecular mechanisms underlying the anti-inflammatory activity of 15d-PGJ₂

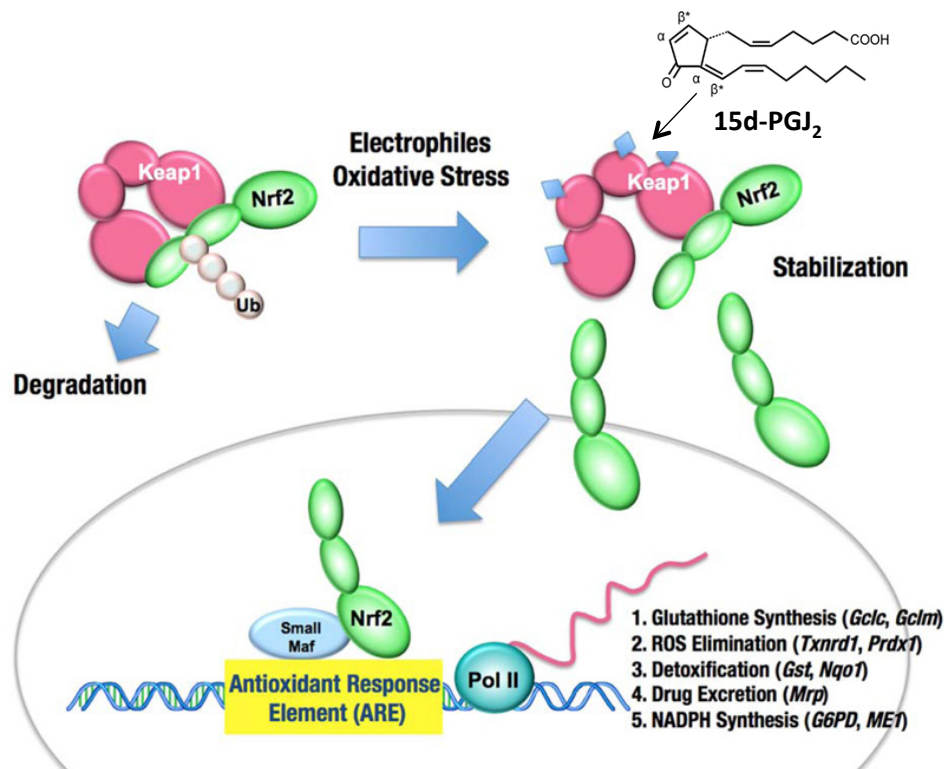


Figure 5.1: 15d-PGJ₂ is an activator of the Nrf2-Keap-1 pathway. Under normal conditions, Nrf2 is constantly ubiquitinated through Keap-1 and degraded in the proteasome. Following exposure to electrophiles or oxidative stress, Keap-1 is inactivated. Stabilized Nrf2 accumulates in the nucleus and activates many cytoprotective genes. 15d-PGJ₂ is an electrophilic lipid, which alkylates Keap-1 and inactivates it. As a result, *de novo* synthesized Nrf2 translocates to the nucleus where it activates the transcription of ARE-dependent genes. Ub, ubiquitin; (adapted from Mitsuishi et al. (2012)).

presumably through activation of effector caspases such as caspase-3 and up-regulation of pro-apoptotic proteins like Bax (Lee et al. (2015)), hence impeding our goal.

Next, we aimed at depleting Keap-1 in the THP-1 cells, also by using a siRNA-based approach. This led to enhanced accumulation of Nrf2 in the nucleus and constitutive expression of cytoprotective Nrf2-target genes such as, e.g., HO-1. Under normal homeostatic conditions, Keap-1 serves as a scaffold for substrate proteins of a Cullin3/RBX1-dependent E3 ubiquitin ligase complex, which apart from Nrf2 also targets other proteins for degradation like I κ B kinase β (IKK β), the major upstream activator of the NF- κ B pathway (Lee et al. (2009a); Kim et al. (2010)). As an integrator of both pathways, loss of Keap-1 function has been shown to augment activation, i.e., nuclear translocation of both Nrf2 and NF- κ B and to simultaneously up-regulate expression of target genes of both TFs. However, Keap-1 deficiency may have differential effects on pro-inflammatory gene expression, depending on the TF that is mostly affected. Thus, it up-regulates expression of IL-6 (Lv et al. (2013)) and IL-8 (Lee et al. (2009a)) in murine macrophages, whereas expression of IL-1 α is down-regulated in several human breast cancer cell lines

(Lee et al. (2009a)). These effects were primarily ascribed to the activation of NF- κ B though (Lv et al. (2013)). Our results show that knockdown of Keap-1, which led to the constitutive activation of Nrf2, significantly attenuated expression of the *IL-1B* gene in TNF- α -stimulated THP-1 cells, corroborating a role of Nrf2 signaling downstream of 15d-PGJ₂ in the transcriptional control of this pro-inflammatory gene. It is likely therefore that constitutive activation of Nrf2 or up-regulation of Nrf2-dependent genes upon loss of Keap-1 markedly alters the cellular redox/antioxidant status (e.g., alteration in GSH levels, expression of antioxidant proteins such as Prx, glutathione peroxidases, etc.) and may thus counteract activation of redox-sensitive TFs (other than NF- κ B) and signaling proteins involved in transactivation of the *IL-1B* gene (e.g., JNK and p38 MAPK).

5.2.3 Investigating the mechanism of action of Nrf2 in THP-1 cells

Based on the data obtained herein, we proposed a model (*cf.* Figure 4.9) summarizing the mechanism by which the relative loss of the NO-dependent anti-inflammatory capacity of the endothelium in homozygous carriers of the T-786C SNP of the *NOS3* gene is counterbalanced. CC-genotype ECs respond to their reduced capacity to synthesize NO with an adaptive up-regulation of the synthesis of 15d-PGJ₂ whereby the shear stress-dependent up-regulation of 15d-PGJ₂-producing enzymes, COX-2 and L-PGDS, in the CC-genotype ECs is driven by the reduced bioavailability of NO in these cells. The intriguing finding that it is the Nrf2-Keap-1 pathway that mediates the anti-inflammatory effects of this prostanoid in monocytes, prompted us to investigate the precise molecular mechanism(s) involved therein.

Because the anti-inflammatory effects of 15d-PGJ₂ in the monocytes coincided with a profound accumulation of Nrf2 in the nucleus, we considered two possibilities for a potential molecular mechanism: i) 15d-PGJ₂-induced nuclear Nrf2 drives the expression of antioxidant enzymes and proteins, such as HO-1 and PrxI, which in turn contribute to the overall repression of pro-inflammatory gene expression; ii) Nrf2 directly interferes with the expression of pro-inflammatory genes at the transcriptional level, e.g., *IL-1B* gene (*cf.* Figure 4.10A). The first option is not unprecedented. For example, the anti-inflammatory activity of Nrf2-controlled antioxidant proteins, including HO-1, is well described in the literature. In fact, amongst all of the cytoprotective enzymes induced by Nrf2, HO-1 probably plays the most prominent role in the cellular defense against inflammation. HO-1 has been demonstrated to mediate the anti-inflammatory effects of 15d-PGJ₂ (Lee et al. (2003)), as well as of other anti-inflammatory mediators such as IL-10, e.g., in murine macrophages *in vitro* as well as in *in vivo* mouse models of inflammation (Lee and Chau (2002)). Many of these anti-inflammatory functions have primarily been attributed to products derived from the degradation of heme by HO-1, namely carbon monoxide (CO) and biliverdin that is rapidly converted to bilirubin.

CO, for example, has been shown to differentially affect cytokine expression in LPS-stimulated murine macrophages (Otterbein et al. (2000)) by blocking the release of pro-inflammatory cytokines such as TNF- α and IL-1 β but augmenting that of the anti-inflammatory cytokine IL-10. Moreover, CO has been demonstrated to alter the plasma levels of pro- and anti-inflammatory cytokines also *in vivo*, e.g. in mice subjected to a sublethal dose of LPS (Otterbein et al. (2000); Otterbein et al. (2003)). Furthermore, inhibition of HO-1 activity in LPS-challenged murine macrophages as well as scavenging of CO abolished the inhibitory effect of 15d-PGJ₂ on NF- κ B-mediated pro-inflammatory gene expression in these cells (Lee et al. (2003)). In this work, neither blockade of HO-1 activity nor scavenging of CO (data not shown) lessened the inhibitory potency of 15d-PGJ₂ in terms of TNF- α -stimulated *IL-1B* gene expression in the THP-1 monocytes, hence arguing against this hypothesis. However, given that Nrf2 controls the expression of over 250 cytoprotective genes, many of which have demonstrated anti-inflammatory activities themselves, a functional redundancy between HO-1 and other Nrf2-dependent antioxidant enzymes cannot be ruled out.

The *in silico* identification of three high-scoring Nrf2-like binding sites, i.e. ARE-like motifs at positions -225 (ARE1), -162 (ARE2) and -63 (ARE3) relative to the transcription start site (*cf.* Figure 4.10B) in the human proximal *IL-1B* promoter substantiated our second hypothesis of a potential direct interaction between Nrf2 and the *IL-1B* promoter. Upon translocation to the nucleus, Nrf2 normally recruits the transcriptional machinery to induce cytoprotective genes. In particular, Nrf2 increases the rate of transcription of these genes by binding to (an) ARE site(s) present in their promoter regions. The concept that Nrf2 might act as a repressor of gene transcription therefore is rather unusual. To date, only few studies have demonstrated Nrf2 as a negative regulator of gene expression. By directly inhibiting promoter activity of the RON gene, which encodes a tyrosine kinase receptor overexpressed in various cancers with epithelial origin, Nrf2 has been identified as a direct repressor of gene expression, mediating the anti-tumour effects of sulforaphane, a natural Nrf2 inducer (Thangasamy et al. (2011)). In addition, Nrf2-small Maf protein heterodimers have been proposed not only to activate ARE-mediated gene expression, but also to negatively regulate the inducible expression of ARE-dependent genes encoding detoxifying enzymes such as glutathione S-transferase and NQO-1 in the rat, presumably in the context of a late response to electrophilic/xenobiotic stress (Dhakshinamoorthy and Jaiswal (2000); Nguyen (2000)).

In our hands, ChIP analysis confirmed the validity of the “direct repressor” hypothesis, as it demonstrated a potential binding of Nrf2 to the *IL-1B* promoter region comprising the putative ARE-like motifs in 15d-PGJ₂-treated THP-1 cells. Moreover, deletion of the core sequences of two of the three identified ARE motifs (i.e., ARE2 and ARE3) attenuated the repressor effect of 15d-PGJ₂ on *IL-1B* promoter activity in a reporter gene assay, indicating that Nrf2 may in fact be capable of acting as a direct transcriptional repressor of the *IL-1B* gene. On the other hand, deletion of either motif yielded

relatively weak effects, implying a possible functional redundancy between these *cis*-regulatory elements, i.e., disruption of one ARE motif at a time has a little or no effect because the other ARE motif can compensate for the loss of function of the other. As a consequence, deletion of single motifs may not be sufficient to completely abrogate the repressor effect of 15d-PGJ₂. Conversely, the three Nrf2-binding sites might be non-redundant but functional only when bound simultaneously by Nrf2. Hence, they will have to be disrupted all at once in order to clarify whether only one or in fact all three ARE-like motifs are critical for the inhibitory effect of Nrf2 on *IL-1β* expression. Moreover, because two of the three identified ARE-like motifs (i.e., ARE1 and ARE2; cf. Figure 4.10B) are spaced only 64 bp apart from each other, it is likely that they are located within the same nucleosome. Therefore, synergistic action of both motifs to drive the repression of the *IL-1B* gene cannot be ruled out. Further studies are required to verify these hypotheses.

Given that 15d-PGJ₂ is a prostaglandin exerting pleiotropic effects on gene expression and regulation, there may be other ARE-interacting proteins with regulatory function except Nrf2 acting together to mediate the repressor activity of 15d-PGJ₂ on the *IL-1B* gene. It is also plausible that ARE motifs may be regulated by the synergistic action of multiple proteins that can bind adjacent or ARE-overlapping *cis*-regulatory elements (both positive and negative) and thereby influence gene expression. Thus, it has been described that variations in the ARE motif result in an overlapping DNA binding of other ARE-recognizing factors, besides Nrf2, thereby antagonizing or synergistically enhancing its effects on gene expression. It is therefore also possible that another ARE-interacting factor conferring transcriptional repression binds to any of the three ARE motifs of interest, irrespective of the absence of intact motif cores, and by that obscures the effect of the deletion mutations. As shown herein, Bach1, a competitor of Nrf2 with transcriptional repressor function (cf. section 4.2.8), is not one of these TFs.

The dimerization partners of Nrf2, small Maf proteins (sMafs), further illustrate the complex interplay between proteins interacting with the ARE *cis*-regulatory element. In fact, sMafs can work both as transcriptional activators and repressors depending on their dimerization partners. Generally, sMafs act as co-activators of ARE-mediated gene expression when heterodimerized with Nrf2 or with some of the other CNC TF family members, or as repressors when they bind to the ARE in the form of a homodimer (Dhakshinamoorthy and Jaiswal (2000); Nguyen (2000)). Deletion of each of the three ARE core motifs in the *IL-1B* promoter could therefore trigger dissociation of Nrf2, hence disassembly of the Nrf2-sMaf transactivating complex. Small Mafs, which associate with a GC-flanking element outside of the ARE core sequence, may in turn homodimerize and thus repress the activity of the *IL-1B* promoter, masking the effect of the deletion mutations.

As a third option for a potential molecular mechanism, we considered the 15d-PGJ₂-driven negative crosstalk of Nrf2 with pro-inflammatory TFs to impede transactivation

5.2. Investigation of molecular mechanisms underlying the anti-inflammatory activity of 15d-PGJ₂

of the *IL-1B* gene. A time course analysis for activation of the Nrf2-Keap-1 pathway in THP-1 cells pre-treated with 15d-PGJ₂ for 1 hour revealed that Nrf2 already accumulates in the nucleus at the time of exposure to the pro-inflammatory stimulus TNF- α . Moreover, the inhibitory effect of 15d-PGJ₂ on *IL-1B* gene expression became discernible immediately after the onset of the TNF- α -induced rise in IL-1 β mRNA abundance. Furthermore, pre-treatment with 15d-PGJ₂ did not completely block expression of the *IL-1B* transcript but rather restrained the ability of TNF- α to fully activate the *IL-1B* gene, indicating a potential negative crosstalk between Nrf2 and a pro-inflammatory TF activated by TNF- α . In this context, the p65 subunit of NF- κ B has been shown to repress Nrf2-dependent gene expression by competing with Nrf2 for its principal co-activator CBP, a co-activator with intrinsic HAT activity (Liu et al. (2008)). In addition, p65 recruits the co-repressor, HDAC-3 (Liu et al. (2008)), leading to deacetylation of the small MafK protein and deacetylation of histone H4, thereby promoting disassembly of the Nrf2-sMaf transactivating complex (Figure 5.3). The reverse mechanism, wherein Nrf2 counteracts NF- κ B-dependent pro-inflammatory gene expression is likely to exist as well, and could therefore constitute yet another mode of action of 15d-PGJ₂ underlying the anti-inflammatory effects of this prostanoid in the THP-1 cells.

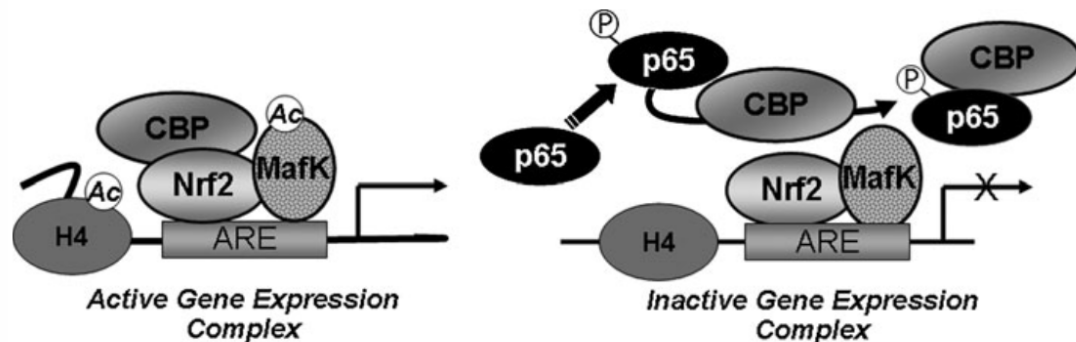


Figure 5.2: Repression of Nrf2-mediated gene transactivation by the p65 subunit of NF- κ B. p65 competes with Nrf2 for co-activator binding proteins (e.g., CBP) or recruits HDACs to the ARE, thereby altering chromatin dynamics and promoting repression of Nrf2-dependent gene transcription (Wakabayashi et al. (2010)).

15d-PGJ₂ on the other hand has been shown to exert direct effects on chromatin-modifying factors such as histone acetyl transferases and histone deacetylases. For example, 15d-PGJ₂ represses activity of the *TNFA* (TNF- α gene) promoter in human THP-1 and mouse RAW 264.7 cell lines, an effect which was claimed to correlate with the recruitment of HDACs (Engdahl et al. (2007)) that would increase chromatin condensation and thus render the enhancer DNA sequence inaccessible for TFs. Moreover, 15d-PGJ₂ antagonizes activity of the *COX2* promoter in human synovial fibroblasts by preventing IL-1 β -induced recruitment and activation of p300/CBP, which by way of histone H3 hyperacetylation relaxes the chromatin structure and/or recruits the basal transcriptional machinery to enhancer elements (Farrajota et al. (2005)). In this work,

we demonstrated that a generic HDAC inhibitor, TSA, is not capable of reversing the 15d-PGJ₂-mediated repression of the *IL-1B* promoter in THP-1 cells, which to some extent is at variance with Engdahl et al. (2007). These authors did not consider the effect of TSA alone on LPS-induced *TNFA* gene promoter activity. However, TSA typically causes global histone hyperacetylation and thus enhances the (basal) activity of gene promoters. Accordingly, in our reporter gene assay, the *IL-1B* promoter-driven basal and inducible expression of the luciferase reporter was strongly potentiated by pre-treatment with TSA. Nonetheless, 15d-PGJ₂ was able to overcome the impact not only of TSA but also that of the CBP inhibitor C646 on both the endogenous and the experimental *IL-1B* promoter, thereby arguing against the claim that inhibition of HDACs or HATs alike abrogates the repressor effect of 15d-PGJ₂ on pro-inflammatory gene expression in the THP-1 monocytes.

5.3 Clinical relevance of 15d-PGJ₂ in patients with chronic inflammatory diseases such as CHD

Although inflammation is an intrinsic protective mechanism of the body to neutralize foreign pathogens or facilitate wound healing, failure of endogenous inhibitory mechanisms to terminate such inflammatory responses may result in chronic inflammatory diseases. Co-existing with pro-inflammatory processes is an anti-inflammatory state characterized by increased levels of anti-inflammatory mediators, which terminate the inflammatory program (Haworth and Buckley (2007)). Arachidonic acid (AA) metabolites play a pivotal role in the establishment of pro-inflammatory responses. However, AA-derived lipid mediators not only exert pro-inflammatory effects in the course of an acute inflammation (e.g., PGE₂ or leukotrienes), but they may also function as anti-inflammatory mediators to promote resolution of the pro-inflammatory response and re-establish tissue homeostasis (e.g., lipoxins, resolvins or 15d-PGJ₂). For example, in the carrageenan-induced acute inflammation model of pleurisy in the rat, COX-2 expression and activity exhibits two peaks: initially at 2 hours after the onset of inflammation, correlating with the maximal synthesis of pro-inflammatory PGE₂; and a second rise in COX-2 expression observed at the late phase of inflammation (48 hours), associated with minimal production of PGE₂, but with markedly elevated levels of PGD₂ and 15d-PGJ₂. Accordingly, selective COX-2 and dual COX-1/COX-2 inhibition attenuated the early phase of inflammation but significantly exacerbated inflammation at 48 hours, which was reversed by the administration of PGD₂ and 15d-PGJ₂ (Gilroy et al. (1999)). Therefore, COX-2 might be pro-inflammatory at the onset and early phases of inflammation but may likewise contribute to the resolution of inflammation by generating anti-inflammatory prostanoids including 15d-PGJ₂.

In fact, formation of 15d-PGJ₂ has been detected *in vivo* in a mouse model of self-resolving peritonitis, wherein H-PGDS-derived prostanoids, i.e., PGD₂ and 15d-PGJ₂

5.3. Clinical relevance of 15d-PGJ₂ in patients with chronic inflammatory diseases such as CHD

have been proposed to mediate resolution of the inflammation. By orchestrating the trafficking of leukocytes to the site of inflammation and the efflux of macrophages (e.g., monocyte-derived macrophages engulfing apoptotic polymorphonuclear leukocytes during the termination of peritonitis) from the inflamed peritoneal cavity to draining lymph nodes, these two prostanoids have been shown to switch off acute inflammation (Rajakariar et al. (2007)). Consequently, exogenous administration of 15d-PGJ₂ in animal models of acute and chronic inflammation has demonstrated to be effective in alleviating several features of the experimentally induced inflammatory processes. Amongst these, 15d-PGJ₂ has been found to limit excessive neuroinflammation upon stress-induced cerebrospinal injury in diverse rodent models of CNS inflammation. It ameliorates different forms of experimentally-induced pulmonary and gastrointestinal injury, and it has demonstrated pronounced cardioprotective effects when administered at the site of myocardial ischemia/reperfusion injury induced in rats (Wayman et al. (2002)). A potent anti-inflammatory activity of 15d-PGJ₂ has been described also in the murine cyclophosphamide-induced model of bladder inflammation (Masuda et al. (2006)), the murine carrageenan-induced acute model of pleurisy (Itoh et al. (2004)) and the murine zymosan-induced non-septic shock (Marzocco et al. (2005)).

In humans, 15d-PGJ₂ has been suggested to exert neuroprotective effects by attenuating the inflammatory cascade triggered by ischemic stroke. The plasma levels of 15d-PGJ₂, for example, were significantly higher in acute ischemic stroke patients with vascular risk factors (such as history of hypertension and diabetes), as compared to patients without such risk factors and healthy controls. In addition, elevated 15d-PGJ₂ plasma concentrations exclusively correlated with the presence of atherothrombotic infarct and not with other infarct subtypes in these patients (Blanco et al. (2005)). Therefore, atherosclerosis, hypertension and diabetes may be driving stimuli for the synthesis of this prostanoid. As a consequence, high plasma levels of 15d-PGJ₂ in patients with acute ischemic stroke significantly associated with a favorable early and late neurological outcome and reduced infarct volume. Although the authors found no association between the increased release of 15d-PGJ₂ and the acute phase response or cerebral ischemia elicited within the first 24 hours of acute ischemic stroke, these findings were not confirmed with a prospective follow-up study. Blanco et al. speculated that high levels of plasma 15d-PGJ₂ detected in the stroke study group reflect a previous inflammatory event underlying vascular diseases, wherein formation and release of this anti-inflammatory lipid mediator has been triggered by activation of COX-2.

On the other hand, the concentration of plasma 15d-PGJ₂ was found to be unaltered in patients with multiple sclerosis (Comabella et al. (2009)), or even decreased in patients with chronic schizophrenia (Martínez-Gras et al. (2011)), thus somewhat obscuring a protective role of 15d-PGJ₂ in neuroinflammation. In this regard, variation in human plasma levels of 15d-PGJ₂ and their correlation with a disease strongly depends on the pathophysiological conditions. Moreover, variation among studies due to differences in

study designs such as, e.g. patient selection criteria or patient baseline clinical characteristics, as well as specificity of the methods employed to quantify the plasma levels of 15d-PGJ₂ could limit generalization of the findings from such studies.

Given its powerful immunomodulatory properties, 15d-PGJ₂ has also been proposed to have anti-atherogenic potential. As an important inflammation-resolving and anti-inflammatory mediator, 15d-PGJ₂ is likely to modulate the degree of plaque inflammation and thus vulnerability in individuals with atherosclerosis (Shibata et al. (2002); Seno et al. (2011)). We therefore, analyzed the plasma levels of 15d-PGJ₂ in human subjects suffering from CHD (i.e., at least one coronary artery with a 50% stenosis objectified by coronary angiography) and compared them to plasma 15d-PGJ₂ levels of age-matched CHD-free “healthy” controls. Interestingly, we found a positive association between plasma 15d-PGJ₂ concentrations and the presence of CHD, which was elevated 6-fold in the diseased group. No patient received any COX-2 inhibitors. In addition, the regular anti-thrombogenic low-dose aspirin therapy in patients with CHD would not have a major impact on 15d-PGJ₂ plasma levels because aspirin primarily blocks the COX-1-dependent synthesis of pro-thrombotic/pro-aggregatory TXA₂ in platelets, without affecting the endothelial cell synthesis of COX-1 or COX-2-derived anti-inflammatory as well as anti-aggregatory prostanoids such as e.g., prostacyclin (Laufer et al. (2003)). Hence, our finding is valid and corroborates a possible clinical relevance of this bioactive lipid as a biomarker.

Based on our hypothesis that 15d-PGJ₂ constitutes a compensatory mechanism which stabilizes the anti-atherosclerotic EC phenotype in individuals homozygous for the C-variant of the *NOS3* promoter, which predisposes them to endothelial dysfunction and hence CHD, we investigated the potential association between 15d-PGJ₂ plasma levels and homozygosity for the C-allele within the CHD cohort. The lack of a significant difference among the three *NOS3* genotype cohorts might be, on the one hand, attributed to the as yet relatively small sample size. On the other hand, endogenous 15d-PGJ₂ could represent a general defense mechanism to antagonize the ongoing chronic inflammatory process in affected individuals, independent of their genotype, and as such its plasma level is rather associated with the severity of the disease. And, all patients analyzed in the CHD group clearly had a multi-vessel disease. In this context, 15d-PGJ₂ may be acting as a feedback regulator of inflammatory responses, for example, by modulating the biosynthesis of other prostanoids involved in inflammation as well as its own production. 15d-PGJ₂ could thus redirect arachidonic acid metabolism towards inflammation-resolving lipid mediators, thereby controlling the degree of inflammation in a developing atherosclerotic plaque. In line with this, 15d-PGJ₂ has been demonstrated to modulate expression of both PLA₂ and COX-2 (Tsubouchi et al. (2001)), indicating the capability of this prostanoid to induce a lipid-mediator class switching during inflammation. By controlling the balance between pro- and anti-inflammatory AA-derived lipid mediators that regulate leukocyte trafficking and differentiation (Itoh et al. (2004); Rajakariar et al. (2007)), the relative abundance of 15d-PGJ₂ may influence the stability of atherosclerotic

lesions and thus alter the progression of coronary/systemic atherosclerosis altogether. Furthermore, 15d-PGJ₂ has been shown to inhibit oxLDL-induced macrophage proliferation and survival by suppressing the production of granulocyte/macrophage-colony stimulating factor, which has been implicated in the pathogenesis of atherosclerosis and other chronic inflammatory diseases (Matsuo et al. (2004)). Finally, 15d-PGJ₂ can trigger apoptosis of human IFN- γ /TNF- α -stimulated macrophages *in vitro* (Chinetti et al. (1998)). Therefore, given its modulatory activity on the macrophage phenotype, 15d-PGJ₂ could potentially influence myeloid cell-driven processes and thus the degree of inflammation in the lesion, plaque progression and vulnerability.

Because 15d-PGJ₂ inhibits the expression of a number of proteins involved in the pathogenesis of rheumatoid arthritis, it has been proposed to be a physiological mediator released to restrain chronic inflammation. For example, 15d-PGJ₂ suppressed the growth of arthritis-associated synoviocytes *in vitro* and in a dose-dependent manner attenuated chronic inflammation and pannus formation in an adjuvant-induced arthritis model in rats (Kawahito et al. (2000); Tsubouchi et al. (2001)). Furthermore, 15d-PGJ₂ has been reported to interfere with the IL-1 β -driven synthesis of PGE₂, a key mediator of synovial inflammation, in arthritis-associated synovial fibroblasts by inhibiting the expression of COX-2 and cytosolic PLA₂, corroborating its therapeutic potential in inflammatory diseases (Tsubouchi et al. (2001)).

In this context, we will not only expand our analysis of the plasma concentrations of 15d-PGJ₂ in patients with CHD (and the three different T-786C SNP genotypes) but also include patients with rheumatoid arthritis to elucidate whether presence of the 15d-PGJ₂-mediated compensatory mechanism is a general indicator for chronic inflammatory diseases that resemble each other with regard to the underlying pathogenesis and thus also evaluate its potential as a prognostic marker for the severity of the disease.

5.4 Implications of the T-786C *NOS3* SNP for T helper cell-endothelial cell interactions

CD4⁺ T helper cells play a central role throughout all stages of atherogenesis. In fact, they are the most abundant T cells in atherosclerotic plaques. CD4⁺ T cells from the Th1 phenotype, in particular, represent 10-20% (Hansson et al. (2002)) of the cells in advanced human atherosclerotic lesions. Th1 cells release various cytokines such as IFN- γ , IL-2 and TNF- α , which exert autocrine and paracrine effects on other lesional cell types, thereby modulating the inflammatory process in the plaque. Accumulation of IFN- γ -producing Th1 cells in atherosclerotic lesions directly accelerates the disease through their effects on macrophages and vascular cells. Consequently, inhibition of

differentiation to the Th1 phenotype (Laurat et al. (2001); Buono et al. (2005)) or deficiency of the IFN- γ receptor (Gupta et al. (1997)) substantially reduced atherosclerosis in hypercholesterolemic mice.

Besides atherosclerosis, effector CD4⁺ T cells have been postulated to drive the pathogenesis of chronic inflammatory disorders and autoimmune conditions such as rheumatoid arthritis, multiple sclerosis, psoriasis and inflammatory bowel diseases such as Crohn's disease to mention a few. Although IFN- γ -producing Th1 cells have long been considered as the causative agents in the pathogenesis of autoimmunity, targeting IL-17 and Th17 cell-related cytokines (e.g., IL-23) led to the notion that Th17 cells (i.e., cells from the IL-17-producing CD4⁺ effector cell lineage) are the chief contributors to autoimmune inflammation. Therefore, Th1 and Th17 cells, as well as their inflammatory products, are potential therapeutic targets to inhibit inflammation in chronic inflammatory diseases.

15d-PGJ₂ has the capacity to modify the production of T cell cytokines and thus to modulate the differentiation and effector function of distinct T lymphocyte subsets. 15d-PGJ₂ has been demonstrated, for example, to regulate Th1/Th17 responses in the EAE rodent model of human multiple sclerosis by suppressing the secretion of IFN- γ and IL-17 both in the central nervous system and in lymphoid organs (Kanakasabai et al. (2012)). Moreover, treatment with 15d-PGJ₂, both *in vitro* and *ex vivo*, inhibited neural antigen-induced release of IFN- γ , IL-17, IL-12 and IL-23, whereas it augmented IL-4, IL-10 and PPAR- γ in the lymphoid organs of the mice suffering from EAE. Moreover, 15d-PGJ₂ impairs the activation and maturation of human monocyte-derived dendritic cells (DCs) in response to Toll-like receptor (TLR)-mediated stimulation and through this mechanism reduces their capacity to induce T-cell proliferation (Appel (2005); Farnesi-de Assunção et al. (2014)). In addition, by down-regulating the expression of co-stimulatory and adhesion molecules on activated DCs as well as the secretion of cytokines/chemokines involved in T-cell activation and recruitment by these cells, 15d-PGJ₂ has been shown to attenuate the immunogenicity of DCs and could thus mediate the resolution of immune responses. At the molecular level, 15d-PGJ₂ has been demonstrated to negatively regulate DNA binding and transcriptional activity of nuclear factor of activated T cells (NFAT) in a PPAR- γ -dependent manner, thereby suppressing the production of IL-2, which governs T cell activation and clonal expansion upon antigen priming, as well as the antigen-driven proliferation of human peripheral blood T lymphocytes (Yang et al. (2000)).

In this study, we highlighted 15d-PGJ₂ as an anti-inflammatory prostanoid implicated in a compensatory mechanism counteracting the early development of chronic vascular inflammation in individuals genetically predisposed to endothelial dysfunction. Since 15d-PGJ₂ is a potent modulator of T lymphocyte differentiation and effector function, it may play an important role in the outcome of immune responses. Given that Th1- and Th17-cell-driven responses are detrimental to atherogenesis and autoimmune tissue

inflammation alike, we intend to investigate the impact of the 15d-PGJ₂-mediated compensatory mechanism on the differentiation, effector functions and migratory capacity of Th1 and Th17 lymphocytes. The significance of the T-786C SNP of the human *NOS3* gene for the interactions between ECs and T cells of both Th1 and Th17 phenotypes will be addressed in addition. For this purpose, we have established an *in vitro* transmigration model mimicking the disturbed flow pattern at arterial bifurcation or curvatures, to study transmigration of leukocytes in a setting closely approximating the flow conditions at atherosclerosis predilection sites (for detailed description of the model, see section 3.1.6). In this pathophysiologically relevant experimental setup, 15d-PGJ₂ potentially reduced the transmigration of *in vitro* differentiated Th1 cells across monolayers of human ECs, indicating that this prostanoid could potentially modulate the migratory capacity of this cell type as well, and possibly also *in vivo*. Because 15d-PGJ₂ affects the expression of adhesion molecules, both on leukocytes and ECs (*cf.* section 5.1), as well as the release of chemokines under pro-inflammatory conditions, it may thus impede the recruitment and infiltration of Th1 cells into atherosclerotic lesions and inflamed synovial tissue, thereby counteracting the progression of diseases such as CHD or RA. The effects of 15d-PGJ₂ on cytoskeletal organization might also be attributed to its anti-migratory activity (Napimoga et al. (2008)).

T-cell anergy can arise when a T-cell does not receive appropriate co-stimulation during antigen recognition. From here, the ability of 15d-PGJ₂ to modulate the expression of co-stimulatory molecules on the surface of antigen-presenting cells (e.g., DCs) might be implicated in the balance between T-cell priming and anergy *in vivo*. If 15d-PGJ₂ is in fact capable of eliciting tolerance to self-antigens through the anergy of auto-reactive effector CD4⁺ T cells, its effects could be harnessed in therapies for autoimmune/chronic inflammatory diseases such as RA.

In conclusion, the compensatory shear stress-dependent up-regulation of 15d-PGJ₂ synthesis effectively stabilizes the anti-atherosclerotic phenotype of CC-genotype ECs and may explain the comparatively slow onset of endothelial dysfunction and chronic inflammation in homozygous carriers of the C-variant of the *NOS3* promoter. By counteracting inflammation on several levels, 15d-PGJ₂ has the potential to avert the development of chronic inflammatory diseases. Strategies to improve the *in vivo* efficacy and pharmacokinetics of 15d-PGJ₂ as well as its tissue targeting specificity are essential for the therapeutic application of this anti-inflammatory prostanoid and are already under way (Alves et al. (2011)). Besides that, 15d-PGJ₂ may turn out as an important novel biomarker the plasma level of which is associated with the severity of a chronic inflammatory disease such as CHD and hence the risk for, e.g., myocardial infarction.

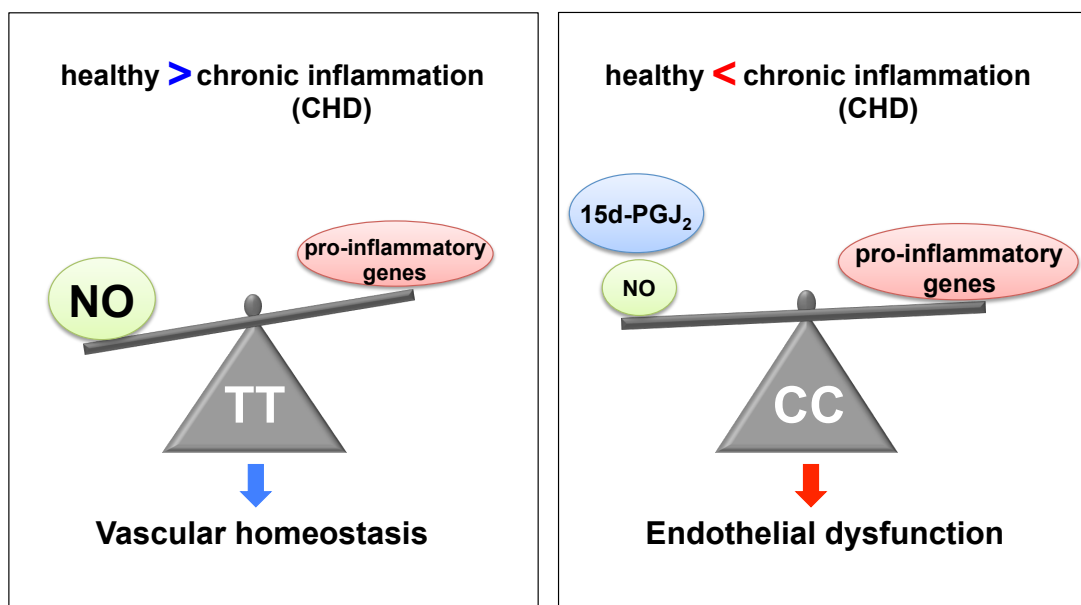


Figure 5.3: 15d-PGJ₂ balances for the anti-inflammatory properties of NO in ECs with genetically determined NO deficit. TT-genotype ECs produce normal levels of NO sufficient to maintain vascular homeostasis and health. Reduced bioavailability of NO in ECs homozygous for the C-variant of the *NOS3* promoter lifts the brake on pro-inflammatory gene expression resulting in endothelial dysfunction and increased risk of contracting chronic inflammatory diseases, such as CHD. However, a compensatory up-regulation of 15d-PGJ₂ synthesis stabilizes the anti-inflammatory phenotype of dysfunctional CC-genotype ECs, hence preventing the early onset of chronic inflammation in individuals homozygous for this genetic defect. 15d-PGJ₂ may turn out as a general indicator for chronic inflammation and a biomarker associated with the severity of chronic inflammatory diseases.

Summary

Blood flow-generated shear stress (FSS) is the major determinant of endothelial nitric oxide synthase (NOS-3) expression. In humans, a promoter variant of the *NOS3* gene, the C-variant of the T-786C single nucleotide polymorphism, renders the gene insensitive to shear stress, resulting in a reduced endothelial cell (EC) capacity to generate nitric oxide (NO). Endothelial dysfunction, commonly associated with decreased NO bioavailability, may facilitate vascular inflammation. Consequently, individuals homozygous for the C-variant have an increased risk of developing cardiovascular (e.g., coronary heart disease (CHD)) and rheumatic diseases (e.g., rheumatoid arthritis (RA)).

However, there are at least two mechanisms by which insufficient NO production can be counterbalanced in CC-genotype endothelial cells (ECs), one of which involves a multi-component pathway leading to the increased release of the anti-inflammatory prostanoid 15-deoxy- $\Delta^{12,14}$ -prostaglandin J₂ (15d-PGJ₂).

Exposure of human ECs to physiological levels of FSS effectively reduced monocyte migration, not only through monolayers of TT- but most notably also of NO-deficient CC-genotype ECs. FSS up-regulated the expression of COX-2 and L-PGDS, the rate-limiting enzymes for 15d-PGJ₂ synthesis, solely in CC-genotype ECs, and only these cells revealed an increased release of 15d-PGJ₂ in response to FSS. Exogenously added 15d-PGJ₂ significantly reduced the transmigration of monocytes through EC monolayers. In addition, pre-treatment with 15d-PGJ₂ or exposure to FSS-pretreated CC-genotype ECs exerted a pronounced anti-inflammatory effect on the (transmigrated) monocytes, as demonstrated e.g. by an inhibitory effect on interleukin-1 β (IL-1 β) expression, a marker for monocyte pro-inflammatory activation. This inhibition occurs at the transcriptional level, as 15d-PGJ₂ repressed tumor necrosis factor- α -induced IL-1 β promoter activity in transiently transfected HEK293 cells.

The anti-inflammatory activity of 15d-PGJ₂ in monocytes involves the Nrf2-antioxidant response element (ARE) pathway. Similar to 15d-PGJ₂, constitutive activation of Nrf2 reduced the expression of IL-1 β . Bioinformatic analysis revealed three putative Nrf2-responsive elements (i.e., AREs) in the human *IL-1B* promoter, suggesting that Nrf2 may act through an as yet unknown mechanism to repress transcription of the *IL-1B* gene. Chromatin immunoprecipitation showed a 15d-PGJ₂-induced binding of Nrf2 to the promoter of the *IL-1B* gene. Deletion of two of the identified ARE motifs attenuated the inhibitory potency of 15d-PGJ₂ toward *IL-1B* promoter activity, thereby corroborating Nrf2 as a downstream effector of this prostanoid's transcriptional effects.

Given its powerful immunomodulatory properties, 15d-PGJ₂ has been proposed to have anti-atherogenic potential. To evaluate its prognostic relevance, the relationship between plasma 15d-PGJ₂ levels and disease severity and outcome in patients suffering from CHD, RA or both was investigated. The levels of 15d-PGJ₂ were found to be significantly increased in the CHD group compared to age-matched controls, suggesting that 15d-PGJ₂ may constitute a general defense mechanism to counteract the ongoing chronic inflammatory process in affected individuals. Moreover, pre-treatment with 15d-PGJ₂ potently inhibited the *in vitro* transendothelial migration of interferon- γ -producing human T helper type 1 cells, major players in atherosclerosis as well as various other chronic inflammatory disorders.

Despite an inadequate capacity to form NO, CC-genotype ECs maintain a robust anti-inflammatory phenotype by enhancing the shear stress-dependent synthesis of 15d-PGJ₂. Its anti-inflammatory activity on human monocytes may ascribe a novel role to Nrf2 as a direct repressor of pro-inflammatory gene expression.

Zusammenfassung

Die durch den Blutfluss generierte Schubspannung (fluid shear stress, FSS) ist der wichtigste bestimmende Faktor für die Expression der endothelialen NO-Synthase (NOS-3). Beim Menschen macht eine Promotorvariante des *NOS3* Gens, die C-Variante des T-786C Einzelnukleotid-Polymorphismus, das Gen unempfindlich gegen Schubspannung, wodurch die Fähigkeit endothelialer Zellen (endothelial cells, EC) Stickstoffmonoxid (NO) zu erzeugen vermindert wird. Eine endotheliale Dysfunktion, die gewöhnlich mit einer verminderten NO-Bioverfügbarkeit assoziiert ist, kann Entzündungsreaktionen in den Gefäßen fördern. Infolgedessen haben Individuen, die homozygot für die C-Variante sind, ein erhöhtes Risiko, Herz-Kreislauf-Erkrankungen (z. B. koronare Herzkrankheit (coronary heart disease, CHD)) und rheumatische Erkrankungen (z. B. rheumatoide Arthritis (RA)) zu entwickeln.

Es gibt aber mindestens zwei Mechanismen, durch die eine unzureichende NO-Produktion in Endothelzellen (ECs) mit dem CC-Genotyp kompensiert werden kann. Einer davon basiert auf einem Mehrkomponenten-Stoffwechselweg, der zu einer erhöhten Freisetzung des entzündungshemmenden Prostanoids 15-Desoxy- $\Delta^{12,14}$ -Prostaglandin J₂ (15d-PGJ₂) führt.

Die Exposition menschlicher ECs gegenüber physiologischen FFS-Werten vermindert effektiv die Migration von Monozyten nicht nur durch Monolayer von ECs vom TT- sondern vor allem auch vom NO-defizienten CC-Genotyp. Nur in CC-Genotyp ECs reguliert FSS die Expression von COX-2 und L-PGDS, den geschwindigkeitsbestimmenden Enzymen bei der 15d-PGJ₂-Synthese, hoch, und nur diese Zellen zeigten eine erhöhte Freisetzung von 15d-PGJ₂ als Reaktion auf FSS. Exogen zugegebenes 15d-PGJ₂ reduzierte signifikant die Transmigration von Monozyten durch EC-Monolayer. Darüber hinaus übte die Vorbehandlung mit 15d-PGJ₂ oder die Exposition gegenüber FSS-vorbehandelten CC-Genotyp ECs eine ausgeprägte entzündungshemmende Wirkung auf die (transmigrierten) Monozyten aus, wie z. B. der hemmende Einfluss auf die Expression von Interleukin-1 β (IL-1 β), einem Marker für die pro-inflammatorische Aktivierung von Monozyten, zeigte. Diese Hemmung erfolgt auf der Transkriptionsebene, da 15d-PGJ₂ die durch Tumornekrosefaktor- α induzierte IL-1 β -Promotoraktivität in transient transfizierten HEK 293-Zellen hemmte.

Die entzündungshemmende Aktivität von 15d-PGJ₂ in Monozyten wird über den Nrf2-Antioxidans-Response-Element (ARE)-Signalweg ausgeübt. Ähnlich wie bei 15d-PGJ₂ reduziert eine konstitutive Aktivierung von Nrf2 die Expression von IL-1 β . Eine bioinformatische Analyse zeigte drei putative Nrf2-responsive Elemente (d. h. AREs) im

humanen *IL-1B*-Promotor, was darauf hindeutet, dass Nrf2 durch einen noch unbekanntem Mechanismus die Transkription des *IL-1B*-Gens reprimiert. Eine Chromatin-Immunopräzipitation ergab, dass 15d-PGJ₂ die Bindung von Nrf2 an den Promotor des *IL-1B*-Gens induziert. Die Deletion von zwei der identifizierten ARE-Motive schwächte die hemmende Wirkung von 15d-PGJ₂ auf die *IL-1B*-Promotoraktivität ab, was Nrf2 als nachgeschalteten Effektor bei der die Transkription beeinflussenden Wirkung des Prostanoids bestätigte.

Aufgrund seiner starken immunmodulatorischen Eigenschaften geht man davon aus, dass 15d-PGJ₂ antiatherogen wirken kann. Um seine prognostische Relevanz zu bewerten, wurde der Zusammenhang zwischen dem 15d-PGJ₂-Plasmaspiegel und der Schwere bzw. dem Ausgang der Erkrankung bei Patienten, die an CHD, rheumatoider Arthritis oder beiden leiden, untersucht. Verglichen mit altersangepassten Kontrollen war der 15d-PGJ₂-Spiegel in der CHD-Gruppe signifikant erhöht, was darauf hindeutet, dass 15d-PGJ₂ einen allgemeine Abwehrmechanismus darstellen könnte, um bei den betroffenen Personen dem laufenden chronischen Entzündungsprozess entgegenzuwirken. Außerdem hemmte die Vorbehandlung mit 15d-PGJ₂ *in vitro* stark die transendotheliale Migration von Interferon- γ -produzierenden humanen T-Helfer-Typ-1-Zellen, Hauptakteuren bei der Arteriosklerose sowie verschiedenen anderen chronisch entzündlichen Erkrankungen.

Trotz einer unzureichenden Fähigkeit zur Bildung von NO halten CC-Genotyp ECs durch die schubspannungsabhängige Synthese von 15d-PGJ₂ einen stabilen anti-inflammatorischen Phänotyp aufrecht. Seine entzündungshemmende Wirkung auf menschliche Monozyten könnte Nrf2 eine neue Rolle als direkter Repressor einer pro-inflammatorischen Genexpression zuschreiben.

Bibliography

- Ait-Oufella, H., Salomon, B. L., Potteaux, S., Robertson, A.-K. L., Gourdy, P., Zoll, J., Merval, R., Esposito, B., Cohen, J. L., Fisson, S., Flavell, R. A., Hansson, G. K., Klatzmann, D., Tedgui, A., and Mallat, Z. (2006). Natural regulatory T cells control the development of atherosclerosis in mice. *Nature Medicine*, 12(2):178–180.
- Alfranca, A., Iniguez, M., Fresno, M., and Redondo, J. (2006). Prostanoid signal transduction and gene expression in the endothelium: Role in cardiovascular diseases. *Cardiovascular Research*, 70(3):446–456.
- Alves, C. F., de Melo, N., Fraceto, L. F., de Araújo, D. R., and Napimoga, M. H. (2011). Effects of 15d-PGJ2-loaded poly(D,L-lactide-co-glycolide) nanocapsules on inflammation. *British Journal of Pharmacology*, 162(3):623–632.
- An, J.-d., Li, X.-y., Yu, J.-b., Zhao, Y., and Jin, Z.-s. (2012). Association between the eNOS gene polymorphisms and rheumatoid arthritis risk in a northern Chinese population. *Chinese medical journal*, 125(8):1496–1499.
- Appel, S. (2005). PPAR- agonists inhibit toll-like receptor-mediated activation of dendritic cells via the MAP kinase and NF- B pathways. *Blood*, 106(12):3888–3894.
- Asif, A. R., Hecker, M., and Cattaruzza, M. (2009a). Disinhibition of SOD-2 Expression to Compensate for a Genetically Determined NO Deficit in Endothelial Cells—Brief Report. *Arteriosclerosis, Thrombosis, and Vascular Biology*, 29(11):1890–1893.
- Asif, A. R., Oellerich, M., Armstrong, V. W., Hecker, M., and Cattaruzza, M. (2009b). T-786C Polymorphism of the nos-3 Gene and the Endothelial Cell Response to Fluid Shear Stress—A Proteome Analysis. *Journal of Proteome Research*, 8(6):3161–3168.
- Baccarelli, A., Rienstra, M., and Benjamin, E. J. (2010). Cardiovascular Epigenetics: Basic Concepts and Results From Animal and Human Studies. *Circulation: Cardiovascular Genetics*, 3(6):567–573.

- Badimon, L., Padró, T., and Vilahur, G. (2012). Atherosclerosis, platelets and thrombosis in acute ischaemic heart disease. *European heart journal. Acute cardiovascular care*, 1(1):60–74.
- Balligand, J. L., Feron, O., and Dessy, C. (2009). eNOS Activation by Physical Forces: From Short-Term Regulation of Contraction to Chronic Remodeling of Cardiovascular Tissues. *Physiological Reviews*, 89(2):481–534.
- Bentzon, J. F., Otsuka, F., Virmani, R., and Falk, E. (2014). Mechanisms of Plaque Formation and Rupture. *Circulation Research*, 114(12):1852–1866.
- Blanco, M., Moro, M. A., Davalos, A., Leira, R., Castellanos, M., Serena, J., Vivancos, J., Rodriguez-Yanez, M., Lizasoain, I., and Castillo, J. (2005). Increased Plasma Levels of 15-Deoxy Prostaglandin J2 Are Associated With Good Outcome in Acute Atherothrombotic Ischemic Stroke. *Stroke*, 36(6):1189–1194.
- Boon, R. A. and Horrevoets, A. J. G. (2009). Key transcriptional regulators of the vasoprotective effects of shear stress. *Hämostaseologie*, 29(1):39–40– 41–3.
- Buono, C., Binder, C. J., Stavrakis, G., Witztum, J. L., Glimcher, L. H., and Lichtman, A. H. (2005). T-bet deficiency reduces atherosclerosis and alters plaque antigen-specific immune responses. *Proceedings of the National Academy of Sciences of the United States of America*, 102(5):1596–1601.
- Caligiuri, G., Rudling, M., Ollivier, V., Jacob, M.-P., Michel, J.-B., Hansson, G. K., and Nicoletti, A. (2003). Interleukin-10 deficiency increases atherosclerosis, thrombosis, and low-density lipoproteins in apolipoprotein E knockout mice. *Molecular medicine (Cambridge, Mass.)*, 9(1-2):10–17.
- Castrillo, A., Díaz-Guerra, M. J., Hortelano, S., Martín-Sanz, P., and Boscá, L. (2000). Inhibition of I κ B kinase and I κ B phosphorylation by 15-deoxy-Delta(12,14)-prostaglandin J(2) in activated murine macrophages. *Molecular and Cellular Biology*, 20(5):1692–1698.
- Cattaruzza, M., Guzik, T. J., Słodowski, W., Pelvan, A., Becker, J., Halle, M., Buchwald, A. B., Channon, K. M., and Hecker, M. (2004). Shear stress insensitivity of endothelial nitric oxide synthase expression as a genetic risk factor for coronary heart disease. *Circulation Research*, 95(8):841–847.
- Cattaruzza, M., Nogoy, N., Wojtowicz, A., and Hecker, M. (2012). Zinc finger motif-1 antagonizes PDGF-BB-induced growth and dedifferentiation of vascular smooth muscle cells. *The FASEB Journal*, 26(12):4864–4875.
- Cattaruzza, M., Słodowski, W., Stojakovic, M., Krzesz, R., and Hecker, M. (2003). Interleukin-10 Induction of Nitric-oxide Synthase Expression Attenuates CD40-mediated Interleukin-12 Synthesis in Human Endothelial Cells. *Journal of Biological Chemistry*, 278(39):37874–37880.

- Cernuda-Morollon, E., Pineda-Molina, E., Canada, F. J., and Perez-Sala, D. (2001). 15-Deoxy- 12,14-prostaglandin J2 Inhibition of NF- B-DNA Binding through Covalent Modification of the p50 Subunit. *Journal of Biological Chemistry*, 276(38):35530–35536.
- Chinetti, G., Griglio, S., Antonucci, M., Torra, I. P., Delerive, P., Majd, Z., Fruchart, J. C., Chapman, J., Najib, J., and Staels, B. (1998). Activation of proliferator-activated receptors alpha and gamma induces apoptosis of human monocyte-derived macrophages. *The Journal of biological chemistry*, 273(40):25573–25580.
- Chiu, J. J., Wung, B. S., Hsieh, H. J., Lo, L. W., and Wang, D. L. (1999). Nitric Oxide Regulates Shear Stress Induced Early Growth Response-1 : Expression via the Extracellular Signal Regulated Kinase Pathway in Endothelial Cells. *Circulation Research*, 85(3):238–246.
- Cippitelli, M., Fionda, C., Di Bona, D., Lupo, A., Piccoli, M., Frati, L., and Santoni, A. (2003). The Cyclopentenone-Type Prostaglandin 15-Deoxy- 12,14-Prostaglandin J2 Inhibits CD95 Ligand Gene Expression in T Lymphocytes: Interference with Promoter Activation Via Peroxisome Proliferator-Activated Receptor- -Independent Mechanisms. *The Journal of Immunology*, 170(9):4578–4592.
- Colombo, M. G., Paradossi, U., Andreassi, M. G., Botto, N., Manfredi, S., Masetti, S., Biagini, A., and Clerico, A. (2003). Endothelial nitric oxide synthase gene polymorphisms and risk of coronary artery disease. *Clinical chemistry*, 49(3):389–395.
- Comabella, M., Pradillo, J. M., Fernández, M., Ríó, J., Lizasoain, I., Julià, E., Moro, M. A., Sastre-Garriga, J., and Montalban, X. (2009). Plasma levels of 15d-PGJ 2 are not altered in multiple sclerosis. *European Journal of Neurology*, 16(11):1197–1201.
- Cousins, D. J., Lee, T. H., and Staynov, D. Z. (2002). Cytokine Coexpression During Human Th1/Th2 Cell Differentiation: Direct Evidence for Coordinated Expression of Th2 Cytokines. *The Journal of Immunology*, 169(5):2498–2506.
- Dancy, B. M. and Cole, P. A. (2015). Protein Lysine Acetylation by p300/CBP. *Chemical Reviews*, 115(6):2419–2452.
- Deloukas, P., Kanoni, S., Willenborg, C., Farrall, M., Assimes, T. L., Thompson, J. R., Ingelsson, E., Saleheen, D., Erdmann, J., Goldstein, B. A., Stirrups, K., König, I. R., Cazier, J.-B., Johansson, Å., Hall, A. S., Lee, J.-Y., Willer, C. J., Chambers, J. C., Esko, T., Folkersen, L., Goel, A., Grundberg, E., Havulinna, A. S., Ho, W. K., Hopewell, J. C., Eriksson, N., Kleber, M. E., Kristiansson, K., Lundmark, P., Lyytikäinen, L.-P., Rafelt, S., Shungin, D., Strawbridge, R. J., Thorleifsson, G., Tikkanen, E., Van Zuydam, N., Voight, B. F., Waite, L. L., Zhang, W., Ziegler, A., Absher, D., Altshuler, D., Balmforth, A. J., Barroso, I., Braund, P. S., Burgdorf, C., Claudi-Boehm, S., Cox, D., Dimitriou, M., Do, R., Doney, A. S. F., El Mokhtari, N., Eriksson, P., Fischer, K., Fontanillas, P., Franco-Cereceda, A., Gigante, B., Groop, L.,

- Gustafsson, S., Hager, J., Hallmans, G., Han, B.-G., Hunt, S. E., Kang, H. M., Illig, T., Kessler, T., Knowles, J. W., Kolovou, G., Kuusisto, J., Langenberg, C., Langford, C., Leander, K., Lokki, M.-L., Lundmark, A., McCarthy, M. I., Meisinger, C., Melander, O., Mihailov, E., Maouche, S., Morris, A. D., Müller-Nurasyid, M., Nikus, K., Peden, J. F., Rayner, N. W., Rasheed, A., Rosinger, S., Rubin, D., Rumpf, M. P., Schäfer, A., Sivananthan, M., Song, C., Stewart, A. F. R., Tan, S.-T., Thorgeirsson, G., van der Schoot, C. E., Wagner, P. J., Wells, G. A., Wild, P. S., Yang, T.-P., Amouyel, P., Arveiler, D., Basart, H., Boehnke, M., Boerwinkle, E., Brambilla, P., Cambien, F., Cupples, A. L., de Faire, U., Dehghan, A., Diemert, P., Epstein, S. E., Evans, A., Ferrario, M. M., Ferrières, J., Gauguier, D., Go, A. S., Goodall, A. H., Gudnason, V., Hazen, S. L., Holm, H., Iribarren, C., Jang, Y., Kähönen, M., Kee, F., Kim, H.-S., Klopp, N., Koenig, W., Kratzer, W., Kuulasmaa, K., Laakso, M., Laaksonen, R., Lee, J.-Y., Lind, L., Ouwehand, W. H., Parish, S., Park, J. E., Pedersen, N. L., Peters, A., Quertermous, T., Rader, D. J., Salomaa, V., Schadt, E., Shah, S. H., Sinisalo, J., Stark, K., Stefansson, K., Trégouët, D.-A., Virtamo, J., Wallentin, L., Wareham, N., Zimmermann, M. E., Nieminen, M. S., Hengstenberg, C., Sandhu, M. S., Pastinen, T., Syvänen, A.-C., Hovingh, G. K., Dedoussis, G., Franks, P. W., Lehtimäki, T., Metspalu, A., Zalloua, P. A., Siegbahn, A., Schreiber, S., Ripatti, S., Blankenberg, S. S., Perola, M., Clarke, R., Boehm, B. O., O'Donnell, C., Reilly, M. P., März, W., Collins, R., Kathiresan, S., Hamsten, A., Kooner, J. S., Thorsteinsdottir, U., Danesh, J., Palmer, C. N. A., Roberts, R., Watkins, H., Schunkert, H., and Samani, N. J. (2012). Large-scale association analysis identifies new risk loci for coronary artery disease. *Nature Publishing Group*, 45(1):25–33.
- Dhakshinamoorthy, S., Jain, A. K., and Bloom, D. A. (2005). Bach1 competes with Nrf2 leading to negative regulation of the antioxidant response element (ARE)-mediated NAD (P) H: quinone oxidoreductase 1 gene expression *Journal of Biological . . .*
- Dhakshinamoorthy, S. and Jaiswal, A. K. (2000). Small Maf (MafG and MafK) Proteins Negatively Regulate Antioxidant Response Element-mediated Expression and Antioxidant Induction of the NAD(P)H:Quinone Oxidoreductase1 Gene. *Journal of Biological Chemistry*, 275(51):40134–40141.
- Diab, A., Deng, C., Smith, J. D., Hussain, R. Z., Phanavanh, B., Lovett-Racke, A. E., Drew, P. D., and Racke, M. K. (2002). Peroxisome Proliferator-Activated Receptor-Agonist 15-Deoxy- 12,1412,14-Prostaglandin J2 Ameliorates Experimental Autoimmune Encephalomyelitis. *The Journal of Immunology*, 168(5):2508–2515.
- Drechsler, M., Megens, R. T. A., van Zandvoort, M., Weber, C., and Soehnlein, O. (2010). Hyperlipidemia-Triggered Neutrophilia Promotes Early Atherosclerosis. *Circulation*, 122(18):1837–1845.
- Dunn, J., Simmons, R., Thabet, S., and Jo, H. (2015). The International Journal of Biochemistry & Cell Biology. *International Journal of Biochemistry and Cell Biology*, 67:167–176.

- Engdahl, R., Monroy, M. A., and Daly, J. M. (2007). 15-Deoxy- Δ 12,14-prostaglandin J2 (15d-PGJ2) mediates repression of TNF- α by decreasing levels of acetylated histone H3 and H4 at its promoter. *Biochemical and Biophysical Research Communications*, 359(1):88–93.
- Farnesi-de Assunção, T. S., Carregaro, V., da Silva, C. A. T., de Pinho, Jr, A. J., and Napimoga, M. H. (2014). The Modulatory Effect of 15d-PGJ2 in Dendritic Cells. *Nuclear Receptor Research*, 1:1–7.
- Farrajota, K., Cheng, S., Martel-Pelletier, J., Afif, H., Pelletier, J.-P., Li, X., Ranger, P., and Fahmi, H. (2005). Inhibition of interleukin-1 β -induced cyclooxygenase 2 expression in human synovial fibroblasts by 15-deoxy- Δ 12,14-prostaglandin J2 through a histone deacetylase-independent mechanism. *Arthritis & Rheumatism*, 52(1):94–104.
- Fleming, I. (2010). Molecular mechanisms underlying the activation of eNOS. *Pflügers Archiv - European Journal of Physiology*, 459(6):793–806.
- Förstermann, U. (2010). Nitric oxide and oxidative stress in vascular disease. *Pflügers Archiv - European Journal of Physiology*, 459(6):923–939.
- Förstermann, U. and Sessa, W. C. (2012). Nitric oxide synthases: regulation and function. *European Heart Journal*, 33(7):829–837.
- Full, L. E., Ruisanchez, C., and Monaco, C. (2009). The inextricable link between atherosclerosis and prototypical inflammatory diseases rheumatoid arthritis and systemic lupus erythematosus. *Arthritis Research & Therapy*, 11(2):217.
- Galkina, E. and Ley, K. (2007). Vascular Adhesion Molecules in Atherosclerosis. *Arteriosclerosis, Thrombosis, and Vascular Biology*, 27(11):2292–2301.
- Galkina, E. and Ley, K. (2009). Immune and Inflammatory Mechanisms of Atherosclerosis *. *Annual Review of Immunology*, 27(1):165–197.
- Gilroy, D. W., Colville-Nash, P. R., Willis, D., Chivers, J., Paul-Clark, M. J., and Willoughby, D. A. (1999). Inducible cyclooxygenase may have anti-inflammatory properties. *Nature Medicine*, 5(6):698–701.
- Gotsman, I., Sharpe, A. H., and Lichtman, A. H. (2008). T-cell costimulation and coinhibition in atherosclerosis. *Circulation Research*, 103(11):1220–1231.
- Gupta, S., Pablo, A. M., Jiang, X. c., Wang, N., Tall, A. R., and Schindler, C. (1997). IFN-gamma potentiates atherosclerosis in ApoE knock-out mice. *Journal of Clinical Investigation*, 99(11):2752–2761.
- Haberland, M., Montgomery, R. L., and Olson, E. N. (2009). The many roles of histone deacetylases in development and physiology: implications for disease and therapy. *Nature Reviews Genetics*, 10(1):32–42.

- Hansson, G. K., Libby, P., Schönbeck, U., and Yan, Z.-Q. (2002). Innate and adaptive immunity in the pathogenesis of atherosclerosis. *Circulation Research*, 91(4):281–291.
- Haworth, O. and Buckley, C. D. (2007). Resolving the problem of persistence in the switch from acute to chronic inflammation. *Proceedings of the National Academy of Sciences of the United States of America*, 104(52):20647–20648.
- Hellemans, J., Mortier, G., De Paepe, A., Speleman, F., and Vandesompele, J. (2007). qBase relative quantification framework and software for management and automated analysis of real-time quantitative PCR data. *Genome Biology*, 8(2):R19.
- Hemmens, B. and Mayer, B. (1998). Enzymology of nitric oxide synthases. *Methods in molecular biology (Clifton, N.J.)*, 100:1–32.
- Ito, K., Barnes, P. J., and Adcock, I. M. (2000). Glucocorticoid receptor recruitment of histone deacetylase 2 inhibits interleukin-1 β -induced histone H4 acetylation on lysines 8 and 12. *Molecular and Cellular Biology*, 20(18):6891–6903.
- Ito, K., Lim, S., Caramori, G., Cosio, B., Chung, K. F., Adcock, I. M., and Barnes, P. J. (2002). A molecular mechanism of action of theophylline: Induction of histone deacetylase activity to decrease inflammatory gene expression. *Proceedings of the National Academy of Sciences of the United States of America*, 99(13):8921–8926.
- Itoh, K., Tong, K. I., and Yamamoto, M. (2004). Molecular mechanism activating nrf2–keap1 pathway in regulation of adaptive response to electrophiles. *Free Radical Biology and Medicine*, 36(10):1208–1213.
- Jain, M. K. and Berg, O. G. (1989). The kinetics of interfacial catalysis by phospholipase A2 and regulation of interfacial activation: hopping versus scooting. *Biochimica et biophysica acta*, 1002(2):127–156.
- Jeremy, J. Y., Rowe, D., Emsley, A. M., and Newby, A. C. (1999). Nitric oxide and the proliferation of vascular smooth muscle cells. *Cardiovascular Research*, 43(3):580–594.
- Jiang, Y.-Z., Manduchi, E., Jiménez, J. M., and Davies, P. F. (2015). Endothelial epigenetics in biomechanical stress: disturbed flow-mediated epigenomic plasticity in vivo and in vitro. *Arteriosclerosis, Thrombosis, and Vascular Biology*, 35(6):1317–1326.
- Jin, W., Wang, H., Yan, W., Xu, L., Wang, X., Zhao, X., Yang, X., Chen, G., and Ji, Y. (2008). Disruption of Nrf2 enhances upregulation of nuclear factor- κ B activity, proinflammatory cytokines, and intercellular adhesion molecule-1 in the brain after traumatic brain injury. *Mediators of Inflammation*, 2008:725174.
- Kanakasabai, S., Casalini, E., Walline, C. C., Mo, C., Chearwae, W., and Bright, J. J. (2012). Differential regulation of CD4(+) T helper cell responses by curcumin in experimental autoimmune encephalomyelitis. *The Journal of nutritional biochemistry*, 23(11):1498–1507.

- Kannan, M. B., Solovieva, V., and Blank, V. (2012). *Biochimica et Biophysica Acta. BBA - Molecular Cell Research*, 1823(10):1841–1846.
- Kansanen, E., Kivelä, A. M., and Levonen, A.-L. (2009). *Free Radical Biology & Medicine. Free Radical Biology and Medicine*, 47(9):1310–1317.
- Kawahito, Y., Kondo, M., Tsubouchi, Y., Hashiramoto, A., Bishop-Bailey, D., Inoue, K., Kohno, M., Yamada, R., Hla, T., and Sano, H. (2000). 15-deoxy-delta(12,14)-PGJ(2) induces synoviocyte apoptosis and suppresses adjuvant-induced arthritis in rats. *Journal of Clinical Investigation*, 106(2):189–197.
- Ketelhuth, D. F. J. and Hansson, G. K. (2016). Adaptive Response of T and B Cells in Atherosclerosis. *Circulation Research*, 118(4):668–678.
- Kim, J.-E., You, D.-J., Lee, C., Ahn, C., Seong, J. Y., and Hwang, J.-I. (2010). Suppression of NF-kappaB signaling by KEAP1 regulation of IKKbeta activity through autophagic degradation and inhibition of phosphorylation. *Cellular Signalling*, 22(11):1645–1654.
- Kisucka, J., Chauhan, A. K., Patten, I. S., Yesilaltay, A., Neumann, C., Van Etten, R. A., Krieger, M., and Wagner, D. D. (2008). Peroxiredoxin1 prevents excessive endothelial activation and early atherosclerosis. *Circulation Research*, 103(6):598–605.
- Kobayashi, A., Kang, M. I., Watai, Y., Tong, K. I., Shibata, T., Uchida, K., and Yamamoto, M. (2006). Oxidative and Electrophilic Stresses Activate Nrf2 through Inhibition of Ubiquitination Activity of Keap1. *Molecular and Cellular Biology*, 26(1):221–229.
- Kobayashi, M., Li, L., Iwamoto, N., Nakajima-Takagi, Y., Kaneko, H., Nakayama, Y., Eguchi, M., Wada, Y., Kumagai, Y., and Yamamoto, M. (2009). The Antioxidant Defense System Keap1-Nrf2 Comprises a Multiple Sensing Mechanism for Responding to a Wide Range of Chemical Compounds. *Molecular and Cellular Biology*, 29(2):493–502.
- Kondoh, K., Tsuji, N., Asanuma, K., Kobayashi, D., and Watanabe, N. (2007). Inhibition of estrogen receptor β -mediated human telomerase reverse transcriptase gene transcription via the suppression of mitogen-activated protein kinase signaling plays an important role in 15-deoxy- Δ 12,14-prostaglandin J2-induced apoptosis in cancer cells. *Experimental Cell Research*, 313(16):3486–3496.
- Kovacic, S. and Bakran, M. (2012). Genetic Susceptibility to Atherosclerosis. *Stroke Research and Treatment*, 2012(20):1–5.
- Laufer, S., Gay, S., and Brune, K. (2003). *Inflammation and Rheumatic Diseases. The Molecular Basis of Novel Therapies*. Georg Thieme Verlag.

- Laurat, E., Poirier, B., Tupin, E., Caligiuri, G., Hansson, G. K., Bariéty, J., and Nicoletti, A. (2001). In vivo downregulation of T helper cell 1 immune responses reduces atherogenesis in apolipoprotein E-knockout mice. *Circulation*, 104(2):197–202.
- Lee, D.-F., Kuo, H.-P., Liu, M., Chou, C.-K., Xia, W., Du, Y., Shen, J., Chen, C.-T., Huo, L., Hsu, M.-C., Li, C.-W., Ding, Q., Liao, T.-L., Lai, C.-C., Lin, A.-C., Chang, Y.-H., Tsai, S.-F., Li, L.-Y., and Hung, M.-C. (2009a). Short Article. *Molecular Cell*, 36(1):131–140.
- Lee, I.-T., Luo, S.-F., Lee, C.-W., Wang, S.-W., Lin, C.-C., Chang, C.-C., Chen, Y.-L., Chau, L.-Y., and Yang, C.-M. (2009b). Overexpression of HO-1 Protects against TNF- α -Mediated Airway Inflammation by Down-Regulation of TNFR1-Dependent Oxidative Stress. *The American Journal of Pathology*, 175(2):519–532.
- Lee, T.-S. and Chau, L.-Y. (2002). Heme oxygenase-1 mediates the anti-inflammatory effect of interleukin-10 in mice. *Nature Medicine*, 8(3):240–246.
- Lee, T. S., Tsai, H. L., and Chau, L. Y. (2003). Induction of Heme Oxygenase-1 Expression in Murine Macrophages Is Essential for the Anti-inflammatory Effect of Low Dose 15-Deoxy- 12,14-prostaglandin J2. *Journal of Biological Chemistry*, 278(21):19325–19330.
- Lee, Y.-J., Lee, D. M., and Lee, S.-H. (2015). Nrf2 Expression and Apoptosis in Quercetin-treated Malignant Mesothelioma Cells. *Molecules and Cells*, 38(5):416–425.
- Libby, P., Lichtman, A. H., and Hansson, G. K. (2013). Immune Effector Mechanisms Implicated in Atherosclerosis: From Mice to Humans. *Immunity*, 38(6):1092–1104.
- Lin, W., Wu, R. T., Wu, T., Khor, T. O., and Wang, H. (2008). Sulforaphane suppressed LPS-induced inflammation in mouse peritoneal macrophages through Nrf2 dependent pathway. *Biochemical . . .*
- Liu, G.-H., Qu, J., and Shen, X. (2008). NF- κ B/p65 antagonizes Nrf2-ARE pathway by depriving CBP from Nrf2 and facilitating recruitment of HDAC3 to MafK. *Biochimica et Biophysica Acta (BBA) - Molecular Cell Research*, 1783(5):713–727.
- Löffers, C., Heilig, B., and Hecker, M. (2015). T-786C single nucleotide polymorphism of the endothelial nitric oxide synthase gene as a risk factor for endothelial dysfunction in polymyalgia rheumatica. *Clinical and experimental rheumatology*, 33(5):726–730.
- Lusis, A. J. (2012). Genetics of atherosclerosis. *Trends in Genetics*, 28(6):267–275.
- Lv, P., Xue, P., Dong, J., Peng, H., Clewell, R., Wang, A., Wang, Y., Peng, S., Qu, W., Zhang, Q., Andersen, M. E., and Pi, J. (2013). Toxicology and Applied Pharmacology. *Toxicology and Applied Pharmacology*, 272(3):697–702.

- Maier, N. K., Leppla, S. H., and Moayeri, M. (2015). The Cyclopentenone Prostaglandin 15d-PGJ2 Inhibits the NLRP1 and NLRP3 Inflammasomes. *The Journal of Immunology*, 194(6):2776–2785.
- Mallat, Z., Besnard, S., Duriez, M., Deleuze, V., Emmanuel, F., Bureau, M. F., Soubrier, F., Esposito, B., Duez, H., Fievet, C., Staels, B., Duverger, N., Scherman, D., and Tedgui, A. (1999). Protective role of interleukin-10 in atherosclerosis. *Circulation Research*, 85(8):e17–24.
- Martínez-Gras, I., Pérez-Nievas, B. G., García-Bueno, B., Madrigal, J. L. M., Andrés-Esteban, E., Rodríguez-Jiménez, R., Hoenicka, J., Palomo, T., Rubio, G., and Leza, J. C. (2011). Schizophrenia Research. *Schizophrenia Research*, 128(1-3):15–22.
- Marzocco, S., Di Paola, R., Mazzon, E., Genovese, T., Britti, D., Pinto, A., Autore, G., and Cuzzocrea, S. (2005). The cyclopentenone prostaglandin 15-deoxy Δ 12,14-prostaglandin J2 attenuates the development of zymosan-induced shock. *Intensive Care Medicine*, 31(5):693–700.
- Mason, J. C. and Libby, P. (2015). Cardiovascular disease in patients with chronic inflammation: mechanisms underlying premature cardiovascular events in rheumatologic conditions. *European Heart Journal*, 36(8):482–489.
- Massberg, S., Grahl, L., von Bruehl, M.-L., Manukyan, D., Pfeiler, S., Goosmann, C., Brinkmann, V., Lorenz, M., Bidzhekov, K., Khandagale, A. B., Konrad, I., Kernerkecht, E., Reges, K., Holdenrieder, S., Braun, S., Reinhardt, C., Spannagl, M., Preissner, K. T., and Engelmann, B. (2010). Reciprocal coupling of coagulation and innate immunity via neutrophil serine proteases. *Nature Medicine*, 16(8):887–896.
- Masuda, H., Chancellor, M. B., Kihara, K., and Yoshimura, N. (2006). 15-Deoxy- Δ 12,14-prostaglandin J2 attenuates development of cyclophosphamide-induced cystitis in rats. *Urology*, 67(2):435–439.
- Matsuo, T., Matsumura, T., Sakai, M., Senokuchi, T., Yano, M., Kiritoshi, S., Sonoda, K., Kukidome, D., Pestell, R. G., Brownlee, M., Nishikawa, T., and Araki, E. (2004). 15d-PGJ2 inhibits oxidized LDL-induced macrophage proliferation by inhibition of GM-CSF production via inactivation of NF- κ B. *Biochemical and Biophysical Research Communications*, 314(3):817–823.
- Melchers, I., Blaschke, S., Hecker, M., and Cattaruzza, M. (2006). The -786C/T single-nucleotide polymorphism in the promoter of the gene for endothelial nitric oxide synthase: Insensitivity to physiologic stimuli as a risk factor for rheumatoid arthritis. *Arthritis & Rheumatism*, 54(10):3144–3151.
- Miao, F., Gonzalo, I. G., Lanting, L., and Natarajan, R. (2004). In Vivo Chromatin Remodeling Events Leading to Inflammatory Gene Transcription under Diabetic Conditions. *Journal of Biological Chemistry*, 279(17):18091–18097.

- Michie, C. A., McLean, A., Alcock, C., and Beverley, P. C. (1992). Lifespan of human lymphocyte subsets defined by CD45 isoforms. *Nature*, 360(6401):264–265.
- Mitsuishi, Y., Motohashi, H., and Yamamoto, M. (2012). The Keap1-Nrf2 system in cancers: stress response and anabolic metabolism. *Frontiers in oncology*, 2:200.
- Miyamoto, Y., Saito, Y., Nakayama, M., Shimasaki, Y., Yoshimura, T., Yoshimura, M., Harada, M., Kajiyama, N., Kishimoto, I., Kuwahara, K., Hino, J., Ogawa, E., Hamanaka, I., Kamitani, S., Takahashi, N., Kawakami, R., Kangawa, K., Yasue, H., and Nakao, K. (2000). Replication protein A1 reduces transcription of the endothelial nitric oxide synthase gene containing a -786T→C mutation associated with coronary spastic angina. *Human Molecular Genetics*, 9(18):2629–2637.
- Moore, K. J., Sheedy, F. J., and Fisher, E. A. (2013). Macrophages in atherosclerosis: a dynamic balance. *Nature Reviews Immunology*, 13(10):709–721.
- Moore, K. J. and Tabas, I. (2011). Macrophages in the Pathogenesis of Atherosclerosis. *CELL*, 145(3):341–355.
- Moriai, M., Tsuji, N., Kobayashi, D., Kuribayashi, K., and Watanabe, N. (2009). Down-regulation of hTERT expression plays an important role in 15-deoxy-Delta12,14-prostaglandin J2-induced apoptosis in cancer cells. *International journal of oncology*, 34(5):1363–1372.
- Morishita, R., Higaki, J., Tomita, N., and Ogihara, T. (1998). Application of transcription factor “decoy” strategy as means of gene therapy and study of gene expression in cardiovascular disease. *Circulation Research*.
- Morse, D., Lin, L., Choi, A. M. K., and Ryter, S. W. (2009). Heme oxygenase-1, a critical arbitrator of cell death pathways in lung injury and disease. *Free Radical Biology and Medicine*, 47(1):1–12.
- Murray, P. C. J. L. M., PhD, P. T. V., MD, P. R. L., PhD, M. N., PhD, A. D. F., MD, C. M., PhD, P. M. E., MD, P. K. S., PhD, P. J. A. S., MBBS, S. A., MD, P. V. A., MPH, J. A., and PhD... (2012). Disability-adjusted life years (DALYs) for 291 diseases and injuries in 21 regions, 1990–2010: a systematic analysis for the Global Burden of Disease Study 2010. *The Lancet*, 380(9859):2197–2223.
- Nadkarni, S., Mauri, C., and Ehrenstein, M. R. (2007). Anti-TNF- α therapy induces a distinct regulatory T cell population in patients with rheumatoid arthritis via TGF- β . *The Journal of Experimental Medicine*, 204(1):33–39.
- Nakayama, M., Yasue, H., Yoshimura, M., Shimasaki, Y., Kugiyama, K., Ogawa, H., Motoyama, T., Saito, Y., Ogawa, Y., Miyamoto, Y., and Nakao, K. (1999). T-786-C Mutation in the 5'-Flanking Region of the Endothelial Nitric Oxide Synthase Gene Is Associated With Coronary Spasm. *Circulation*, 99(22):2864–2870.

- Nakayama, M., Yasue, H., Yoshimura, M., Shimasaki, Y., Ogawa, H., Kugiyama, K., Mizuno, Y., Harada, E., Nakamura, S., Ito, T., Saito, Y., Miyamoto, Y., Ogawa, Y., and Nakao, K. (2000). T(-786)- ζ C mutation in the 5'-flanking region of the endothelial nitric oxide synthase gene is associated with myocardial infarction, especially without coronary organic stenosis. *The American journal of cardiology*, 86(6):628–634.
- Napimoga, M. H., Vieira, S. M., Dal-Secco, D., Freitas, A., Souto, F. O., Mestriner, F. L., Alves-Filho, J. C., Grespan, R., Kawai, T., Ferreira, S. H., and Cunha, F. Q. (2008). Peroxisome Proliferator-Activated Receptor- Ligand, 15-Deoxy- 12,14-Prostaglandin J2, Reduces Neutrophil Migration via a Nitric Oxide Pathway. *The Journal of Immunology*, 180(1):609–617.
- Narasimhan, M., Mahimainathan, L., Rathinam, M. L., Riar, A. K., and Henderson, G. I. (2011). Overexpression of Nrf2 protects cerebral cortical neurons from ethanol-induced apoptotic death. *Molecular pharmacology*, 80(6):988–999.
- Nguyen, T. (2000). Transcriptional Regulation of the Antioxidant Response Element. ACTIVATION BY Nrf2 AND REPRESSION BY MafK. *Journal of Biological Chemistry*, 275(20):15466–15473.
- Nikpay, M., Goel, A., Won, H.-H., Hall, L. M., Willenborg, C., Kanoni, S., Saleheen, D., Kyriakou, T., Nelson, C. P., Hopewell, J. C., Webb, T. R., Zeng, L., Dehghan, A., Alver, M., Armasu, S. M., Auro, K., Bjornnes, A., Chasman, D. I., Chen, S., Ford, I., Franceschini, N., Gieger, C., Grace, C., Gustafsson, S., Huang, J., Hwang, S.-J., Kim, Y. K., Kleber, M. E., Lau, K. W., Lu, X., Lu, Y., Lyttikäinen, L.-P., Mihailov, E., Morrison, A. C., Pervjakova, N., Qu, L., Rose, L. M., Salfati, E., Saxena, R., Scholz, M., Smith, A. V., Tikkanen, E., Uitterlinden, A., Yang, X., Zhang, W., Zhao, W., de Andrade, M., de Vries, P. S., van Zuydam, N. R., Anand, S. S., Bertram, L., Beutner, F., Dedoussis, G., Frossard, P., Gauguier, D., Goodall, A. H., Gottesman, O., Haber, M., Han, B.-G., Huang, J., Jalilzadeh, S., Kessler, T., König, I. R., Lannfelt, L., Lieb, W., Lind, L., Lindgren, C. M., Lokki, M.-L., Magnusson, P. K., Mallick, N. H., Mehra, N., Meitinger, T., Memon, F.-u.-R., Morris, A. P., Nieminen, M. S., Pedersen, N. L., Peters, A., Rallidis, L. S., Rasheed, A., Samuel, M., Shah, S. H., Sinisalo, J., Stirrups, K. E., Trompet, S., Wang, L., Zaman, K. S., Ardisino, D., Boerwinkle, E., Borecki, I. B., Bottinger, E. P., Buring, J. E., Chambers, J. C., Collins, R., Cupples, L. A., Danesh, J., Demuth, I., Elosua, R., Epstein, S. E., Esko, T., Feitosa, M. F., Franco, O. H., Franzosi, M. G., Granger, C. B., Gu, D., Gudnason, V., Hall, A. S., Hamsten, A., Harris, T. B., Hazen, S. L., Hengstenberg, C., Hofman, A., Ingelsson, E., Iribarren, C., Jukema, J. W., Karhunen, P. J., Kim, B.-J., Kooner, J. S., Kullo, I. J., Lehtimäki, T., Loos, R. J. F., Melander, O., Metspalu, A., März, W., Palmer, C. N., Perola, M., Quertermous, T., Rader, D. J., Ridker, P. M., Ripatti, S., Roberts, R., Salomaa, V., Sanghera, D. K., Schwartz, S. M., Seedorf, U., Stewart, A. F., Stott, D. J., Thiery, J., Zalloua, P. A., O'Donnell, C. J., Reilly, M. P.,

- Assimes, T. L., Thompson, J. R., Erdmann, J., Clarke, R., Watkins, H., Kathiresan, S., McPherson, R., Deloukas, P., Schunkert, H., Samani, N. J., Farrall, M., and CARDIoGRAMplusC4D Consortium (2015). A comprehensive 1,000 Genomes-based genome-wide association meta-analysis of coronary artery disease. *Nature Publishing Group*, 47(10):1121–1130.
- Noels, H. and Weber, C. (2011). Atherosclerosis: current pathogenesis and therapeutic options. *Nature Medicine*, 17(11):1410–1422.
- Oliveira-Paula, G. H., Lacchini, R., and Tanus-Santos, J. E. (2016). Endothelial nitric oxide synthase: From biochemistry and gene structure to clinical implications of NOS3 polymorphisms. *Gene*, 575(Part 3):584–599.
- Otterbein, L. E., Bach, F. H., Alam, J., Soares, M., Tao Lu, H., Wysk, M., Davis, R. J., Flavell, R. A., and Choi, A. M. (2000). Carbon monoxide has anti-inflammatory effects involving the mitogen-activated protein kinase pathway. *Nature Medicine*, 6(4):422–428.
- Otterbein, L. E., Soares, M. P., Yamashita, K., and Bach, F. H. (2003). Heme oxygenase-1: unleashing the protective properties of heme. *Trends in Immunology*, 24(8):449–455.
- Oyake, T., Itoh, K., Motohashi, H., Hayashi, N., Hoshino, H., Nishizawa, M., Yamamoto, M., and Igarashi, K. (1996). Bach proteins belong to a novel family of BTB-basic leucine zipper transcription factors that interact with MafK and regulate transcription through the NF-E2 site. *Molecular and Cellular Biology*, 16(11):6083–6095.
- Pagel, J.-I. and Deindl, E. (2011). Early growth response 1—a transcription factor in the crossfire of signal transduction cascades. *Indian journal of biochemistry & biophysics*, 48(4):226–235.
- Paine, A., Eiz-Vesper, B., Blasczyk, R., and Immenschuh, S. (2010). Biochemical Pharmacology. *Biochemical Pharmacology*, 80(12):1895–1903.
- Park, E. J., Park, S. Y., Joe, E. h., and Jou, I. (2003). 15d-PGJ2 and Rosiglitazone Suppress Janus Kinase-STAT Inflammatory Signaling through Induction of Suppressor of Cytokine Signaling 1 (SOCS1) and SOCS3 in Glia. *Journal of Biological Chemistry*, 278(17):14747–14752.
- Park, G. Y., Joo, M., Pedchenko, T., Blackwell, T. S., and Christman, J. W. (2004). Regulation of macrophage cyclooxygenase-2 gene expression by modifications of histone H3. *American journal of physiology. Lung cellular and molecular physiology*, 286(5):L956–62.
- Perez-Sala, D., Cernuda-Morollon, E., and Canada, F. J. (2003). Molecular Basis for the Direct Inhibition of AP-1 DNA Binding by 15-Deoxy- 12,14-prostaglandin J2. *Journal of Biological Chemistry*, 278(51):51251–51260.

- Pfaffl, M. W. (2001). A new mathematical model for relative quantification in real-time RT-PCR. *Nucleic acids research*, 29(9):e45.
- Pober, J. S. and Sessa, W. C. (2007). Evolving functions of endothelial cells in inflammation. *Nature Reviews Immunology*, 7(10):803–815.
- Qin, Z. (2012). Atherosclerosis. *Atherosclerosis*, 221(1):2–11.
- Quah, B. J. C., Warren, H. S., and Parish, C. R. (2007). Monitoring lymphocyte proliferation in vitro and in vivo with the intracellular fluorescent dye carboxyfluorescein diacetate succinimidyl ester. *Nature Protocols*, 2(9):2049–2056.
- Rafikov, R., Fonseca, F. V., Kumar, S., Pardo, D., Darragh, C., Elms, S., Fulton, D., and Black, S. M. (2011). eNOS activation and NO function: structural motifs responsible for the posttranslational control of endothelial nitric oxide synthase activity. *The Journal of endocrinology*, 210(3):271–284.
- Rajakariar, R., Hilliard, M., Lawrence, T., Trivedi, S., Colville-Nash, P., Bellingan, G., Fitzgerald, D., Yaqoob, M. M., and Gilroy, D. W. (2007). Hematopoietic prostaglandin D2 synthase controls the onset and resolution of acute inflammation through PGD2 and 15-deoxyDelta12 14 PGJ2. *Proceedings of the National Academy of Sciences of the United States of America*, 104(52):20979–20984.
- Ricciotti, E. and FitzGerald, G. A. (2011). Prostaglandins and Inflammation. *Arteriosclerosis, Thrombosis, and Vascular Biology*, 31(5):986–1000.
- Robertson, A.-K. L., Rudling, M., Zhou, X., Gorelik, L., Flavell, R. A., and Hansson, G. K. (2003). Disruption of TGF-beta signaling in T cells accelerates atherosclerosis. *Journal of Clinical Investigation*, 112(9):1342–1350.
- Rossi, A., Kapahi, P., Natoli, G., Takahashi, T., and Chen, Y. I. (2000). Anti-inflammatory cyclopentenone prostaglandins are direct inhibitors of I κ B kinase. *Nature*.
- Rossi, G. P., Cesari, M., and Zanchetta, M. (2003). The T-786C endothelial nitric oxide synthase genotype is a novel risk factor for coronary artery disease in Caucasian patients of the GENICA study. *Journal of the . . .*
- Rushworth, S. A., MacEwan, D. J., and O’Connell, M. A. (2008). Lipopolysaccharide-Induced Expression of NAD(P)H:Quinone Oxidoreductase 1 and Heme Oxygenase-1 Protects against Excessive Inflammatory Responses in Human Monocytes. *The Journal of Immunology*, 181(10):6730–6737.
- Sankaranarayanan, K. and Jaiswal, A. K. (2004). Nrf3 negatively regulates antioxidant-response element-mediated expression and antioxidant induction of NAD (P) H: quinone oxidoreductase1 gene. *Journal of Biological Chemistry*.

- Sasaguri, T. and Miwa, Y. (2004). Prostaglandin J2 family and the cardiovascular system. *Current vascular pharmacology*, 2(2):103–114.
- Scher, J. U. and Pillinger, M. H. (2005). 15d-PGJ2: The anti-inflammatory prostaglandin? *Clinical Immunology*, 114(2):100–109.
- Scher, J. U. and Pillinger, M. H. (2009). The anti-inflammatory effects of prostaglandins. *Journal of investigative medicine : the official publication of the American Federation for Clinical Research*, 57(6):703–708.
- Schmidt, M. V., Brüne, B., and von Knethen, A. (2010). The Nuclear Hormone Receptor PPAR γ as a Therapeutic Target in Major Diseases. *The Scientific World JOURNAL*, 10:2181–2197.
- Schreiber, E., Matthias, P., Müller, M. M., and Schaffner, W. (1989). Rapid detection of octamer binding proteins with 'mini-extracts', prepared from a small number of cells. *Nucleic acids research*, 17(15):6419.
- Sdougos, H. P. and Bussolari, S. R. (1984). Secondary flow and turbulence in a cone-and-plate device. *Journal of Fluid . . .*
- Seno, T., Hamaguchi, M., Ashihara, E., Kohno, M., Ishino, H., Yamamoto, A., Kadoya, M., Nakamura, K., Murakami, K., Matoba, S., Maekawa, T., and Kawahito, Y. (2011). 15-Deoxy- Δ 12,14 Prostaglandin J2 Reduces the Formation of Atherosclerotic Lesions in Apolipoprotein E Knockout Mice. *PLoS ONE*, 6(10):e25541.
- Shibata, T., Kondo, M., Osawa, T., Shibata, N., Kobayashi, M., and Uchida, K. (2002). 15-Deoxy- 12,14-prostaglandin J2: A PROSTAGLANDIN D2 METABOLITE GENERATED DURING INFLAMMATORY PROCESSES. *Journal of Biological Chemistry*, 277(12):10459–10466.
- Steyers, III, C. and Miller, Jr., F. (2014). Endothelial Dysfunction in Chronic Inflammatory Diseases. *International Journal of Molecular Sciences*, 15(7):11324–11349.
- Straus, D. S., Pascual, G., Li, M., Welch, J. S., Ricote, M., Hsiang, C. H., Sengchanthlangsy, L. L., Ghosh, G., and Glass, C. K. (2000). 15-deoxy-delta 12,14-prostaglandin J2 inhibits multiple steps in the NF-kappa B signaling pathway. *Proceedings of the National Academy of Sciences of the United States of America*, 97(9):4844–4849.
- Sun, J., Brand, M., Zenke, Y., Tashiro, S., Groudine, M., and Igarashi, K. (2004). Heme regulates the dynamic exchange of Bach1 and NF-E2-related factors in the Maf transcription factor network. *Proceedings of the National Academy of Sciences of the United States of America*, 101(6):1461–1466.
- Surh, Y.-J., Na, H.-K., Park, J.-M., Lee, H.-N., Kim, W., Yoon, I.-S., and Kim, D.-D. (2011). Biochemical Pharmacology. *Biochemical Pharmacology*, 82(10):1335–1351.

- Suzuki, T., Motohashi, H., and Yamamoto, M. (2013). Toward clinical application of the Keap1–Nrf2 pathway. *Trends in Pharmacological Sciences*, 34(6):340–346.
- Taba, Y., Sasaguri, T., Miyagi, M., Abumiya, T., Miwa, Y., Ikeda, T., and Mitsumata, M. (2000). Fluid shear stress induces lipocalin-type prostaglandin D(2) synthase expression in vascular endothelial cells. *Circulation Research*, 86(9):967–973.
- Taguchi, K., Motohashi, H., and Yamamoto, M. (2011). Molecular mechanisms of the Keap1-Nrf2 pathway in stress response and cancer evolution. *Genes to Cells*, 16(2):123–140.
- Takahashi, M., Ikeda, U., Kasahara, T., Kitagawa, S., Takahashi, Y., Shimada, K., Kano, S., Morimoto, C., and Masuyama, J. (1997). Activation of human monocytes for enhanced production of interleukin 8 during transendothelial migration in vitro. *Journal of clinical immunology*, 17(1):53–62.
- Takahashi, T., Tanaka, M., Brannan, C. I., Jenkins, N. A., Copeland, N. G., Suda, T., and Nagata, S. (1994). Generalized lymphoproliferative disease in mice, caused by a point mutation in the Fas ligand. *CELL*, 76(6):969–976.
- Tanaka, R., Miwa, Y., Mou, K., Tomikawa, M., Eguchi, N., Urade, Y., Takahashi-Yanaga, F., Morimoto, S., Wake, N., and Sasaguri, T. (2009). Biochemical and Biophysical Research Communications. *Biochemical and Biophysical Research Communications*, 378(4):851–856.
- Tanus-Santos, J. E., Desai, M., and Flockhart, D. A. (2001). Effects of ethnicity on the distribution of clinically relevant endothelial nitric oxide variants. *Pharmacogenetics*, 11(8):719–725.
- Thangasamy, A., Rogge, J., Krishnegowda, N. K., Freeman, J. W., and Ammanamanchi, S. (2011). Novel function of transcription factor Nrf2 as an inhibitor of RON tyrosine kinase receptor-mediated cancer cell invasion. *Journal of Biological Chemistry*, 286(37):32115–32122.
- Thimmulappa, R. K., Lee, H., Rangasamy, T., Reddy, S. P., Yamamoto, M., Kensler, T. W., and Biswal, S. (2006). Nrf2 is a critical regulator of the innate immune response and survival during experimental sepsis. *Journal of Clinical Investigation*, 116(4):984–995.
- Tilley, S. L., Coffman, T. M., and Koller, B. H. (2001). Mixed messages: modulation of inflammation and immune responses by prostaglandins and thromboxanes. *Journal of Clinical Investigation*, 108(1):15–23.
- Toaldo, C., Pizzimenti, S., Cerbone, A., Pettazoni, P., Menegatti, E., Daniela, B., Minelli, R., Giglioni, B., Dianzani, M. U., Ferretti, C., and Barrera, G. (2009). PPAR γ ligands inhibit telomerase activity and hTERT expression through modulation of the

- Myc/Mad/Max network in colon cancer cells. *Journal of Cellular and Molecular Medicine*, 14(6a):1347–1357.
- Tse, K., Tse, H., Sidney, J., Sette, A., and Ley, K. (2013). T cells in atherosclerosis. *International Immunology*, 25(11):615–622.
- Tsubouchi, Y., Kawahito, Y., Kohno, M., Inoue, K.-i., Hla, T., and Sano, H. (2001). Feedback Control of the Arachidonate Cascade in Rheumatoid Synoviocytes by 15-deoxy- Δ 12,14-Prostaglandin J2. *Biochemical and Biophysical Research Communications*, 283(4):750–755.
- Vaidya, S., Somers, E. P., Wright, S. D., Detmers, P. A., and Bansal, V. S. (1999). 15-Deoxy-Delta12,1412,14-prostaglandin J2 inhibits the beta2 integrin-dependent oxidative burst: involvement of a mechanism distinct from peroxisome proliferator-activated receptor gamma ligation. *Journal of immunology (Baltimore, Md. : 1950)*, 163(11):6187–6192.
- Vandesompele, J., De Preter, K., Pattyn, F., Poppe, B., Van Roy, N., De Paepe, A., and Speleman, F. (2002). Accurate normalization of real-time quantitative RT-PCR data by geometric averaging of multiple internal control genes. *Genome Biology*, 3(7):RESEARCH0034.
- Varga, T. and Nagy, L. (2008). Nuclear receptors, transcription factors linking lipid metabolism and immunity: the case of peroxisome proliferator-activated receptor gamma. *European journal of clinical investigation*, 38(10):695–707.
- Venugopal, R. and Jaiswal, A. K. (1996). Nrf1 and Nrf2 positively and c-Fos and Fra1 negatively regulate the human antioxidant response element-mediated expression of NAD(P)H:quinone oxidoreductase1 gene. *Proceedings of the National Academy of Sciences of the United States of America*, 93(25):14960–14965.
- Wagner, A. H., Gebauer, M., Pollok-Kopp, B., and Hecker, M. (2002). Cytokine-inducible CD40 expression in human endothelial cells is mediated by interferon regulatory factor-1. *Blood*, 99(2):520–525.
- Wakabayashi, N., Slocum, S. L., and Skoko, J. J. (2010). When NRF2 talks, who’s listening? ... *É redox signaling*.
- Warnatsch, A., Ioannou, M., Wang, Q., and Papayannopoulos, V. (2015). Inflammation. Neutrophil extracellular traps license macrophages for cytokine production in atherosclerosis. *Science*, 349(6245):316–320.
- Watkins, H. and Farrall, M. (2006). Genetic susceptibility to coronary artery disease: from promise to progress. *Nature Reviews Genetics*, 7(3):163–173.
- Wayman, N. S., Hattori, Y., McDonald, M. C., Mota-Filipe, H., Cuzzocrea, S., Pisano, B., Chatterjee, P. K., and Thiernemann, C. (2002). Ligands of the peroxisome

- proliferator-activated receptors (PPAR-gamma and PPAR-alpha) reduce myocardial infarct size. *The FASEB Journal*, 16(9):1027–1040.
- Wierda, R. J., Geutskens, S. B., Jukema, J. W., Quax, P. H. A., and van den Elsen, P. J. (2010). Epigenetics in atherosclerosis and inflammation. *Journal of Cellular and Molecular Medicine*, 14(6a):1225–1240.
- Willems, E., Leyns, L., and Vandesompele, J. (2008). Standardization of real-time PCR gene expression data from independent biological replicates. *Analytical Biochemistry*, 379(1):127–129.
- Wright, D. H., Metters, K. M., Abramovitz, M., and Ford-Hutchinson, A. W. (1998). Characterization of the recombinant human prostanoid DP receptor and identification of L-644,698, a novel selective DP agonist. *British Journal of Pharmacology*, 123(7):1317–1324.
- Xiong, X. Y., Meng, S., and Yang, X. (2015). Methylation and atherosclerosis. *Atherosclerosis: Risks*.
- Yang, J., Manolio, T. A., Pasquale, L. R., Boerwinkle, E., Caporaso, N., Cunningham, J. M., de Andrade, M., Feenstra, B., Feingold, E., Hayes, M. G., Hill, W. G., Landi, M. T., Alonso, A., Lettre, G., Lin, P., Ling, H., Lowe, W., Mathias, R. A., Melbye, M., Pugh, E., Cornelis, M. C., Weir, B. S., Goddard, M. E., and Visscher, P. M. (2011). Genome partitioning of genetic variation for complex traits using common SNPs. *Nature Publishing Group*, 43(6):519–525.
- Yang, X. Y., Wang, L. H., Chen, T., and Hodge, D. R. (2000). Activation of Human T Lymphocytes Is Inhibited by Peroxisome Proliferator-activated Receptor γ (PPAR γ) Agonists PPAR γ CO-ASSOCIATION WITH TRANSCRIPTION *Journal of Biological*
- Zhang, Y. J., Yang, X., Kong, Q. Y., Zhang, Y. F., Chen, W. Y., Dong, X. Q., Li, X. Y., and Yu, X. Q. (2006). Effect of 15d-PGJ2 on the expression of CD40 and RANTES induced by IFN-gamma and TNF-alpha on renal tubular epithelial cells (HK-2). *American journal of nephrology*, 26(4):356–362.
- Zhao, M.-L., Brosnan, C. F., and Lee, S. C. (2004). 15-Deoxy- Δ (12,14)-PGJ2 inhibits astrocyte IL-1 signaling: inhibition of NF- κ B and MAP kinase pathways and suppression of cytokine and chemokine expression. *Journal of Neuroimmunology*, 153(1-2):132–142.

Acknowledgements

I would like to express my gratitude to Prof. Dr. Markus Hecker for giving me the great opportunity to pursue my doctoral studies in his research group at the Institute of Physiology and Pathophysiology. Thank you for guiding me and supporting me throughout the past three and half years. Without your experienced advice and invaluable assistance this PhD thesis would not have been possible.

I would also like to thank Prof. Dr. Gudrun Rappold and Prof. Dr. Marc Freichel for their useful input and inspiring discussions during our thesis advisory committee meetings. Thanks to all principal investigators of the Department of Cardiovascular Physiology, namely PD Dr. Andreas Wagner, apl. Prof. Dr. Thomas Korff, Dr. Oliver Drews and Dr. Nina Ullrich, who all have contributed markedly to the improvement of my scientific thinking and knowledge through their thought-provoking discussions and expertise. I would like to commemorate Dr. Marco Cattaruzza and convey my deepest regret on his early passing away. I am truly sorry for not being able to get to know him and learn from his professional experience. I would like to acknowledge our collaborators Dres. Thomas Fleming, Florian Leuschner and Maik Brune for providing us with patient samples. I am grateful to Jacob Morgenstern for his expert assistance with the 15d-PGJ₂ mass spectrometric measurements. My special thanks to Philipp Rößner for performing all flow cytometric analyses and for his helpful suggestions and critical discussions.

A big thank you to everyone who was there for me during this project. I appreciate the solidarity of all my colleagues who accompanied me throughout this very important time of my life. I am grateful to Cheryl, Subhajit, Hanna, Taslima, Miruna, Caroline, Anne-Sophie, Laura-Ines, Lidia, Felix, Tanja, Sebastian, Florian, Maren, Eda, Anca, Fan, Hannes, Jan, Franziska, Larissa, Cordula and to all other present and former colleagues of mine. Many thanks to the technicians Nadine, Franziska, Marie, Gudrun, Anita and Felicia for their excellent technical assistance. I owe my deepest gratitude to Tilly and Renate for giving me a really warm welcome and introducing me to the lab. Thank you for your support throughout the years. It has been an honor and privilege to work with and learn from the professional expertise of Dr. Gerd König who helped me writing all scientific reports and applications. I am indebted to our secretary Barbara Richards for being so kind and helpful to me no matter what.

There are no enough words of thanks to express my gratitude to my family and friends who have always been there for me and who were most understanding for the little time I had for them throughout the last three and half years. Thank you for your unconditional love and moral support. I want to specially thank my aunt Dr. Stela Lazarova who first inspired my passion for science and raised my love for nature. You will always be the best example to follow in my life.

Most of all I want to express my heartfelt thanks to my boyfriend Severino for being so patient, loving and supporting all the way through my PhD training. I would not have made it without you.